DYNAMIC RESPONSE OF A FLOATING DOCK IN REGULAR AND IRREGULAR WAVES

RONG YU

DYNAMIC RESPONSE OF A FLOATING DOCK IN REGULAR AND IRREGULAR WAVES

by

© Rong Yu, B.Eng.

A thesis submitted to the School of Graduate Studies in partial fulfillment of the requirements for the degree of Master of Engineering

Faculty of Engineering and Applied Science
Memorial University of Newfoundland

May 1995

St. John's Newfoundland Canada

ISBN 0-612-01931-4

Abstract

As a result of the increasing interest by engineers and port operators in floating docks to resolve port construction problems, the need for investigating the dynamic response of such structures increases. Since it is not cost effective to carry out tests on an actual operating floating dock in the ocean, an alternative solution is to undertake parametric model tests. Very few experiments using a floating dock model have been published.

To establish the motion response and mooring forces of a typical floating dock in both regular and irregular waves in beam seas, an experimental program using a 1:9 scale model of a moored floating dock has been conducted. For each mooring configuration (free floating, crossed, crossed-connected and non-crossed), tests were undertaken at a 5:1 mooring ratio (horizontal distance to water depth) with prototype wave periods of 3 to 15 seconds. In all cases roll, heave and sway motion responses were obtained. The experiments were conducted in a wave tank equipped with a pseudo random wave making facility. To obtain the response amplitude operator (RAO) from the ambient response data, spectral analysis techniques were used.

There is very good agreement between regular and irregular wave data. The RAO curves for roll, heave, sway and mooring forces show that the non-crossed mooring configuration should be employed where the situation permits since it will decrease the roll motion and mooring forces with respect to crossed and crossed-connected designs. There appears to be no benefit in either of the mooring designs for heave response. The RAO remains relatively constant regardless of wave height and period.

Based on the findings of the study, areas for further research have been identified and recommendations made for further work on floating dock designs.

Acknowledgements

The author wishes to express her deep gratitude and appreciation to Dr. A.B. Cammaert and Dr. D.B. Muggeridge for their supervision, guidance and encouragement.

A special word of thanks goes to my colleague Mr. B.J. Morey for his constant suggestions and assistance during the study.

I am grateful to many other people for their help, but I shall only mention a few of them. Mr. Stephen K. Foster and Mrs. Diane Ramsay of Technical Services built the experimental model; Mr. Andrew Kuczora provided invaluable assistance throughout the experimental investigation in the wave tank; Mr. Lloyd Little and Mr. Tony Galway of the Centre for Computer Aided Engineering assisted in computer related matters.

The funding for the research by the Department of Fisheries and Oceans under grant # 334081 is gratefully acknowledged. Also, I am indebted to Dr. J.J. Sharp (Associate Dean of Engineering) for the award of a graduate fellowship, and to Dr. F.D. Marsh at the Atlantic Accord Career Development Awards Board for a graduate studies award. Thanks are also expressed to Dr. R. Seshadri (Dean of Engineering) and Dr. A.S.J. Swamidas for their help.

No amount of gratitude can adequately repay my parents for their permanent support and affection. This thesis truly belongs to them.

Contents

List of Figures

List of Tables

List of Symbols

$a(\omega)$	added mass matrix
$b(\omega)$	damping matrix
$BMxx$	metacentric radius about longitudinal axis
$BMzz$	metacentric radius about transverse axis
c	stiffness matrix
d	average distance displaced
$F(t)$	force vector
F_a	amplitude of incoming wave force
$F_a(\omega)$	Fourier transform of $F(t)$
f_o	peak frequency of the JONSWAP spectrum
$GMxx$	metacentric height about longitudinal axis
$GMzz$	metacentric height about transverse axis
g	gravitational acceleration
$H(\omega)$	complex transform function
H_s	significant wave height
H	characteristic height of structural component being investigated
$h(t)$	impulse response function
KG	center of gravity
KB	center of buoyancy
Kxx	radius of gyration about longitudinal axis
Kzz	radius of gyration about transverse axis
L	characteristic length of structural component being investigated
M	mass matrix
N	number of samples

RAO	response amplitude operator
$R_x(t)$	auto-correlation function of $x(t)$
$R_f(t)$	auto-correlation function of $F(t)$
$S(f)$	spectral density function of input
$S_x(\omega)$	spectral density function of $x(t)$
$S_f(\omega)$	spectral density function of $F(t)$
Txx	structural period in seconds about longitudinal axis
Tzz	structural period in seconds about transverse axis
t	time
W	characteristic width of structural component being investigated
W_m	mass of model
W_s	mass of small weight being used
x	displacement vector
$X(\omega)$	Fourier transform of $x(t)$
ω	circular frequency of wave
α	ratio of prototype length to model length
τ	time lag between sample values
γ	peak enhancement factor for the JONSWAP spectrum
ε	phase angle between input and output
σ_{AV}	average change in angle of inclination

Chapter 1

Introduction

1.1 General

The recent dramatic increase in the offshore petroleum industry and continually increasing world requirements for coal, natural gas and a wide range of materials coupled with the ability and willingness of different countries to exchange goods, and the lowering of trade barriers have contributed to a significant increase in seaborne traffic. Ports built to handle this traffic play a major role in the economic development of the surrounding region.

In the past two to three decades there has been highly visible and quickening interest, by marine engineers and port operators, in floating docks to resolve port construction and operation problems.

A dock is the most general designation for a structure or place at which a vessel can be moored. In many instances, floating docks may comprise an entire marine terminal or port. Recent examples include the Falkland Islands "Flexiport" which consists of

seven barges forming a 305-m-long floating quay with transit sheds that can accommodate roll-on/roll-off and general cargo ships. The port of Valdez oil dock berth No. 1 loading dock consists of a semisubmersible-type tubular steel space frame supporting a 119-by 21-m deck buoyed by 7-m-diameter vertical cylinders (Tsinker, 1986). Floating docks have also been utilized as offshore terminals for the storage and transfer of hazardous cargoes such as the LPG storage facility in the Java Sea (Anderson, 1973) and a proposed LNG terminal (Anspach, 1980).

On the local scene, there is a major shift to floating docks in small craft harbours, for a number of reasons. A collapse of the fishing industry has sharply reduced the capital funding for dock replacement and dock repairs. In certain areas where the fishery is still active, the use of floating docks is a practical and economic alternative. Environmental concerns related to the construction of fixed structures, also favour the use of floating docks.

Floating docks offer several advantages over conventional fixed pier construction; these include lower construction costs, modular design, improved expansion capability, speed of construction, and ease of deployment. The technical and economic feasibility will vary depending upon local site conditions such as water depth, tidal variations, seabed materials, availability of construction material and equipment access. Their principal disadvantages include higher maintenance and operating costs, and unacceptable motions in certain wave climates.

1.2 Objectives

Since a better understanding of the dynamic behaviour of floating docks is an important prerequisite for a safe, reliable and effective design, an experimental investigation of

floating docks with a view to minimize their motions under wave action then becomes particularly useful. Although many detailed studies have been carried out for floating docks (Jahren, 1986), they have generally been limited to structural design studies. The motion responses and mooring loads induced by environmental forces, especially wave forces, have received relatively little attention.

The following investigation addresses the problem by providing a quantitative measure of the motion response characteristics and mooring line forces of a floating dock in both regular and irregular waves. The resulting comparison will provide a definitive indication of the changes in response and mooring forces that can be expected relative to different wave conditions and mooring configurations.

1.3 Thesis Outline

This treatise is divided into six chapters. The first (Introduction) has already been presented. In Chapter 2, a literature review of available theoretical, experimental and field studies on the motion response and mooring loads of similar floating structures to waves is presented.

Chapter 3 contains hydrodynamic modelling principles, descriptions of the model and the prototype, the design and fabrication of the model, and modelling of the mooring system.

In Chapter 4, a description of the experimental study is presented. This incorporates a brief description of the instrumentation used in the tests to study the dynamic behaviour of the structure due to wave action, and an outline of the experimental procedure.

Chapter 5 focuses on the analysis and discussion of the results. Theoretical formulations which include the Spectral Analysis Method are explained and experimental results are presented and discussed.

Finally, concluding remarks and recommendations for future research are outline in Chapter 6.

Chapter 2

Literature Review

2.1 Introduction

All free floating structures have six degrees of freedom of motion and these responses are modified by the presence of a mooring system. Such structures are used in offshore for exploration and production.

There are two general approaches to the mathematical simulation of structure responses; (1) frequency domain analysis, and (2) time domain analysis. Frequency domain analysis idealizes the moored structure as a linear system characterized by a mass, spring, and dashpot. The analysis is based on mechanical vibrations theory and involves the solution of an equation of the following form;

$$(M + a(\omega)) \ddot{X} + b(\omega) \dot{X} + cX = F(t), \qquad (2.1)$$

where

M = mass matrix

$a(\omega)$ = added mass matrix

x = displacement vector

$b(\omega)$ = damping matrix

c = stiffness matrix

$F(t)$ = force vector

In reality, there is a separate equation of the form of equation (2.1) for each of the six degrees of freedom. Terms on the left-hand side of equation (2.1) account for forces imposed on the structure as it moves in still water (i.e., in the absence of waves). The added mass, $a_{ij}(\omega)$, and damping coefficient, $b_{ij}(\omega)$, are collectively called the hydrodynamic coefficients and are a function of the structure motion frequency, ω. The spring constant, c_{ij}, accounts for forces that are proportional to the structure displacement and represents either hydrostatic restoring forces or a linearized mooring restraint, or both. $F_i(t)$, on the right-hand side of equation (2.1), is a sinusoidally varying wave force and is a function of wave amplitude, frequency, and direction. $F_i(t)$ normally is computed by assuming that the floating body is held rigidly.

Hydrostatic restoring forces in equation (2.1) are often computed from basic principles of naval architecture. The hydrodynamic coefficients $a_{ij}(\omega)$ and $b_{ij}(\omega)$ usually are computed by using either slender body or wave scattering theory as discussed by van Oortmerssen (1976) for a variety of motion frequencies. Similarly, the wave forcing function is computed for a variety of wave frequencies and directions. Equation (2.1) is then solved for the structure displacement, velocity, and acceleration for each wave frequency and direction of interest. A consequence of this approach is that the floating body responds sinusoidally at a frequency equal to the wave frequency. Because an irregular wave field is characterized by a variety of frequencies and directions, equation (2.1) is solved for the range of wave frequencies and directions present in the wave field. Results of such analysis normally are computed for waves of unit amplitude and

summarized in terms of Response Amplitude Operators (RAOs), the ratios of individual motion responses to individual wave amplitudes, such as presented by Sugin (1983). Since the moored-object system is assumed linear, the motions of the floating structure in an irregular wave field can be determined by using the spectral response techniques which will be described in Chapter 5.

The frequency domain approach has been, and continues to be, widely used as it is simpler and requires less computational effort than time domain analysis. Its shortcomings, however, are fundamental. First of all, the mooring restraints must be linear; that is, the mooring restraint load must be a linear function of displacement. If the mooring restraints are nonlinear, nonnegligible subharmonic motions of the structure can occur at frequencies that differ from the forcing wave frequency (van Oortmerssen, 1976). Such motions are not simulated by frequency domain analysis. Second, as discussed by van Oorshot (1975), Loken (1979) and Chakrabarti (1980), floating bodies are subjected to a low frequency, slowly varying wave drift force. Many moored-object systems are characterized by relatively low natural frequencies in surge, sway, and yaw. This fact, coupled with the fact that damping is small at low frequencies, makes structure mooring prone to low frequency excitation. Soft mooring systems, such as spread moorings and single point moorings, are particularly susceptible to slowly varying drift forces. In fact, the first-order forces at wave frequencies often are neglected in the analysis of soft single point mooring systems. Obviously, the above-described frequency domain analysis cannot be used to evaluate floating body response from slowly varying wave drift force.

The shortcomings of frequency domain analysis are overcome by time domain analysis at the expense of added computational effort. Time domain analysis was developed by Cummins (1962) and has been described in detail by Bomze (1974) and van Oortmerssen

(1976, 1986). The interested reader is referred to the previously cited literature for detailed discussion of the applications of mathematical models to structure mooring problems.

2.2 Review of Related Work

Dynamic response and mooring forces prediction of a floating body in waves is not without precedence. Wilson (1959) showed that a fairly accurate solution for the motions of a floating structure in a monochromatic head or beam sea could be obtained by making assumptions which simplify the problem considerably. He assured that:

1. Linear wave theory applies.
2. The wave is not modified by the presence and motion of the structure.
3. The underwater portion of the structure is a prismoidal rectangular block having the same displacement as the actual structure.

The second assumption, known as the Froude-Krylov Hypothesis, produces a good approximation for floating structure motions, particularly in waves of long period, despite its obvious shortcomings of ignoring the effect of the wave diffracted around the immersed body and the wave radiating away from the body produced by the body motion. Vugts (1968) found that the Froude-Krylov hypothesis produces conservative wave exciting forces and motions for bodies with high stability.

Some investigators, as for instance Kaplan and Putz (1962), Leendertse (1963), Muga (1967) and Seidl (1973) linearized the elasticity characteristics of the mooring system. The restoring forces of the mooring system can then be incorporated in the hydrostatic term cX. The equation (2.1) of motion in the frequency domain can then be easily solved, with the restriction that only harmonic excitations can be used.

Others, including Kilner (1960) and Yang (1972) added non-linear terms to equation (2.1) to account for the restoring forces of the mooring system, and solved the equations by means of the method of equivalent linearization, assuming that the excitation was pure sinusoidal.

Investigations by Ogilvie (1964), Kim (1968), Newman (1970) and Wehausen (1971) treated the floating structure motion problem much more rigorously. The motion of the fluid was described by means of a velocity potential function which satisfied the Laplace equation and the boundary conditions at the water surface, at the bottom and at the interface between the immersed body and the water. However, their method leads to difficulties in the solution for mooring forces if the restraints are non-linear.

Garrison (1974) treated the problem of the wave induced motions of various three-dimensional objects by using Green's function methods developed by John (1950). Adee *et al.* (1974) treated the two-dimensional problems of moored floating objects in deep water, also using John's Method. In these investigations, only freely floating conditions were considered as an approximation of slackly moored conditions. These methods were fairly complicated and might not be easily used by many design engineers.

Ijima (1972) introduced two theories for analyzing the motions of a rectangular body due to waves in finite water depth. These theories assured small amplitudes of the waves and motions of the floating bodies. The solutions were exact, but they were cumbersome to calculate because of the infinite series involved. An approximate solution was proposed by Ito (1972). He showed that the infinite series could be omitted without serious decrease in accuracy and he advocated the advantage of approximate solutions over the exact ones: e.g., saving in computational work, clarity of physical meaning of each term in the solutions and versatility to various mooring conditions.

The work of Wilson and Awadalla (1971, 1973), Lean (1971) and Bomze (1974) was characterized by the assumption that the hydrodynamic coefficients a_{ij} and b_{ij} in equation (2.1) were independent of the frequency, so that this equation was regarded as an actual differential equation. The solution, which is found either by approximate analytical methods or by finite difference integration in the time domain may contain components with frequencies lower (subharmonic) or higher (superharmonic) than that of the forcing function.

Unfortunately, the assumption of constant hydrodynamic coefficients can not be justified. Especially in shallow water, these coefficients appear to be very sensitive to changes in frequency. Van Oortmerssen (1976) developed a mathematical model which was based on the equations of motion in the time domain as they had first been formulated by Cummins (1962). In the study, a time-domain description of the behaviour of the moored structure was used which took into account the frequency dependence of the fluid reaction forces.

A comprehensive survey (which focused on the dynamic response of mooring systems to waves) was presented by Casarella (1970) and Choo (1973), wherein the authors covered a wide territory, ranging from structure moorings and towed cable systems to unprogrammed models and purely static models. Another collected list of the existing programmed mathematical treatments and those employing exact analytical methods was given by Dillon (1973).

Natvig *et al.* (1976) discussed the linearized and non-linear methods for finding motion response for taut or slack moored floating structures. The linearized method was based upon a traditional frequency domain approach, whereas the non-linear method was based upon the time integration method as proposed by Newmark.

Bomze (1980) developed a numerical model for calculating the motions of a moored vessel inside the harbour at Acajutla and the forces in the vessel moorings. The numerical model was validated by comparing the calculated responses with those measured full scale in the Port of Acajutla and in hydraulic model tests. The investigation was performed on the existing harbour excited by an offshore wave spectrum and the resulting motions and mooring forces of a vessel moored inside the harbour. Excellent correlation was found between the calculated and measured results.

In Migliore's (1979) study, a three dimensional response theory had been developed into a computer model that could be applied to both slender and barge-like objects. The study investigated box-like shapes motion response for various drafts, periods of excitation and length-to-beam ratios (L/B) by utilizing both two-dimensional strip theory and three-dimensional theory. Results from the two theories were also compared to published experimental data from model tests. The objects analyzed were a 78 x 52 x 5-cm barge model, and a model of a 90 x 90 x 40-m floating box (1:100 scale). The comparison showed that strip theory did not predict reliable results for those L/B ratios; the three-dimensional theory, however, did agree very well with the model-responses reported.

Yamashita (1981) examined a practical formula for estimating the eddy-making component of the roll-damping moment exerted on the floating box-shaped body for comparison with the results obtained from forced-rolling experiments conducted on a two-dimensional model of the floating body. Because the box-shaped floating structures are characterized by small length-to-beam and large beam-to-draft ratios, a three-dimensional method utilizing pulsating pressure distributions was also used to calculate the motions and the wave-exciting forces of a shallow-draft box-shaped floating body in longitudinal and oblique waves. The results of the calculation were compared with

experiments on box-shaped models characterizing a floating dock.

Ikegami and Matsuura (1983) presented a unified analytical method for predicting of the motions of floating bodies under composite external loads such as mooring loads and loads due to floating bodies connected together. In order to verify the applicability of the method, model experiments were also carried out for several typical cases of moored or connected floating bodies. From the results obtained, it was verified that so far as the composite external loads could be approximated by linear dynamic system, this method appeared to have wide applicability to these types of bodies including the case of rigid connections between floating bodies.

An extensive model study was carried out by Chakrabarti (1983) to investigate the motions of a floating structure and the loads in its mooring line. To achieve this objective, a supertanker model, a small tanker and a barge model were tested. The models were moored in head seas with two linear springs. The spring constants were varied in the test series and the springs were pretensioned so that they never went slack. The tests included regular waves, wave groups and irregular waves. Based on the results obtained, he suggested that the mooring line load would increase with the stiffness in the mooring line and the damping in waves was larger than the damping of the structure in still water.

Maeda *et al.* (1986) conducted experiments on motions of a floating body in two-directional regular waves where the wave directions were perpendicular to each other. From the results obtained, it was indicated that in the case of the two directional waves, the direction and the amplitude of each component regular wave could also be obtained by the M.L.M. (Maximum Likelihood Method) and phase from F.F.T. (Fast Fourier Transform) analysis.

Kulsvehagen and Sandvik (1988) focused on a comparison between theoretical analyses and model tests for dynamic motions and mooring line dynamics carried out for a floating production system. The dynamic motions were calculated in the frequency domain and included both first and second order motions. The line dynamics, however, were analyzed in the time domain. They showed that the dynamic strengthening to the mooring lines due to first order motions was neither negligible for "high pretensions", nor dominating for low pretensions. Mooring lines were mostly dominated by restoring forces and less by drag forces.

A statistical analysis of floating structure motions induced by waves was carried out by Langley and McWilliam (1992). In the study, a new (closed form series) solution for the combined first and second order response probability density function had been derived in terms of the eigen values and eigen vectors of the matrix arising in a discretised Kac-Siegert analysis. The applicability of the method was investigated by comparison with time domain simulation. The result suggested that a good estimate of first term of the series which corresponded to the assumption that the first and second order responses were statistically independent could be obtained, and that a limited number of eigen values would suffice.

Nogata *et al.* (1993) introduced a method for calculating motions of floating bodies in waves, moored by elastic lines in a sea with a breakwater by using the method of velocity potential continuation. In that method they calculated a number of small size matrices instead of a large size matrix. The method was especially efficient with respect to the memory required for the calculation. Experiments for two floating bodies were also carried out. Comparisons between the measured and calculated values of amplitudes of the floating body motions and mooring forces were conducted.

Chapter 3

The Hydrodynamic Model

In this chapter, the hydrodynamic model of the floating dock is discussed. It includes the modelling principles, a description of the prototype, the design and fabrication of the experimental model, modelling of the mooring system, and model characteristics.

3.1 Modelling Principles

The essential requirements of any model are that it provides an adequate representation of the design environment and the structure itself. When the design environment is dominated by wave action and the inertia of the body, similitude between prototype and model is achieved using Froude scaling.

In order to scale from prototype to model, the laws of dynamic, geometric and kinematic similitude must be satisfied. Dynamic similarity is achieved by holding the ratio of the gravity force (assumed dominant for free surface flow) to inertia force constant. This results in a relationship between the model and prototype known as the Froude Number defined as;

$$\left(\frac{V_m^2}{g_m L_m} \right)^{0.5} = \left(\frac{V_p^2}{g_p L_p} \right)^{0.5}, \qquad (3.1)$$

where V is velocity, L is length, g is acceleration due to gravity, and the subscripts m and p denote model and prototype respectively. Geometric similarity is achieved by holding the ratio of prototype length to model length constant, as follows;

$$\frac{L_p}{L_m} = \alpha . \qquad (3.2)$$

Kinematic similarity is achieved by holding the ratio of prototype velocity to model velocity constant. From the Froude relationship above

$$(\frac{V_p}{V_m})^2 = \frac{L_p}{L_m} = \alpha . \qquad (3.3)$$

From these relationships, the following scales are determined:

Length scale	$L_p = \alpha L_m .$	(3.4)
Velocity scale	$V_p = \alpha^{1/2} V_m .$	(3.5)
Time scale	$T_p = \alpha^{1/2} T_m .$	(3.6)
Mass scale	$M_p = \alpha^3 M_m .$	(3.7)
Force scale	$F_p = \alpha^3 F_m .$	(3.8)

The choice of model scale depends mainly on the wave tank dimensions. In any case, the scale factor must allow accurate adjustment of such quantities as wave heights, wave periods, and pretension in mooring lines. It is also assumed that model forces and motion levels can be accurately measured and recorded.

3.2 Description of Prototype

The prototype floating dock consists of treated timber crib construction with six internal styrofoam billets. The crib consists of cross-ties, longitudinals, stringers, and decking which distribute the loading evenly. Timber skids located on the underside of the dock allow for storage and on shore towing. The billets are held in place by a number of slats which rest on the skids. The timber material is treated with a chromium-copper-arsenate (CCA) preservative to increase service life. All joints are secured using hot-dip galvanized M20 machined bolts of various lengths. A plywood skirt and plastic fender provide resistance to boat collisions. A series of wheel-guards and chocks provide protection against equipment sliding off the structure and provide supplementary berthing in addition to the mooring cleats. Four eyebolts are positioned near the corners to provide a means of lifting the structure from the water for repairs or winter storage. Information with respect to the number of members, dimensions and mass distribution is included in Table 3.1. The corresponding three-dimensional (3-D) view is shown in Figure 3.1.

The mooring system usually consists of mooring chains and gravity block anchors. In most cases, there are four lines per unit crossed underneath the dock. These are connected to eyebolts located at or near the water-line. When two or more docks are linked, a single mooring line can be shared and the weight and size of both chain and anchor can increase to offset the increased loads. Typically, chain with a mass of 14-15 kg/m is utilized. Figure 3.2 shows a typical mooring system arrangement.

3.3 Design and Fabrication of the Model

Table 3.2 shows the principal characteristics of the prototype and model. These values were computed using the modelling principles presented earlier in Section 3.1.

Table 3.1 Principle Characteristics of the Prototype

Unit	No. of Units	Length (mm)	Height (mm)	Width (mm)	Mass (kg)
Skids - Wide	2	7300	140	191	293
Skids - narrow	2	7300	140	140	215
Longitudinals (Level 1)	12	1020	191	140	245
Cross Ties (Level 1)	7	140	191	3000	421
Slats	24	38	13	2720	24
Billets	6	1020	610	2720	254
Longitudinals (Level 2)	2	8320	241	140	421
Cross Ties (Level 2)	9	140	241	2720	619
Longitudinals A (Level 3)	12	1020	191	140	245
Longitudinals B (Level 3)	4	318	191	140	26
Cross Ties A (Level 3)	7	140	191	3000	421
Cross Ties B (Level 3)	2	292	191	3000	251
Longitudinals A (Level 4)	2	8320	140	241	421
Longitudinals B (Level 4)	2	5540	140	89	104
Longitudinals C (Level 4)	2	3220	140	89	60
Cross Ties A (Level 4)	4	241	140	759	77
Cross Ties B (Level 4)	2	241	140	822	42
Decking	57	140	38	3000	682
Chocks - Short	8	305	62	140	16
Chocks - Long	2	1000	62	140	13
Railing	2	6410	89	140	120
Siding	2	8320	572	13	91
Lifting Hooks	4	----	----	----	24
Skid Bolts	14	----	331	----	9
Stringer Bolts	20	----	331	----	13
Through Bolts A	8	----	572	----	9
Through Bolts B	30	----	903	----	51

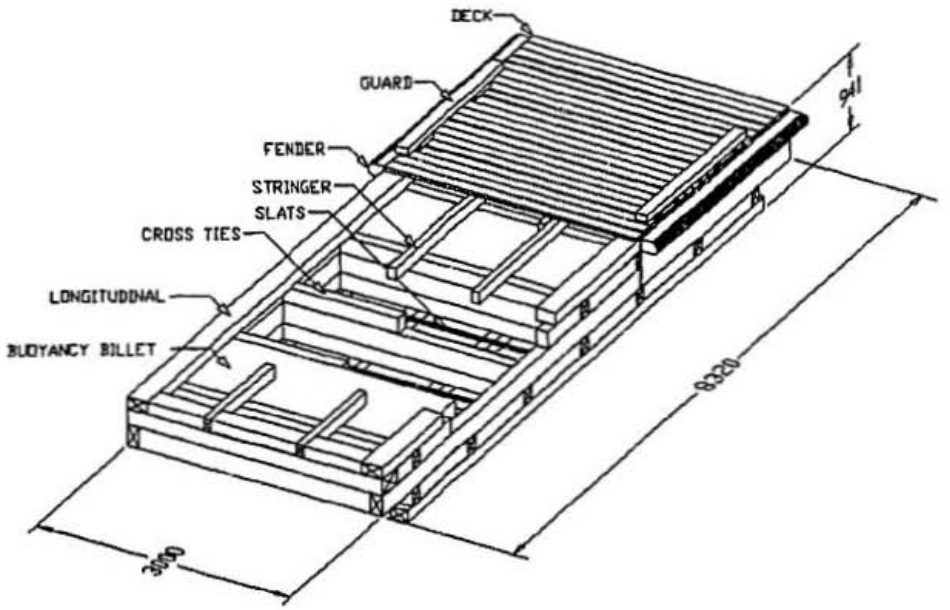

Figure 3.1 3-D View of Floating Dock

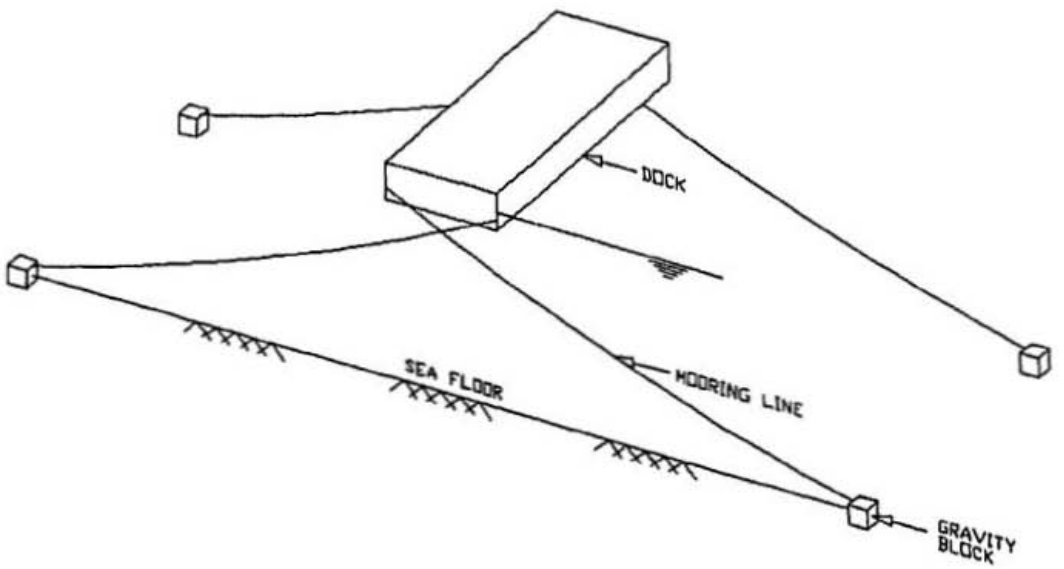

Figure 3.2 Floating Dock Mooring Arrangement

The geometric scale of the model to that of the prototype was determined on the basis of wave frequency range required in comparison to the range which the facility could generate. This resulted in a maximum scaling ratio of 1:9.

Table 3.2 Modelling Parameters

Parameter	Prototype	Model
Length (m)	8.320	0.924
Width (m)	3.000	0.333
Height (m)	0.941	0.105
Draft (m)	0.358	0.039
Centre of Gravity (m)	0.559	0.062
Metacentric Height (m)	2.940	0.327
Radius of Gyration (m)	0.910	0.101
Moment of Inertia ($kg.m^2$)	4329	0.073
Mass (kg)	5169	7.121

The experimental model was fabricated from maple wood which had the same density as the prototype's (750 kN/m^3). The styrofoam for the billet was chosen in the same way to meet the characteristics required.

Each member of the model was cut first and then assembled with wood glue. Eyebolts were placed near the four corners of the model at the water-line to simulate actural mooring attachments.

3.4 Modelling of the Mooring System

A flexible chain of uniform weight per unit length forms a catenary when supported by the two ends. From Alexandrov (1971) the main features of the catenary form are:

1. The horizontal component of tension is constant along the length of line
2. Minimum line tension is equal to the horizontal component of tension
3. Tension at a given point along the line is linearly related to the y-coordinate of the point.

As the tension at the upper end of the mooring line increases, the line geometry progresses from the slack mode (the mooring line makes tangential contact with the seabed applying no vertical force component to the anchor) to the taut mode (the mooring line contacts the seabed at some finite angle thus applying a vertical force component on the anchor).

Field information indicated that 25-mm diameter galvanized chain with a unit mass of 14.3 kg/m is commonly employed as mooring lines. Recommendations from a previous study (Morey, 1993) stated a 5:1 (horizontal distance to vertical distance) mooring line scope should be utilized to reduce motion response and that alternative mooring configurations be examined. As indicated in Figure 3.3, three different configurations (crossed non-connected, crossed connected and non-crossed) were investigated. The free floating condition provides a base which can be utilized to determine the drift forces. The crossed non-connected imitates the configuration utilized in previous studies while the crossed connected and non-crossed design provide alternatives to the crossed non-connected system.

In previous studies, it was also suggested that the chain utilized in the model tests be replaced by a spring system. This would model the global restoring force characteristics of a catenary mooring system. Based on theoretical formulae (Tsinker, 1986), the

mooring forces for the prototype were determined as a function of excursion (Figure 3.4). As shown in Figure 3.5, the seaward and leeward mooring lines exhibit a stiffness of 1.2 and -1.2 kN/m respectively. This translates to a global stiffness of 2.4 kN/m, with an initial pretension of 14.6 kN (Appendix A). Each model mooring line was constructed from a series of elastic bands and calibrated to provide the required stiffness. The lines were attached to eyebolts located near the four corners of the model at the water line.

3.5 Model Characteristics

3.5.1 Mass Properties

Since, each member of the model was made from maple which had the same density as the prototype's, the total mass of the model was very close to the required model mass. Detailed calculations for the centre of gravity, moment of inertia and radius of gyration of the model are presented in Appendix B based on the theoretical formulae (Bhattacharyya, 1978).

3.5.2 Metacentric Height (Inclining Test)

An inclining experiment was used to determine the transverse metacentric height. This involved moving a small mass across the deck under controlled conditions, and recording the resulting angle of inclination.

The dock was free-floating for this test, therefore none of the mooring lines were set in place. The transverse centerline was ascertained and the dock was marked off in 2-cm intervals, starting from the centre point out to each side of the dock. A Shaevitz "Angle

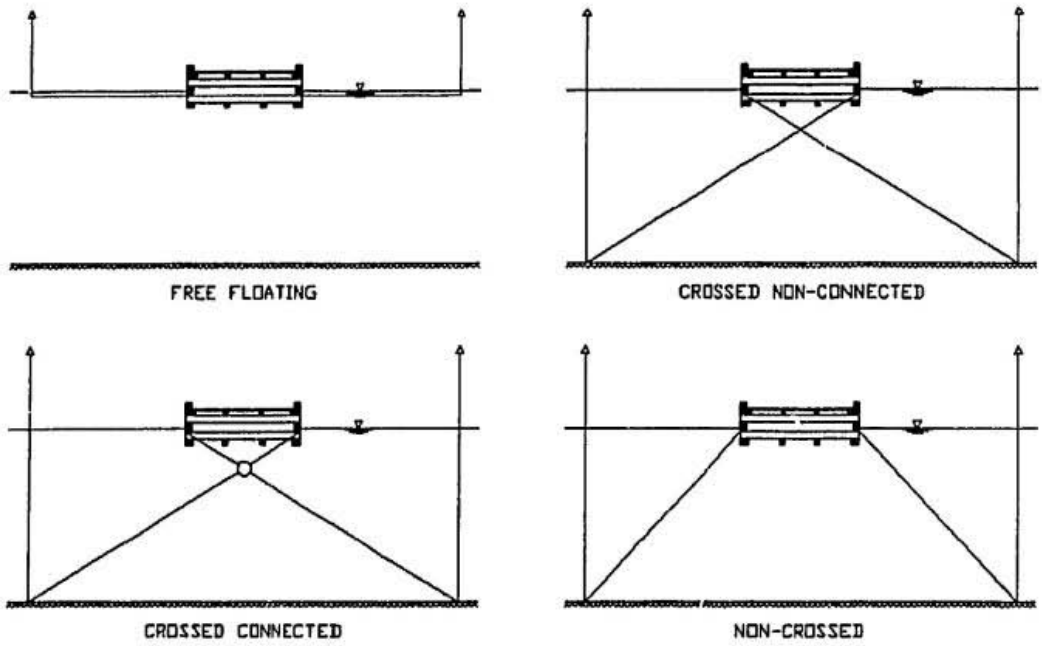

Figure 3.3 Mooring Configurations

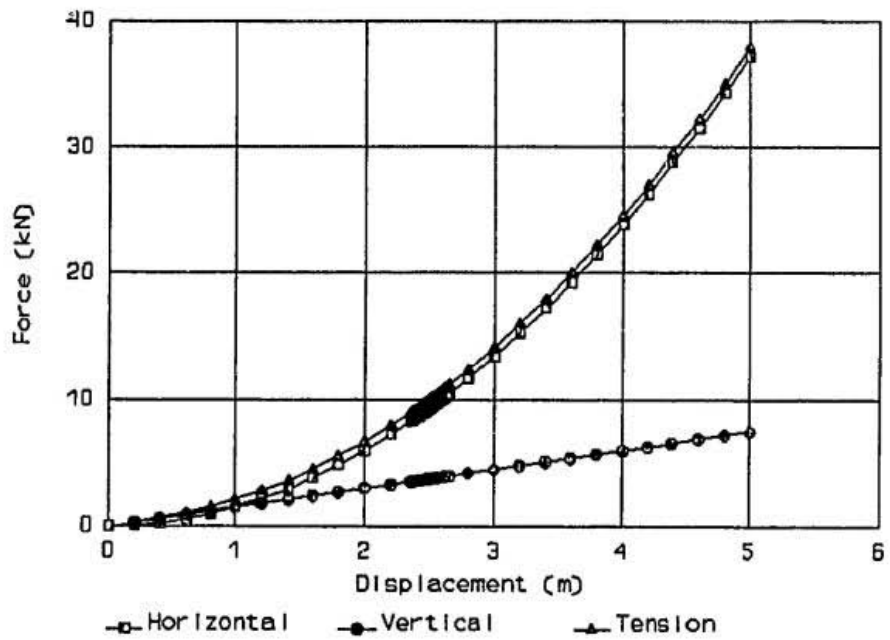

Figure 3.4 Horizontal and Vertical Mooring Forces

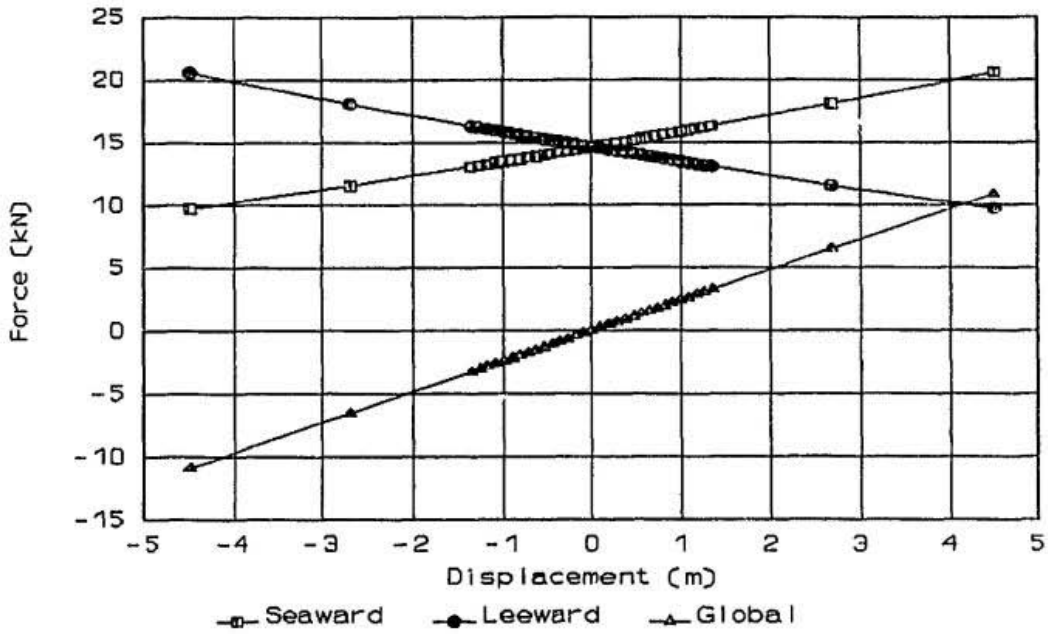

Figure 3.5 Global Stiffness

Star" digital protractor, was centred on the dock so as not to interfere with the stability of the dock and to provide visible readings for the angle of inclination. Figure 3.6 shows the model floating dock before testing.

A 200-g weight was first placed 6 cm from the centre point and the angle of inclination was recorded. The weight was then shifted 2 cm and the angle of inclination was again recorded. This was repeated as the weight was shifted across the dock and back and then across to the other side and back to the centre point to check the zero reading. The measured data can be found in Table 3.3. Figure 3.7 shows the test set-up for the inclining experiment.

Shifting the weight causes the dock's centre of gravity to move out a small distance towards the side to which the weight has been shifted. The metacentric height can now

Figure 3.6 Model Floating Dock Before Testing

Table 3.3 Inclining Experiment Data

INCLINING EXPERIMENT		
Distance Displaced **d** (cm)	Angle of Inclination. σ (°)	Change in Inclination σ_{AV} (°)
0	0.14	-
6	0.53	-
8	0.64	0.11
10	0.74	0.10
8	0.64	0.10
6	0.54	0.10
0	0.14	-
0	0.14	-
-6	-0.21	-
-8	-0.32	0.11
-10	-0.42	0.10
-8	-0.33	0.09
-6	-0.22	0.11
0	0.14	-
Average Difference	2	-	0.1025

Figure 3.7 Test Set-up for the Inclining Test

be calculated using the average displacement, the average change in angle of inclination, and following simple trigonometric calculation:

$$GM = \frac{W_s \cdot d}{W_m \cdot \tan\sigma_{AV}} \tag{3.9}$$

where W_s = mass of small weight being used

d = average distance displaced

W_m = mass of the model

σ_{AV} = average change in angle of inclination

The metacentric height determined from the inclining test is 0.318 m while the value calculated from the prototype is 0.327 m.

3.5.3 Natural Periods

To ascertain the natural period of the model dock, several decay tests were conducted. The natural periods of oscillation in heave and roll motions of the free floating (unmoored) and heave, roll and sway motions of the non-crossed (moored) model were measured in the wave tank using a potentiometer. The natural period was calculated from the record as the average of the peak-to-peak values of the positive (as well as negative) peaks. The values obtained from the analysis are included in Table 3.4, while Figure 3.8-3.12 indicate the decay curves for roll, heave and sway respectively.

Table 3.4 Decay Test Results (Full Scale)

Mooring Configuration	Roll (s)	Heave (s)	Sway (s)
Calculated	1.07	1.77	N/A
Free Floating	1.87	2.43	N/A
Non-crossed	1.81	2.22	18.40

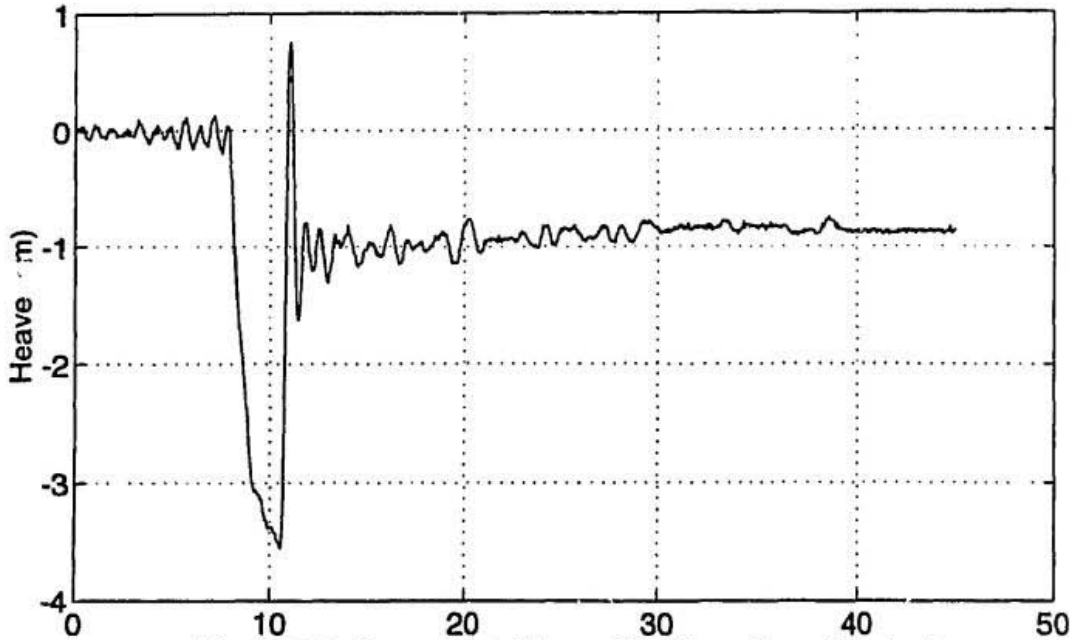

Figure 3.8 Decay Test: Heave Vs. Time (Free Floating)

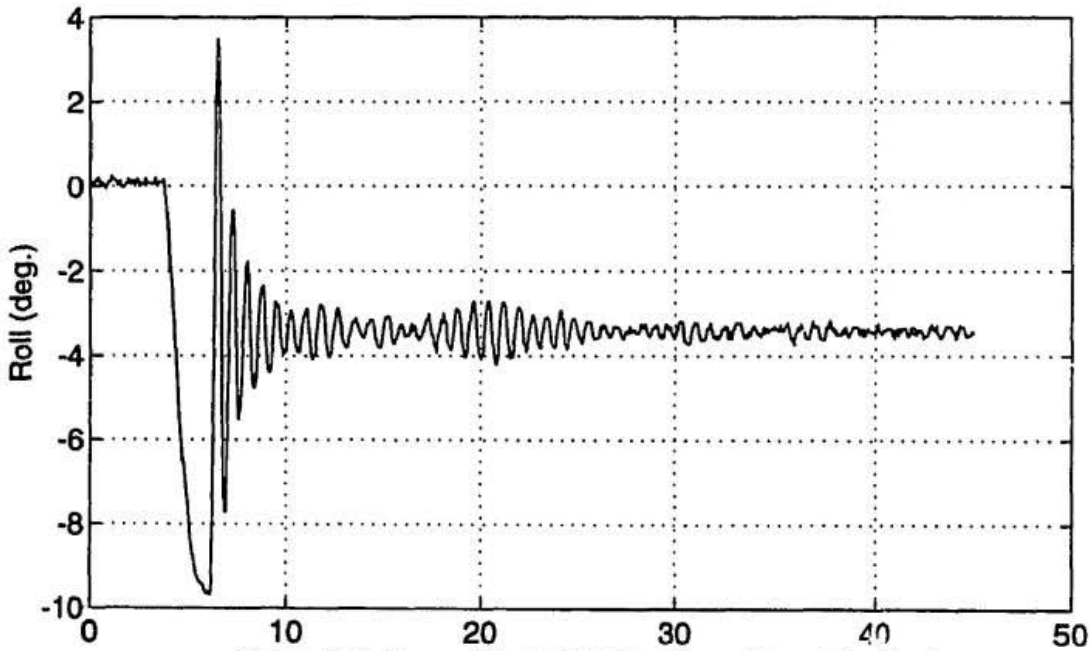

Figure 3.9 Decay Test: Roll Vs. Time (Free Floating)

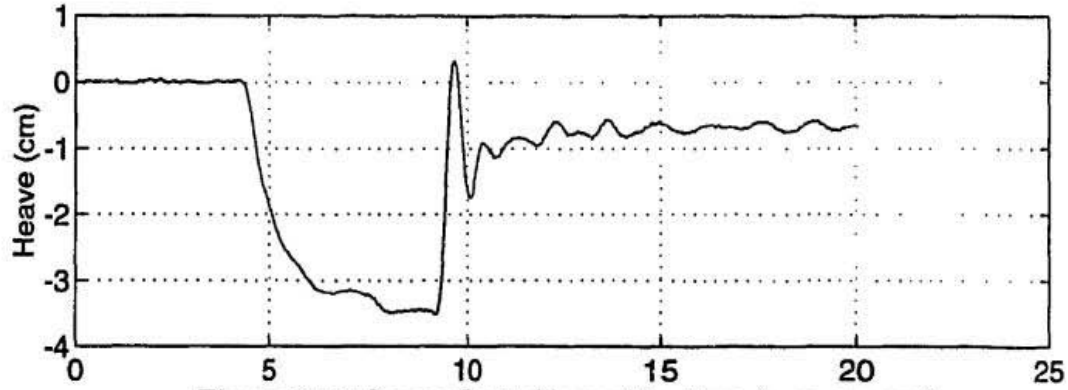

Figure 3.10 Decay Test: Heave Vs. Time (non-crossed)

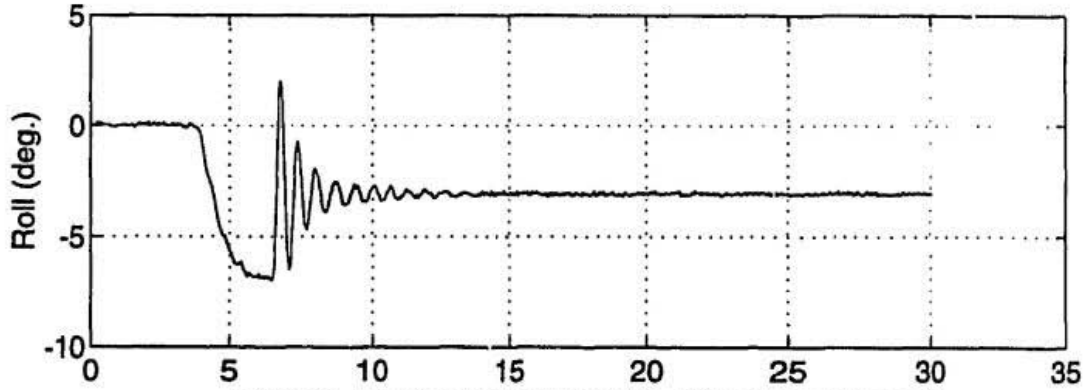

Figure 3.11 Decay Test: Roll Vs. Time (non-crossed)

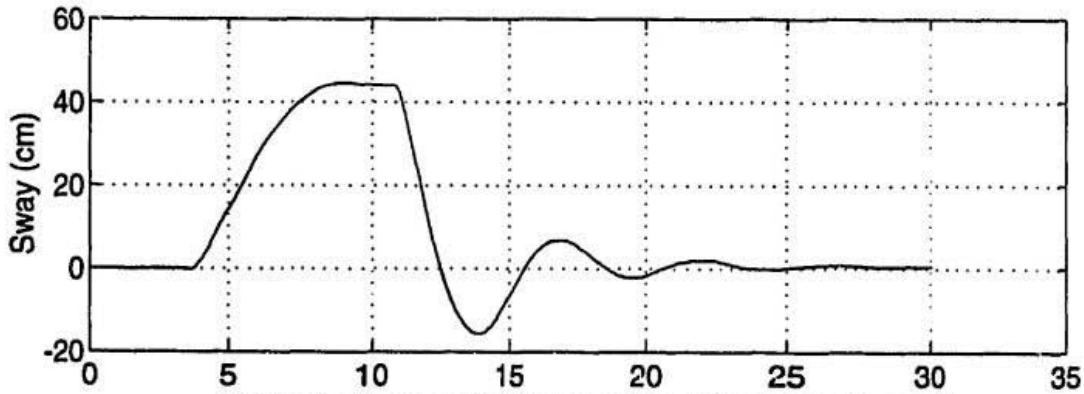

Figure 3.12 Decay Test: Sway Vs. Time (non-crossed)

Chapter 4

Experimental Study

This chapter deals with the dynamic testing of the experimental model. The objective of the dynamic testing is to determine the dynamic response of the structure. Dynamic testing is very advantageous because it can be used to diagnose the response of the structure in a number of configurations and thus be used as a tool to assess design changes.

4.1 Experimental Arrangement

A brief description of the equipment used in the experiments is presented in this section. First the wave maker system is described, then the instrumentation and calibration of the model structure, and finally data acquisition and analysis.

4.1.1 The Wave Maker System

The wave tank facility at Memorial University is 58.27 m in length, 4.57 m in width and 3.04 m in depth (see Figure 4.1). However, the hydraulically operated piston type

wave generator, installed behind the wave board at one end of the tank, restricts the actual operating length to approximately 54.74 m. Wave filter plates fixed directly to the front of the wave generator are used to reduce the presence of cross tank oscillation in the tank. The walls of the tank are of reinforced concrete construction, while the wave board is fabricated from aluminum with a water tight teflon seal along its sides and bottom. Several large viewing windows are conveniently located in one of the tank's walls, enabling visual and photographic analysis of a model's response at surface and sub-surface elevations.

Both regular and irregular waves spectra can be generated by the translatory motion of the wave board. The force capability of the hydraulic actuator is specified at 48.8 kN and limits the actual operating depth to about 2.13 m or less. Wave heights and frequencies are governed by the motions of the actuator. Electronic control for the board is provided from the control room through an MTS closed-loop servo-controlled system with error detection and compensation applied through an LVDT feedback loop. Figure 4.2 shows the wave tank facility.

4.1.2 Instrumentation and Calibration

The experimental model was installed almost at mid length of the wave tank for easy access. One capacitance type wave probe, located on the side of the model, was used to measure the incoming waves; this was designated A for ease of reference. The probe is equipped with a capacitance meter to convert the change in capacitance (resulting as the waves interact with the probe) to a d.c. voltage and was calibrated in units of distance in centimetres per volt. Therefore, the changes in wave elevation above or below the mean water level could be computed. Calibration of the probe was undertaken prior to the start of tests each day and after the wave generator ran for 10 minutes to

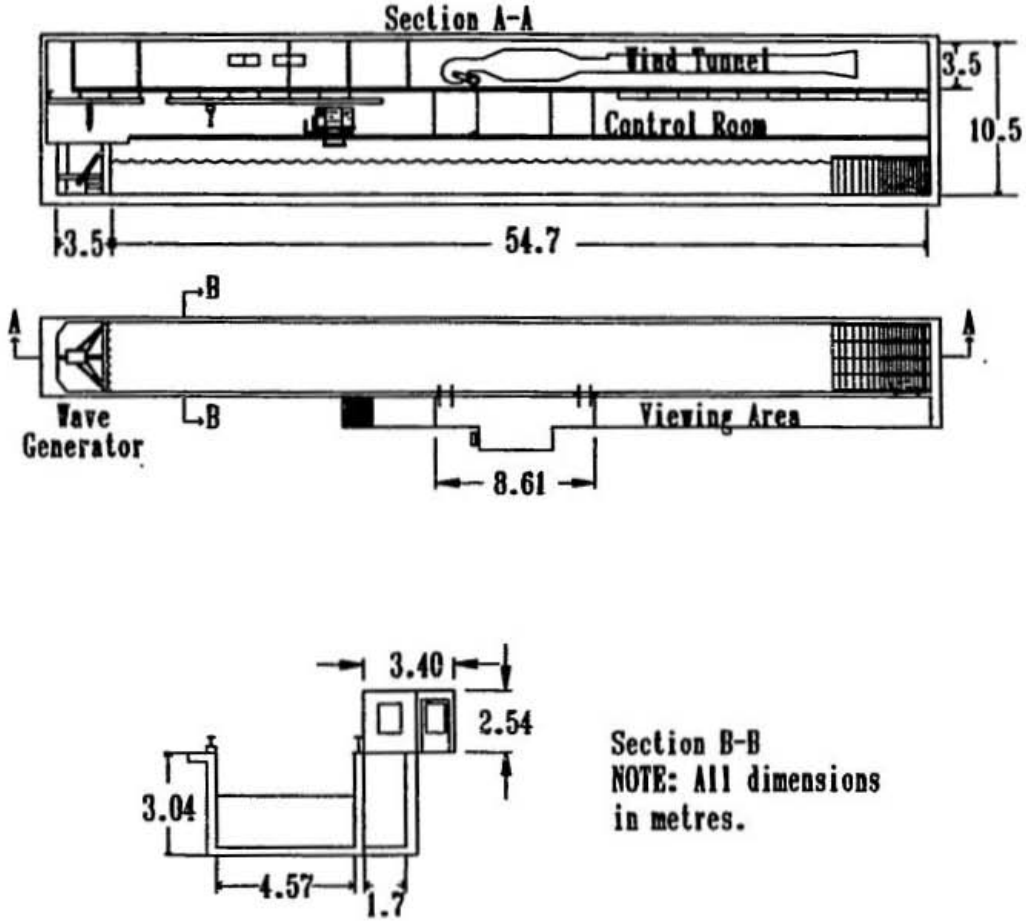

Figure 4.1 Dimensions Of Wave Tank Facility

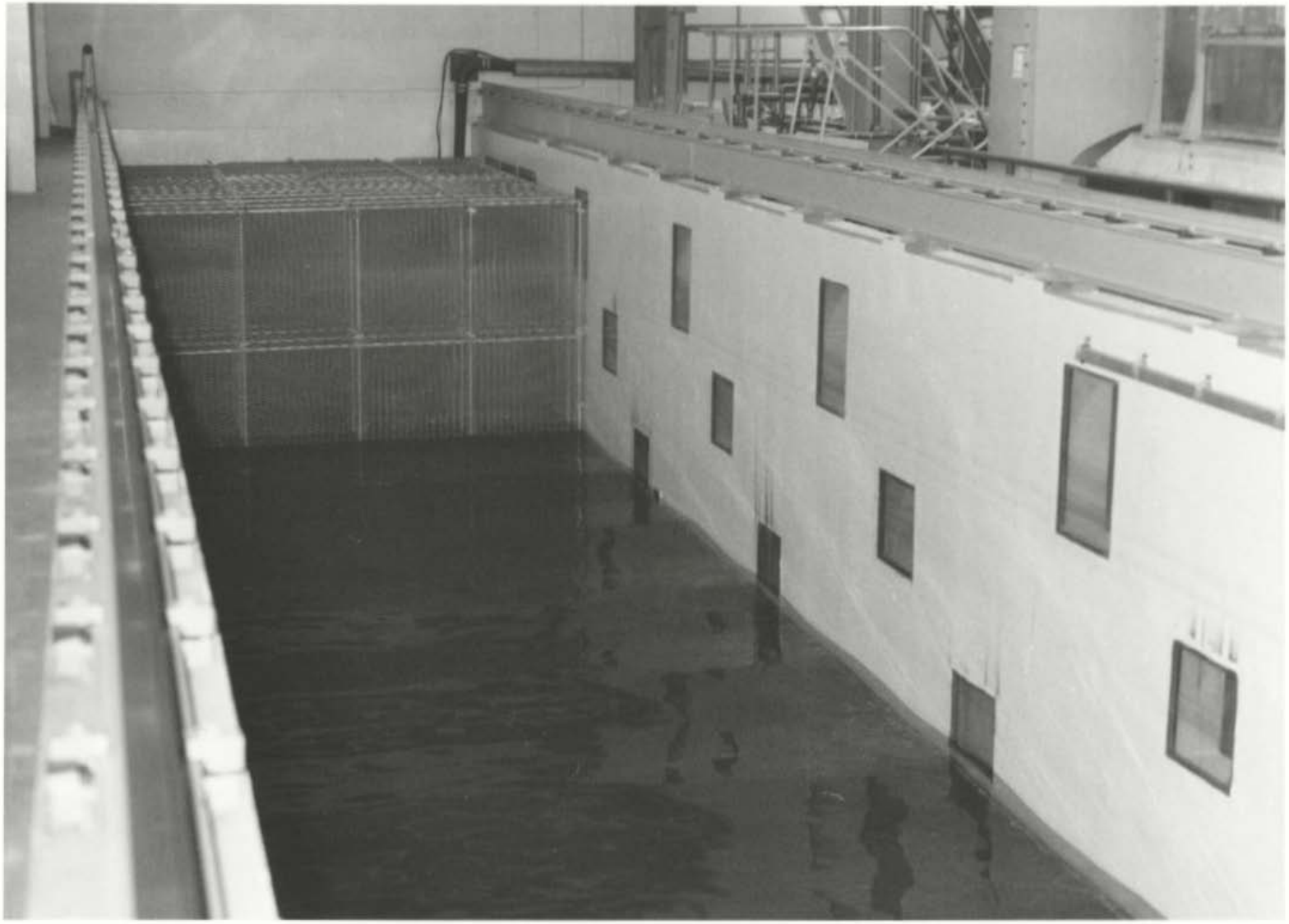

Figure 4.2 View of Wave Tank Facility

eliminate any water temperature differential. The probe was calibrated by raising and lowering the probe $\pm$ 5 cm about its zero position and measuring the voltage across the wires at each 1 cm interval of immersion. For control, calibration of the probe was also done at the completion of each day's tests. No significant difference between daily calibrations occurred and linearity correlation coefficient was always 0.999 or better.

Three rotary transducers were used to measure the motions of the structure; these were designated B, C and D for ease of reference. The rotary transducers were calibrated in still water by adding weights in known increments to the string attached to the transducer. Transducer B was used to measure the sway motion of the model. It was placed approximately 1 m above the water level and was connected to the centre of gravity of the model structure with a string. Transducers designated C and D were also installed approximately 1 m above the water but with two lines which were connected to the centre of the windward and leeward side of the structure; these were used to measure the heave and roll motions respectively.

The force on the mooring line was measured using a ring dynamometer and a strain-gauge conditioner. To prevent difficulties due to waterproofing, the load cell connected to the mooring line was arranged so that they remained well above the water level. The strain-gauge conditioner measured the deflection in the load cell when a load was applied. The load cell was calibrated in the same way as for the rotary transducers. Figure 4.3 indicates the location of the instrumentation and Table 4.1 provides a description of what each position measured.

4.1.3 Data Acquisition and Analysis

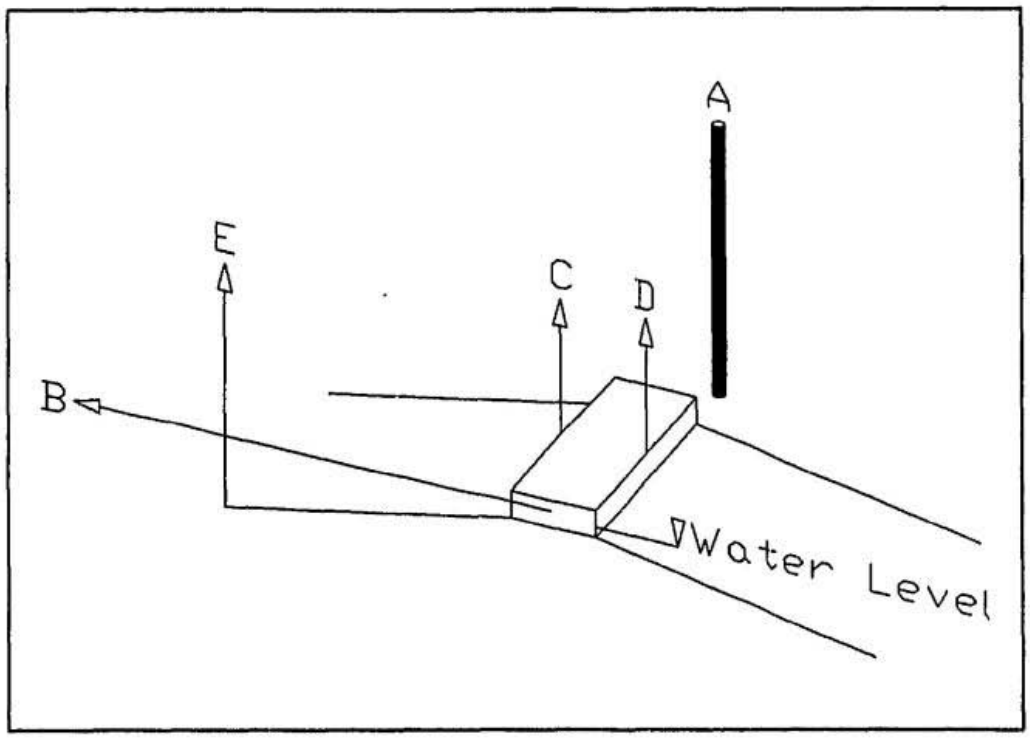

Figure 4.3 Instrumentation Layout

Table 4.1 Data Acquisition Positions

Position	Channel Description
A	Capacitive Wave Probe - Wave Height (channel 1)
B	Rotary Transducer - Sway (channel 2)
C	Rotary Transducer - Heave/Roll (channel 3)
D	Rotary Transducer - Heave/Roll (channel 4)
E	Ring Dynamometer - Mooring Force (channel 5)

Data acquisition and much of the subsequent analyses were carried out in the control room of the wave tank facility, with some on-line equipment producing real-time analyses. Each signal was passed through a charge amplifier where it was calibrated and then through a low pass filter to remove extraneous noise occurring above the maximum cut-off frequency desired. Voltage measurements from the probe meters were filtered in a similar manner. Subsequently, all data were digitized with an analog-to-digital converter. Then the digitized data were transmitted via an Ethernet link system to the Faculty's UNIX for storage. The UNIX system provided additional analysis packages, decreased computation times and increased mass storage capability in a universal format. Figure 4.4 shows the entire experimental equipment installation.

4.2 Experimental Procedure

4.2.1 Test Programme

The model tests were carried out in regular and irregular waves in beam seas with sway, heave, roll and mooring force being recorded. For regular wave tests, the wave heights ranged from 4.4 to 8.9 cm and the wave period varied from 1 to 5 sec. This is equivalent to a full scale wave height range of 0.4 to 0.8 m and a wave period range of 3 to 15 sec. Extremely soft springs were used to allow motions on the dock to be measured as a free floating object for this series of tests.

Another series of irregular wave tests were also conducted using a JONSWAP spectrum for three different mooring configurations, in addition to the free floating case. The wave period used was 10 sec. full scale at a wave height of 0.4 m. A detailed test programme is shown in Table 4.2 and Table 4.3.

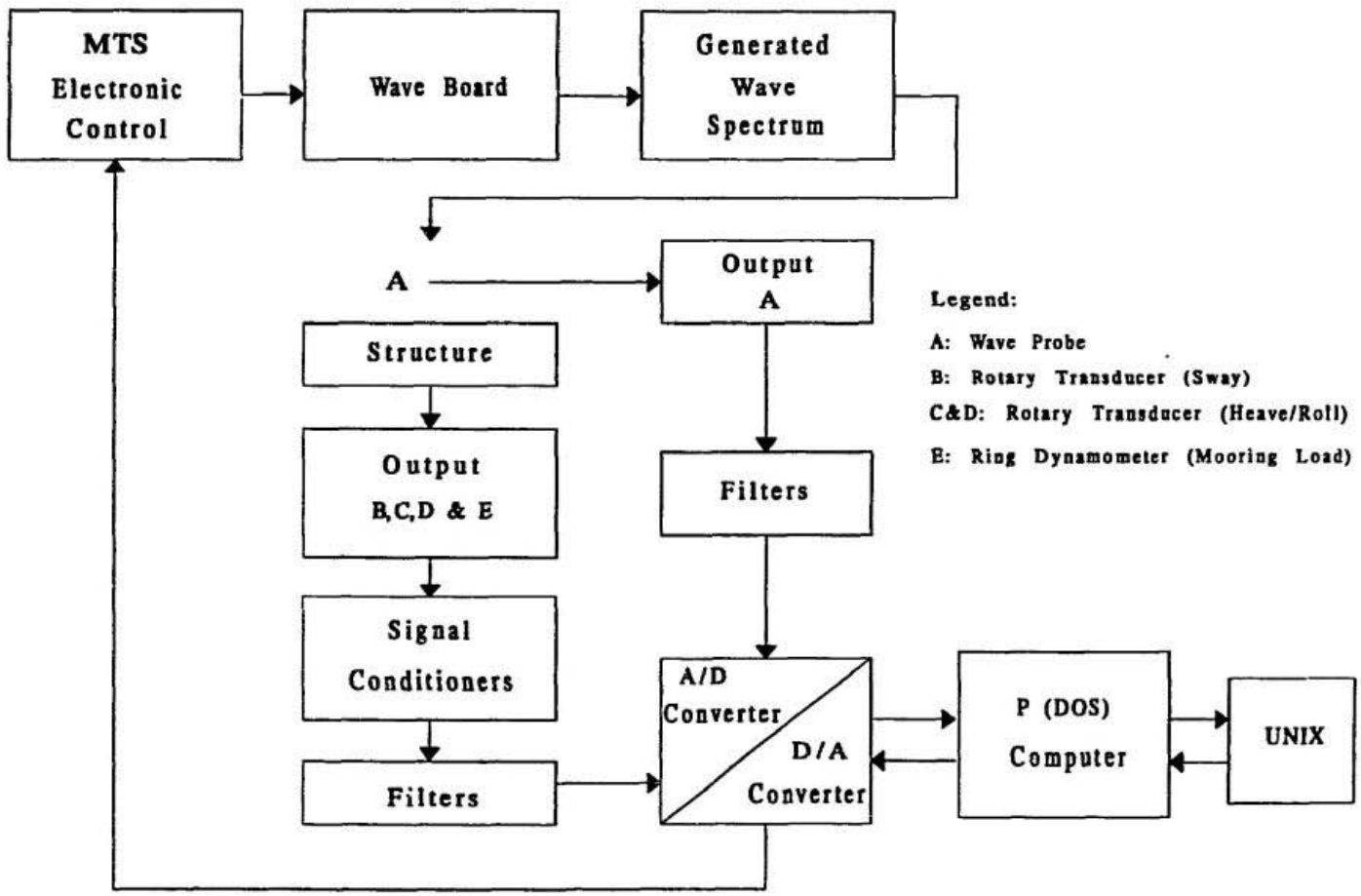

Figure 4.4 Experimental Circuit

Table 4.2 Test Matrix for Regular Waves (Free Floating, Full Scale)

TEST SERIES	FREQUENCY H_z	PERIOD s	HEIGHT m	DEPTH m
A1M1	0.333	3	0.40	4.5
A2M1	0.167	6	0.40	4.5
A3M1	0.111	9	0.40	4.5
A4M1	0.083	12	0.40	4.5
A5M1	0.067	15	0.40	4.5
B1M1	0.333	3	0.60	4.5
B2M1	0.167	6	0.60	4.5
B3M1	0.111	9	0.60	4.5
B4M1	0.083	12	0.60	4.5
B5M1	0.067	15	0.60	4.5
C1M1	0.333	3	0.80	4.5
C2M1	0.167	6	0.80	4.5
C3M1	0.111	9	0.80	4.5
C4M1	0.083	12	0.80	4.5
C5M1	0.067	15	0.80	4.5

4.2.2 Wave Simulation

Since a true sea state is a random phenomena, where waves are continually changing in

Table 4.3 Test Matrix for Irregular Waves (Full Scale)

TEST SERIES	FREQUENCY H_z	PERIOD s	HEIGHT m	DEPTH m
Free Floating				
D1M1	0.100	10	0.40	4.5
D2M1	0.100	10	0.40	4.5
D3M1	0.100	10	0.40	4.5
Crossed Non-connected				
D1M2	0.100	10	0.40	4.5
D2M2	0.100	10	0.40	4.5
D3M2	0.100	10	0.40	4.5
Crossed Connected				
D1M3	0.100	10	0.40	4.5
D2M3	0.100	10	0.40	4.5
D3M3	0.100	10	0.40	4.5
Non-crossed				
D1M4	0.100	10	0.40	4.5
D2M4	0.100	10	0.40	4.5
D3M4	0.100	10	0.40	4.5

height, length and breadth, it is impossible to characterize or define it exactly in terms of its pattern or shape. It is possible, however, to define the sea in terms of the total energy it contains. Furthermore, it is also possible to define the contributions made to its total energy by each of its components. That is, for any given sea state, a wave energy spectrum may be developed which expresses the wave energy density distribution of the sea as a function of wave frequency or as a function of wave number. This is the basis upon which the irregular wave spectra were simulated by the wave maker system.

A JONSWAP spectrum was used in this study to examine the behaviour of the structure under realistic sea conditions. The spectral density equation used to define the spectrum is:

$$S(f) = \frac{A}{f^5}\exp\left(-\frac{B}{f^4}\right)\gamma^{\alpha}, \qquad (4.1)$$

where

$$\alpha = \exp\left[\frac{-(f - f_o)^2}{2\sigma^2 f_o^2}\right],$$

$$\sigma = 0.07 \qquad for\ f \le f_o,$$

$$\sigma = 0.09 \qquad for\ f > f_o,$$

$$A = \frac{5 H_s^2 f_o^4}{16\,\gamma^{1/3}} \qquad for\ 1 < \gamma < 4,$$

$$B = 5\frac{f_o^4}{4}.$$

and where f_o is the peak frequency, H_s is the significant wave height, and γ is a peak

enhancement factor. (The values used for H_s, γ and f_o in the experiments are 0.4 m, 3.3, and 0.1 H_z, respectively.)

4.2.3 Irregular Wave Simulation

To simulate an irregular wave spectrum, the following five steps were carried out:

1. Having defined the desired wave spectrum, the spectral density curve was calculated using equation (4.1). For the JONSWAP spectrum, the inputs included the peak frequency, f_o, the significant wave height, H_s, and the peak enhancement factor, γ.

2. An initial digitized time-history drive signal was calculated by the computer. This signal was subsequently converted to its analog form to drive the wave board and create an irregular sea state in the wave tank.

3. An achieved wave spectrum was then calculated from the waves generated by the initial drive signal. This was achieved by recording the time history data with a wave probe located on the side of the model structure. The data were then manipulated by the computer software to create an achieved wave spectrum.

4. Any discrepancies between the desired wave spectrum and the achieved wave spectrum was corrected via an iterative process. Variations between the two were determined by the computer, and additional drive signals were created until the differences between the desired and the achieved were within acceptable limits.

5. The corrected time history drive signal was applied to the wave board to create irregular waves for model testing. Collected data were finally manipulated by the

system application software to create spectral density information.

4.2.4 Wave Structure Interaction

As a result of the frequency resolution desired, the memory limitation of the data acquisition computer at the wave tank facility, and sufficient data required to allow transfer function analysis, the duration for the wave test was set at ten minutes. Three separate runs, for each test, were carried out for the sake of accuracy. (A set of three runs lasted approximately two hours). This was accomplished by running a test for ten minutes (while collecting data), then stopping the test and allowing the water in the tank to settle. The water was considered settled, when the wave probe readings showed a particular pre-determined value. Figure 4.5 shows the structure in still water, and Figure 4.6 shows the structure as it is acted upon by waves.

Figure 4.5 Model Floating Dock in Still Water

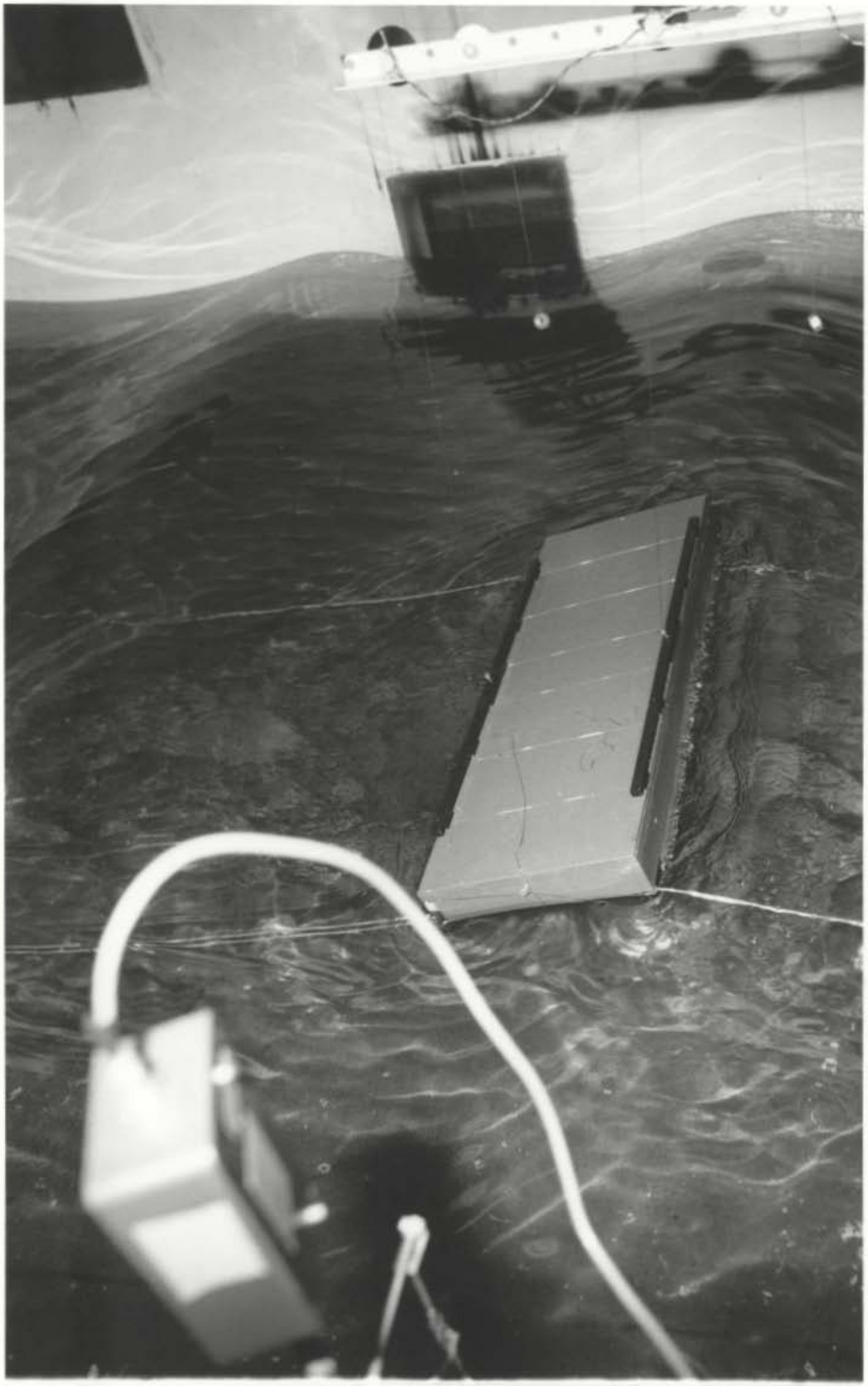

Figure 4.6 Model Floating Dock Acted upon by Waves

Chapter 5

Analysis of Results and Discussion

The signals obtained from the experimental investigation described in chapter 4, were analyzed to extract relevant information. All of the test results are presented and discussed below. Spectral analysis techniques were used to obtain an overview of the response of the floating dock in the frequency domain.

5.1 Analysis of Experimental Results

5.1.1 Model Response in Regular Waves

Body motions of a floating structure obey Newton's law and can be described as either translational or rotational. Assume a sinusoidal force (given in Equation 5.1) is applied to a single degree of freedom system described by Equation (2.1)

$$F(t) = F_a e^{i\omega t} . \qquad (5.1)$$

Taking a particular integral of the form

$$X = X_a e^{i\omega t}, \tag{5.2}$$

and substituting this with Equation (5.1) into (2.1) gives

$$\begin{aligned} X &= \frac{F_a[c - (M + a)\omega^2 - ib\omega]}{[c - (M + a)\omega^2]^2 + b^2\omega^2} e^{i\omega t}, \\ &= H(\omega) F_a e^{i\omega t}. \end{aligned} \tag{5.3}$$

where function $H(\omega)$ is the complex transfer function between force and motion amplitude. Taking the real parts of Equations (5.1) and (5.3) also yields the governing equation and solution to be of the form

$$(M + a(\omega))\ddot{X} + b(\omega)\dot{X} + cX = F_a \cos\omega t, \tag{5.4}$$

$$\begin{aligned} X &= \frac{F_a\{[c - (M + a)\omega^2]\cos\omega t + b\omega \sin\omega t\}}{[c - (M + a)\omega^2]^2 + b^2\omega^2}, \\ &= \frac{F_a}{\{[c - (M + a)\omega^2]^2 + b^2\omega^2\}^{1/2}} \cos(\omega t - \varepsilon), \end{aligned} \tag{5.5}$$

where

$$\varepsilon = \arctan\left[\frac{b\omega}{c - (M + a)\omega^2}\right]. \tag{5.6}$$

The total solution for Equation (2.1) and (5.1) is made up of the sum of the complementary function representing the transient response ($F(t) = 0$) and the particular integral describing the steady state response of Equations (5.3) or (5.5).

From structural dynamics theory, it is known that an arbitrary function $X(t)$ can be related to its frequency composition $X(\omega)$ by the well-known Fourier transform through

the pair of equations

$$X(t) = \int_{-\infty}^{\infty} X(\omega)e^{i\omega t}\, d\omega\,, \tag{5.7}$$

and

$$X(\omega) = \frac{1}{2\pi}\int_{-\infty}^{\infty} X(t)e^{-i\omega t}\, dt\,. \tag{5.8}$$

If the system described by Equation (2.1) is excited by a sinusoidal force of amplitude F_a and frequency ω, then the response $X(t)$ is

$$X(t) = H(\omega)F_a e^{i\omega t}\,. \tag{5.9}$$

Summation by integration of many such sinusoidal components will lead to the equation

$$X(t) = \int_{-\infty}^{\infty} H(\omega)F_a(\omega)e^{i\omega t}\, d\omega\,, \tag{5.10}$$

with $F_a(\omega)$ written as

$$F_a(\omega) = \int_{-\infty}^{\infty} F(t)e^{-i\omega t}\, dt\,. \tag{5.11}$$

Comparing Equation (5.7) and (5.10) then yields

$$X(\omega) = H(\omega)F_a(\omega)\,. \tag{5.12}$$

It is also known that the impulse response function can be related to the transfer function $H(\omega)$ through a Fourier transform. If the system is excited by the unit impulse then $F_a(\omega)$ in Equation (5.11) becomes unity and the dynamic system response will be the impulse response function $h(t)$. Equation (5.10) then becomes

$$h(t) = \int_{-\infty}^{\infty} H(\omega)e^{i\omega t}\, d\omega\,. \tag{5.13}$$

Its Fourier transform is

$$H(\omega) = \frac{1}{2\pi}\int_{-\infty}^{\infty} h(t)e^{-i\omega t}\,dt. \qquad (5.14)$$

Thus the impulse response function and transfer function form a Fourier transfer pair.

5.1.2 Response to Irregular Waves

Two fundamental assumptions are made in the calculation of the response of the structure to irregular waves:

1. The response of a floating body to any individual regular wave component is a linear function of the amplitude of this component, that is, the response is linearly proportional to the wave excitation (i.e., the wave amplitude).

2. The response of the structure to any individual wave component is independent of its response to any other wave component, that is, the sum of the responses of the structure to a number of simple sinusoidal waves is equal to the response of the structure to the sum of the waves.

These assumptions are quite reasonable if the wave condition is moderate and only moderate responses are expected. Numerous model experiments for the similar structures have shown that, although in principle the responses are nonlinear, nonlinearities can be ignored in practice (i.e., Reference 5).

Motions of a floating structure in irregular waves can be determined by means of the following steps:

1. For the particular wave condition in which the structure is to operate, a suitable

wave spectrum is chosen.

2. The wave spectrum is calculated to a base of wave frequency interested.

3. A plot is obtained in which the ordinates represent the amplitude of motion to a base of encountering frequency distribution. This can be obtained analytically or by experimentation with regular or irregular waves in a tow tank.

4. The diagram obtained in step 3 is modified so that the ordinates represent the ratio of the square of the motion amplitude divided by the square of the wave amplitude. This diagram is termed the *response amplitude operator* or simply the transform function.

Where wave-induced structure motions and mooring forces can be assumed to be linear and frequency-dependent, their statistical values can be determined by spectral response analysis techniques. This requires that a transfer function, or response amplitude operator be determined. Basically there are two transfer functions that are involved in deriving a body motion response from wave elevation, (1) from wave elevation to wave force, and (2) from wave force to motion. The spectral density function $S_x(f)$ defined in the frequency domain can be evaluated from a random process $X(t)$ defined in the time domain by applying the Fourier transfer as follows

$$S_x(f) = \frac{1}{N}\sum_{n=1}^{N}\frac{2}{T}\left|\int_0^T X(t)\exp^{-i2\pi ft}dt\right|^2, \qquad (5.15)$$

where N is the total number of data points and T is the record length.

There are basically three parameters involved in a spectral analysis:

1). The length of each record to be analyzed

2). The time interval between successive data points in a record

3). The number of intervals along the frequency axis at which the spectra value is estimated

The response of a single degree of freedom dynamic system to random excitation can be obtained by extending the ideas of random processes to the examination of system response. Consider the governing equation given by Equation (2.1) and take $F(t)$ to denote a stationary random excitation force with frequency spectrum $S_f(\omega)$ and auto-correlation function $R_f(t)$. The dynamic system response X will then have some corresponding frequency spectrum $S_x(\omega)$ and auto-correlation function $R_x(t)$. The latter can be rewritten here as

$$R_x(\tau) = \lim_{T\to\infty} \frac{1}{T} \int_0^T X(t)X(t+\tau)dt. \qquad (5.16)$$

The response of a dynamic system to random excitation is equivalent to the system responding to a series of impulses of magnitude $F(\tau)\delta\tau$ with the response equation given by

$$X(t) = \int_0^t F(\tau)h(t-\tau)d\tau. \qquad (5.17)$$

replacing t-τ by τ_1 yields

$$X(t) = \int_0^\infty F(t-\tau_1)h(\tau_1)d\tau_1, \qquad (5.18)$$

and also

$$X(t+\tau) = \int_0^\infty F(t+\tau-\tau_2)h(\tau_2)d\tau_2, \tag{5.19}$$

by replacing t with $t+\tau$ and τ_1 by τ_2 in Equation (5.18). Substituting Equations (5.18) and (5.19) into (5.16) yields

$$\begin{aligned} R_x(\tau) &= \int_0^\infty h(\tau_1) \int_0^\infty h(\tau_2) * \\ &\quad \lim \frac{1}{T} \int_0^T F(t-\tau_1)F(t+\tau-\tau_2)dt d\tau_2 d\tau_1 \\ &= \int_0^\infty h(\tau_1) \int_0^\infty h(\tau_2)\, R_f(\tau-\tau_2+\tau_1)d\tau_2 d\tau_1 . \end{aligned} \tag{5.20}$$

But

$$\begin{aligned} S_x(\omega) &= \frac{1}{\pi} \int_{-\infty}^\infty R_x(\tau)e^{-i\omega\tau}d\tau \\ &= \frac{1}{\pi} \int_{-\infty}^\infty e^{-i\omega\tau} \int_0^\infty h(\tau_1) * \\ &\quad \int_0^\infty h(\tau_2)R_f(\tau-\tau_2+\tau_1)d\tau_2 d\tau_1 d\tau . \end{aligned} \tag{5.21}$$

since $h(\tau) = 0$ for $t<0$, this equation becomes

$$\begin{aligned} S_x(\omega) &= \frac{1}{\pi} \int_{-\infty}^\infty h(\tau_1)e^{i\omega\tau_1} \int_{-\infty}^\infty h(\tau_2)e^{-i\omega\tau_2} \\ &\quad * \int_{-\infty}^\infty R_f(\tau-\tau_2+\tau_1)e^{-i\omega(\tau-\tau_2+\tau_1)}d\tau d\tau_2 d\tau_1 \\ &= \int_{-\infty}^\infty h(\tau_1)e^{i\omega\tau_1} \int_{-\infty}^\infty h(\tau_2)e^{-i\omega\tau_2} \\ &\quad * \frac{1}{\pi} \int_{-\infty}^\infty R_f(\tau_3)e^{-i\omega\tau_3}d\tau_3 d\tau_2 d\tau_1 , \end{aligned} \tag{5.22}$$

where $\tau_3 = \tau - \tau_2 + \tau_1$. Substituting Equations (5.13), (5.14) and (5.21) into Equation (5.22) yields

$$S_x(\omega) = H(-\omega)H(\omega)S_f(\omega). \qquad (5.23)$$

Inspection of the form of $H(\omega)$ in Equation (5.3) shows that $H(-\omega)$ and $H(\omega)$ are complex conjugates permitting Equation (5.23) to be written as

$$S_x(\omega) = |H(\omega)|^2 S_f(\omega), \qquad (5.24)$$

where $S_f(\omega)$ = spectral density function of water surface elevation [m^2-s]

$S_x(\omega)$ = spectral density function of structure response [amplitude^2-s]

and $|H(\omega)|^2$ = response amplitude operator, as follows:

(a) For rolling motion, $|H(\omega)|^2 = (\theta/h)^2$ [deg^2/m^2]

(b) For heaving motion, $|H(\omega)|^2 = (H/h)^2$ [m^2/m^2]

(c) For swaying motion, $|H(\omega)|^2 = (S/h)^2$ [m^2/m^2]

in which θ, H, S and h are amplitudes for roll, heave, sway and incident waves, respectively.

5.2 Experimental Results

Graphical outputs of the experimental results are presented for:

(1) Spectral density functions of the signals measured with the wave probe,

(2) Response of the model to a train of regular waves, and

(3) Response of the model to irregular waves (JONSWAP spectrum)

Wave Probe Signals

As discussed in Chapter 4, Section 4.2.3, five steps were necessary to achieve the

desired wave spectrum. Figures 5.1-5.3 show the measured spectrum at the wave probe designated A using the Welch method. This method involves averaging across adjacent records to obtain more reliable spectral estimates than the conventional Fast Fourier Transform (FFT) method in which no smoothing is done. Confidence limits are also available which can be seen from Figure 5.2.

Structural Response to Regular and Irregular Waves

Before the irregular wave tests were carried out, it was necessary to examine the behaviour of the structure to a train of regular waves. These tests were desirable to test the workability of the instrumentation system. Besides, since the motion of the model to regular waves is not as complex as that due to irregular waves, these tests were done, bearing in mind the shape of the response curve(s) that should be expected.

The RAO obtained from the double amplitude of motion divided by the wave height for roll, sway and heave motions are given in Figures 5.4-5.6 for all regular and irregular waves. In the free floating configuration, the values for drift force were recorded for the regular wave experiments and are shown in Figure 5.7. Mooring forces were also measured and computed for irregular wave tests for the crossed non-connected, crossed connected and non-crossed configurations. The results have been included in Figure 5.8. Appendix C shows the time history plots for all the input waves and structure responses as well as mooring forces.

5.3 Discussion of Results

Dynamic Model Response

When comparing the model motion periods determined by calculation with those obtained from the decay tests for the free floating case, there is an error of 45% and 27% for roll and heave respectively. It is generally accepted that the roll period is not significantly affected by added mass. However, when determining the mass moment of inertia for roll the virtual mass of water entrained in the dock structure should be taken into consideration. It is expected this would increase the period by a factor proportional to the square root of a mass factor (Gaythwaite, 1990). It is also accepted that the heave period is a function of the added mass, and is generally increased by the square root of the added mass factor. If an added mass factor of 2 is applied to the calculated values the corresponding roll and heave periods would be 1.89 and 2.49 seconds respectively. These values would then equate to errors of only 1% and 3% for roll and heave respectively. An added mass factor in the range of 1.5 to 2.0 is very reasonable due to the shape and structure of the design. Comparison between the free floating and non-crossed mooring configurations reveals that the mooring lines decreased the periods of roll, heave and sway.

The significance of determining these periods of oscillation can be seen when considering the motion response. With respect to heave and roll, when the incoming waves have a sufficient height and length they can excite resonant motions when approaching the natural periods of oscillation. For non-crossed test series, the wave periods range from full scale values of 3 to 15 secs as compared to natural periods of 1.81, 2.22 and 18.40 seconds for roll, heave and sway respectively. This indicates that roll and heave motion responses in the 3 second range could be affected.

Motion Response

A comparison for the motion responses between regular and irregular waves indicates

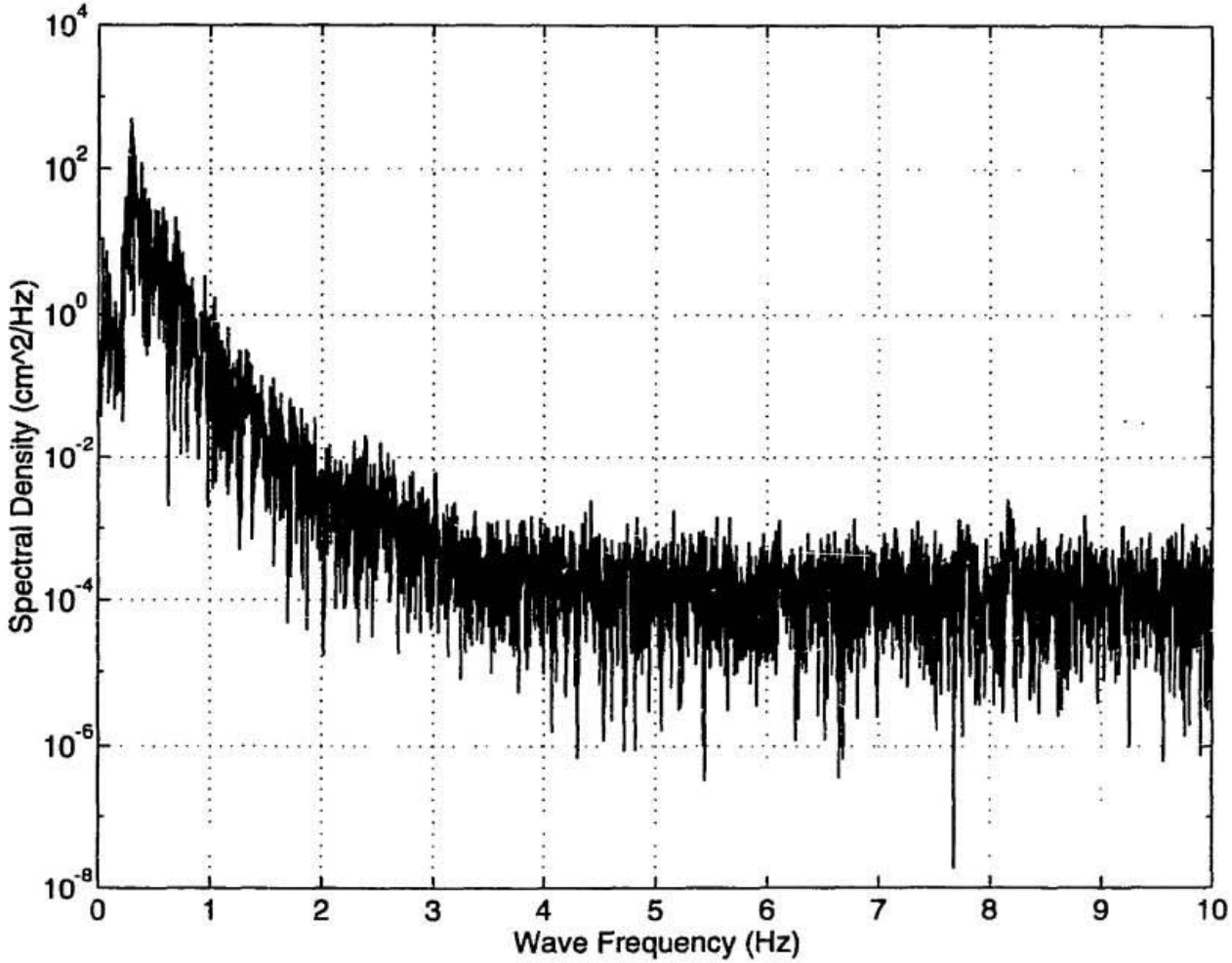

Figure 5.1 Measured Input Wave Spectrum at Wave Probe

(Using Conventional FFT Method)

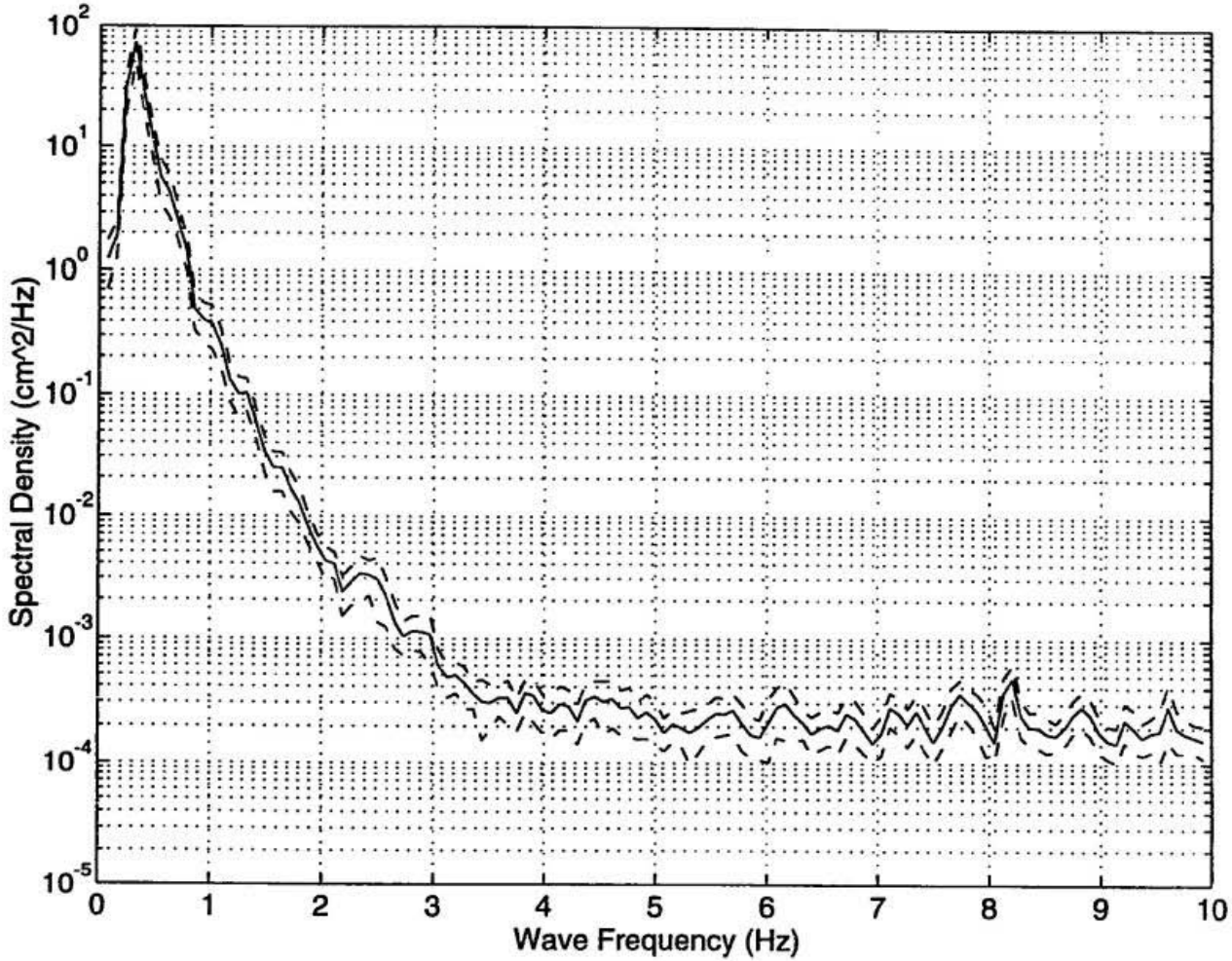

Figure 5.2 Measured Input Wave Spectrum at Wave Probe with 95% Confidence Limits (Using Welch Method)

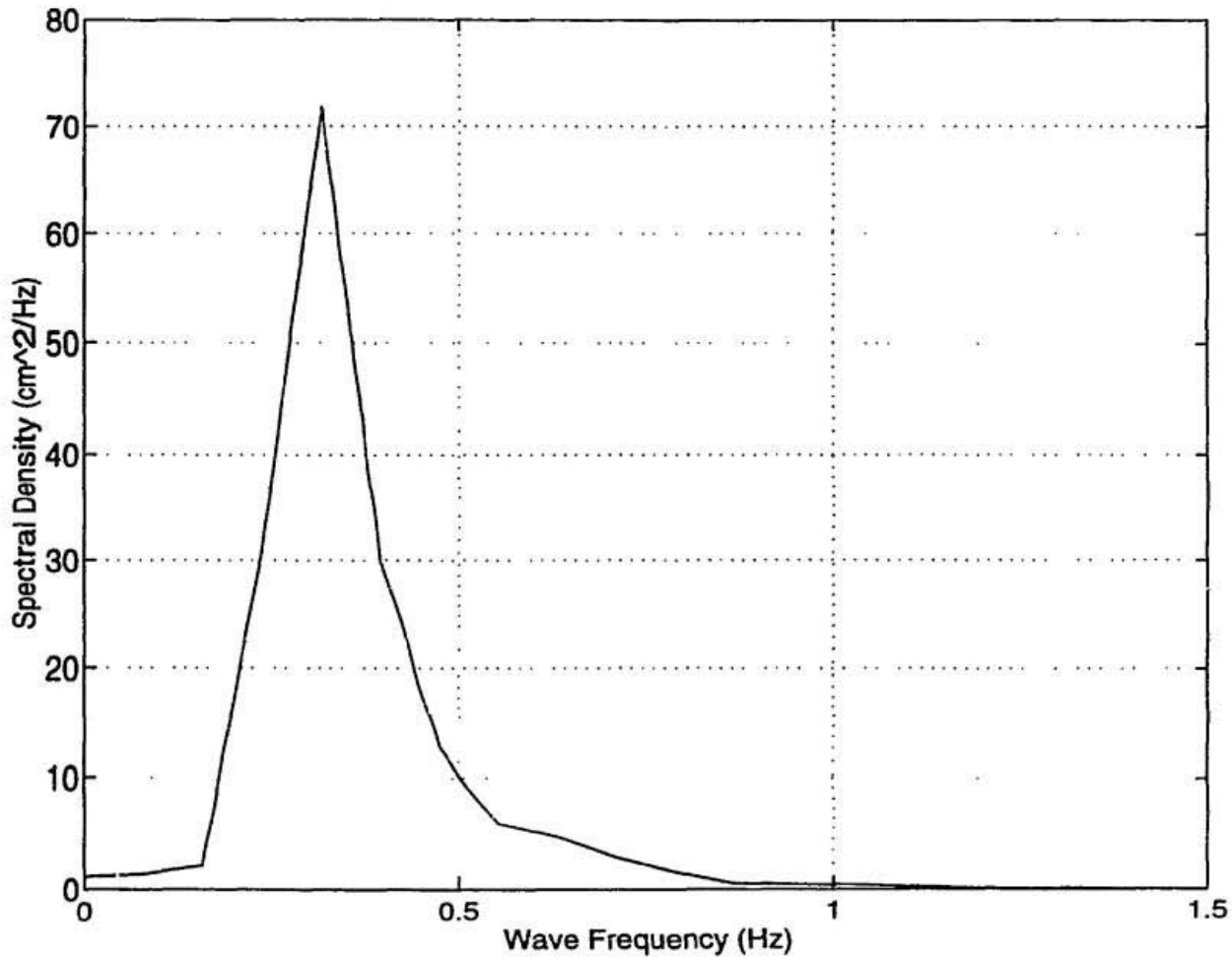

Figure 5.3 Measured Input Wave Spectrum over the Frequency Range of Interest

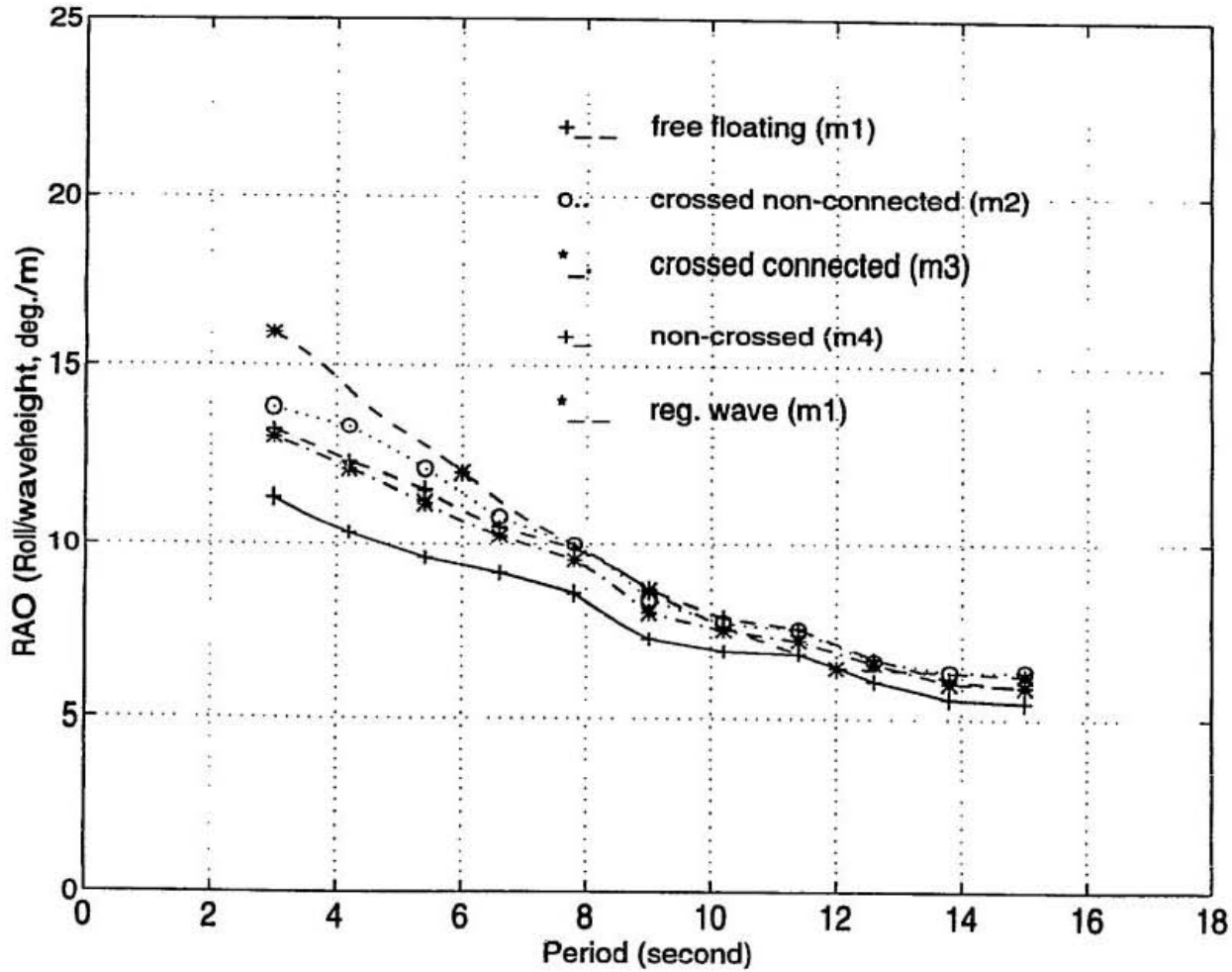

Figure 5.4 Roll Motion Response Vs. Wave Period

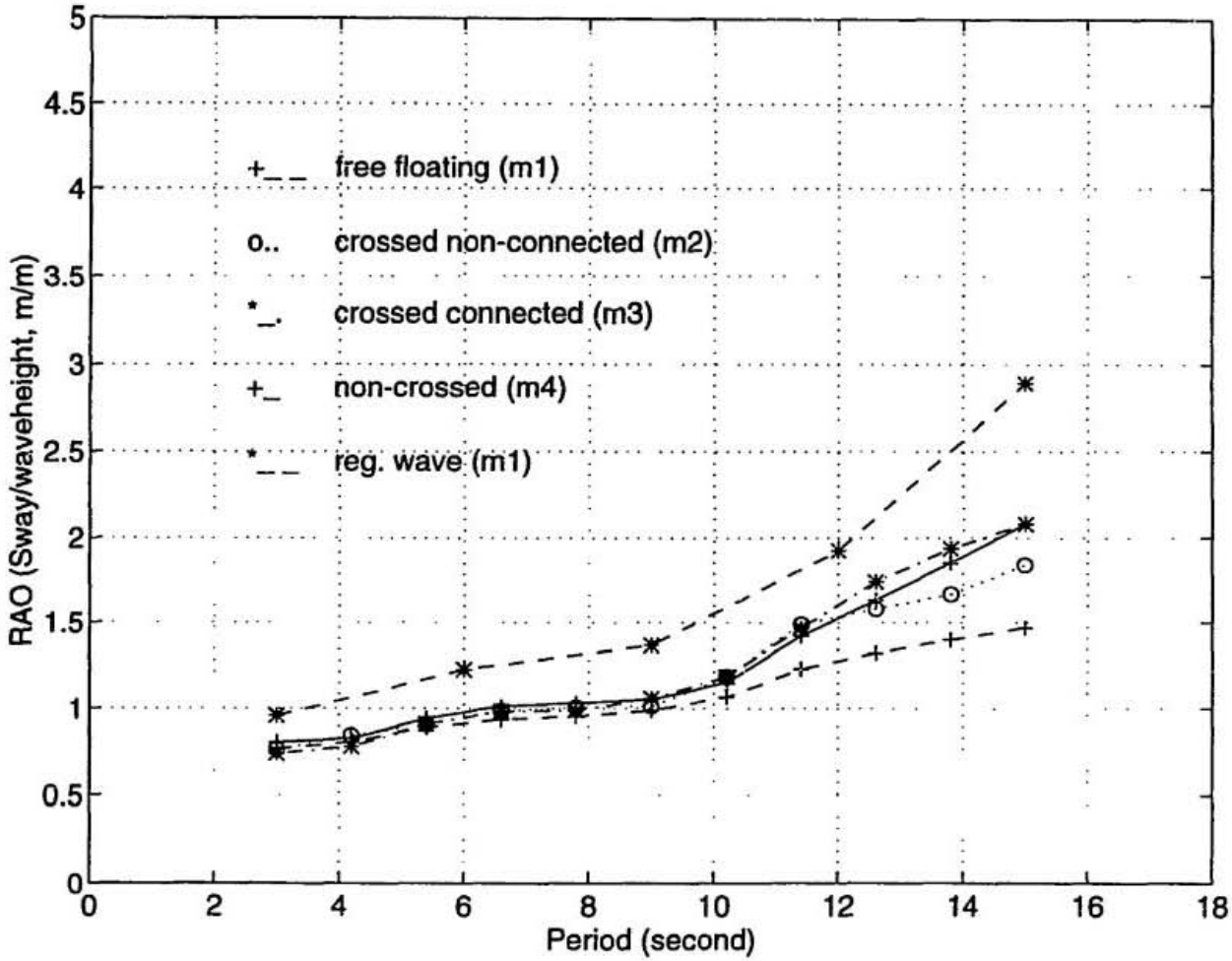

Figure 5.5 Sway Motion Response Vs. Wave Period

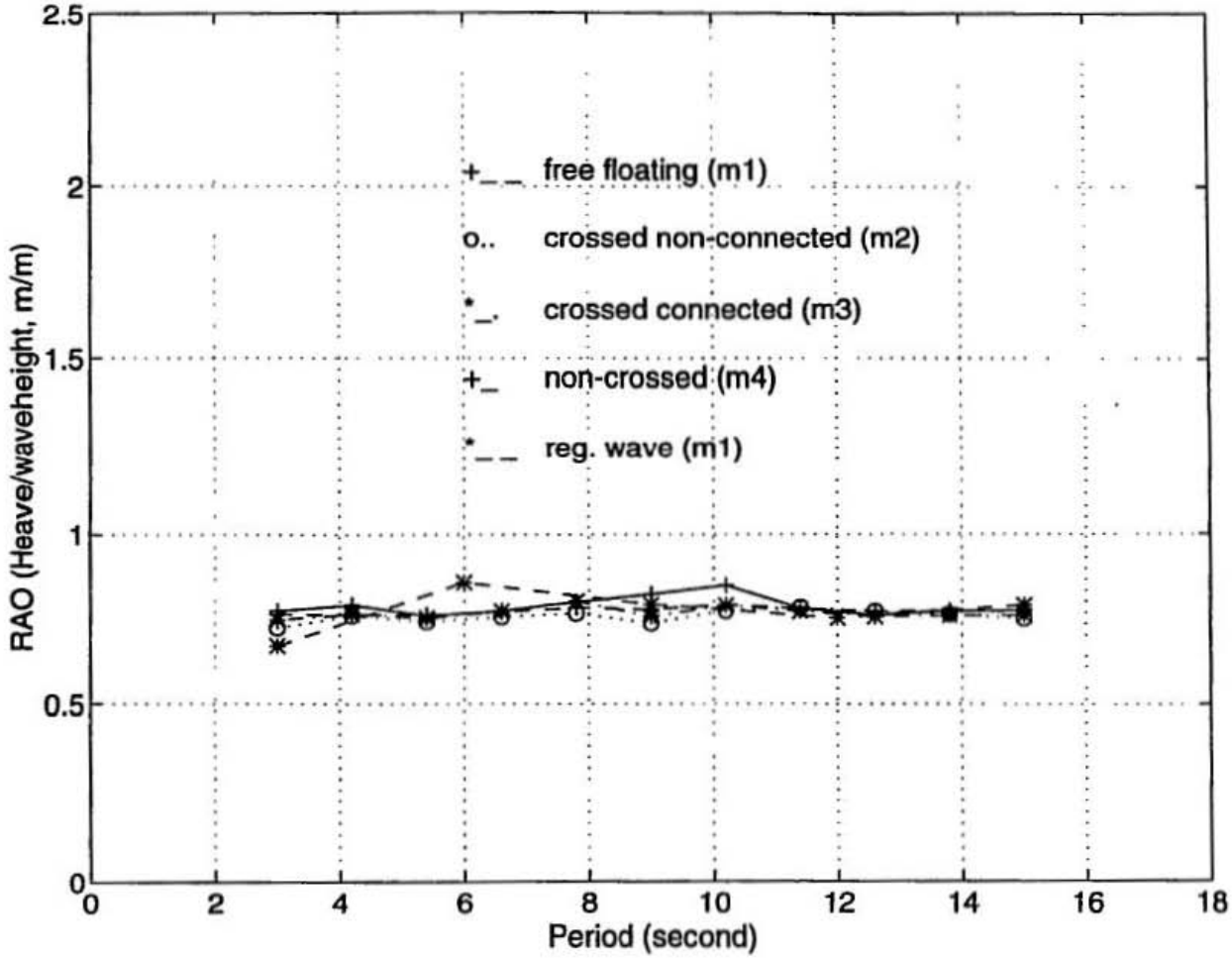

Figure 5.6 Heave Motion Response Vs. Wave Period

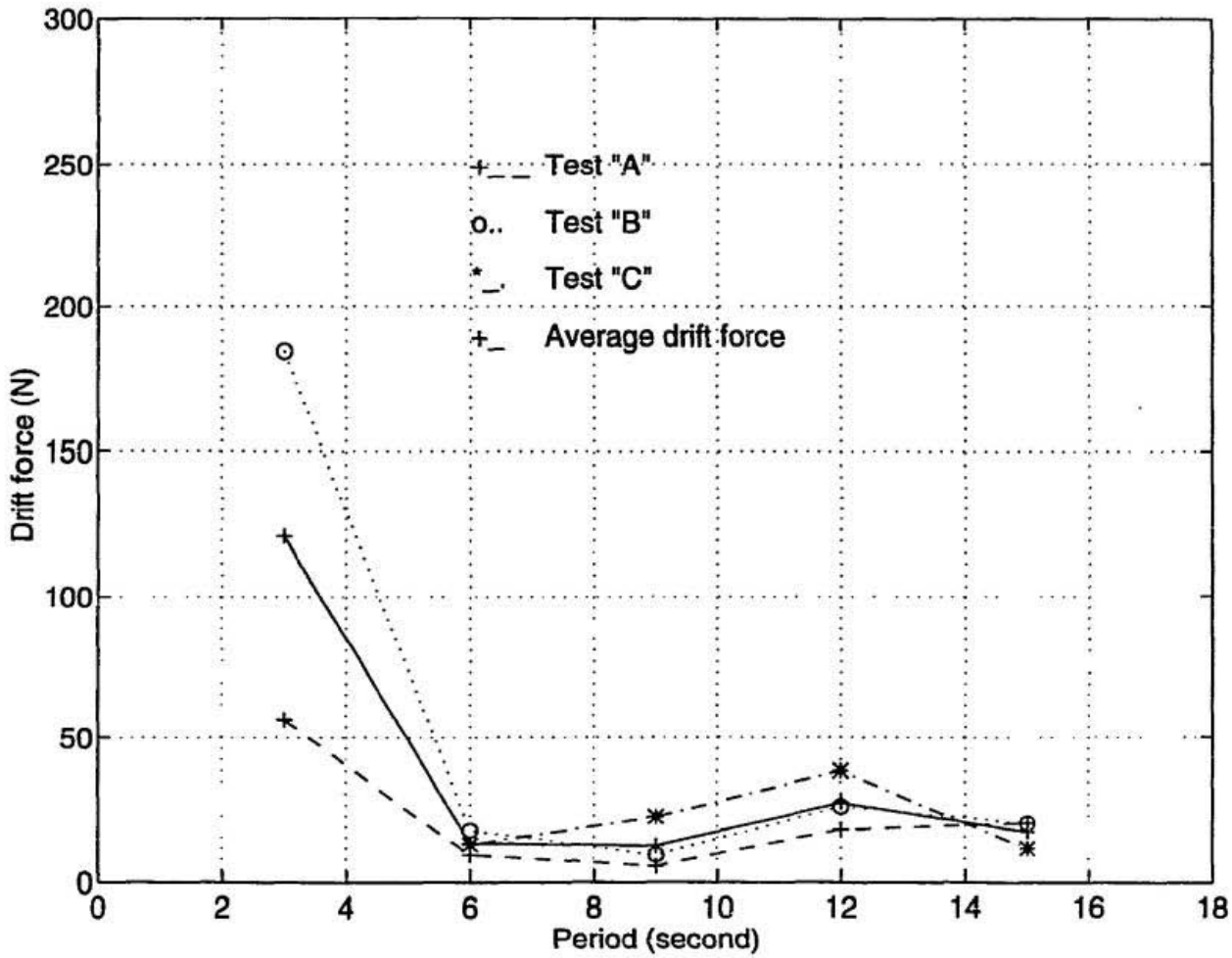

Figure 5.7 Drift Force Vs. Wave Period

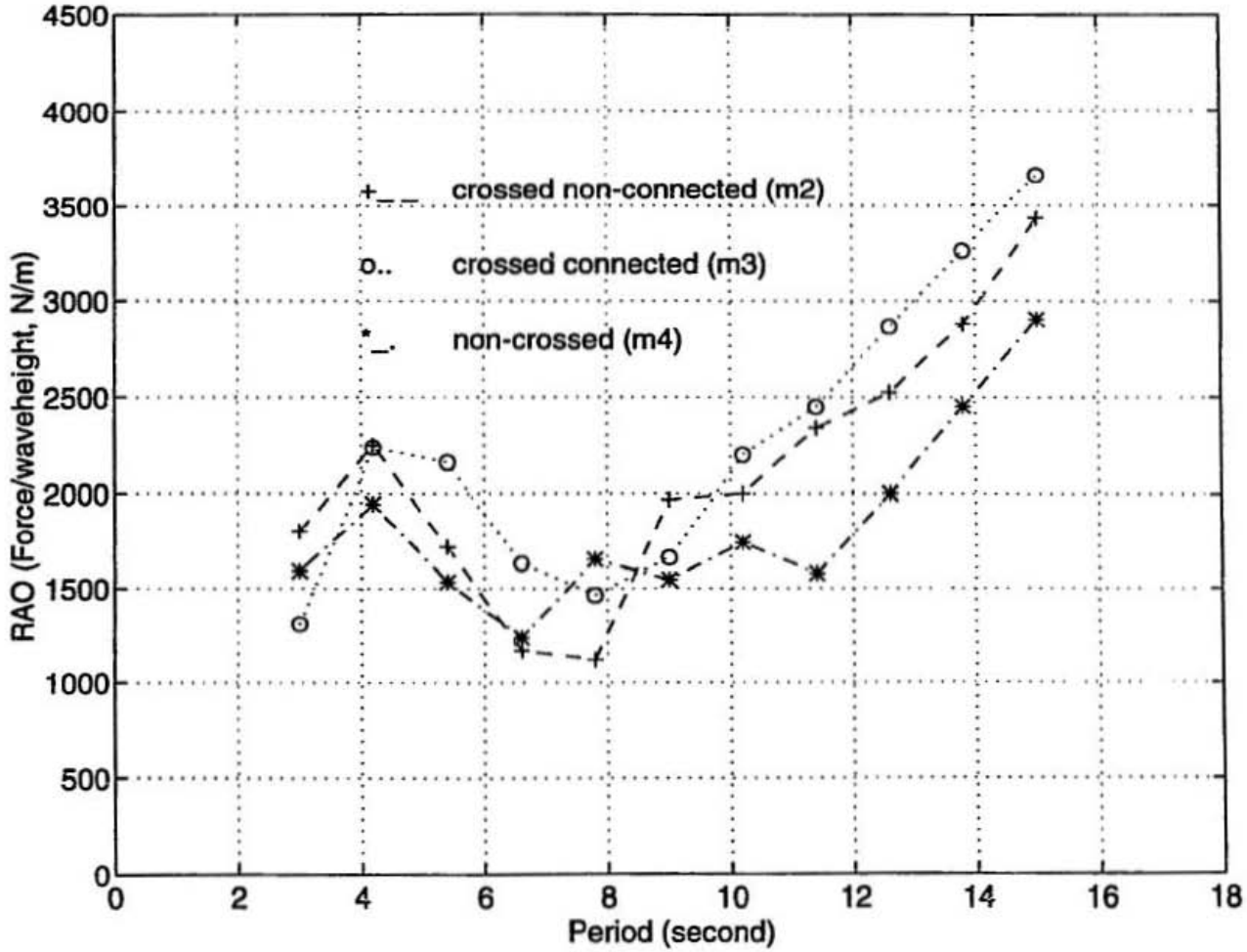

Figure 5.8 Mooring Line Force Vs. Wave Period

good agreement between the two (refer to Figure 5.4, 5.5 and 5.6). The RAO's for the regular waves appear to be slightly higher than for the irregular waves. These slight differences are most probably related to limitations in the measuring devices. Since the response in regular waves is measured from the steady-state part of the response in the regular waves. This assumes that all transients have diminished. For this reason, response to regular waves can be characterized by maximum values while response to irregular waves can be characterized by significant values.

The motions recorded indicate trends which occur with an elastic mooring system which allows a significantly larger range of motion than that of a chain system which can provide no allowance for stretching. As a result the values reported are valid up to a certain displacement at which time the model will react differently. This displacement is primarily a function of the mooring line scope.

Roll

The free floating response provides a control by which to compare the mooring configurations tested. It is apparent that the non-crossed configuration provides the least amount of roll response, approximately 10% - 25% less than the free floating condition (refer to Figure 5.4). The crossed connected design does reduce the motion but is not significant in the savings. The crucial observation concerns the crossed non-connected configuration, which was utilized in previous tests (Morey, 1993). This set-up amplifies the roll response by 20%, which in part explains the high roll amplitudes encountered in earlier model tests. The general trends indicate that roll decreases with increasing period, implying at high periods the dock rides the waves.

Sway

From Figure 5.5, it is apparent that when the period is lower than 10 seconds there is no discernible difference between any of the mooring configurations. For wave periods greater than 10 seconds, a deviation from the free floating configuration occurs. Beyond this period, the crossed non-connected system proved to be 20% more effective than either the crossed connected or non-crossed configurations. The general trends indicate that sway increases with increasing period, implying at high periods the dock sways more significantly. This is reasonable when considering that the sway period for the non-crossed mooring configuration is 18.40 seconds. Theoretically, the sway amplitude would be largest at this period. The data supports this conclusion.

Heave

As indicated in Figure 5.6, there is no discernible difference between the mooring configurations and the RAO remains relatively constant at 0.6 m/m regardless of the magnitude of the wave period or wave height. This is acceptable since the heave motions tend to equal the wave height at long periods and are smaller with short period waves. Since different wave conditions generated the same RAO, the structure can be described as responding "independently" to each frequency component, the total response being the sum of the responses to the various frequencies. This verifies that the superposition principle holds in this experimental study.

Mooring Forces

The mooring lines impart a global restoring force on the system depending upon the horizontal displacement of the model which varies with respect to the wave height and period. The second type of wave force is nonlinear in nature and a result of the irregular sea state. This force, known as the drift force, is primarily a consequence of wave

grouping and set-down effects. The drift force is a steady force in regular waves and a slow-varying/low frequency force in irregular waves. The slow-varying drift force may cause overstressing of mooring lines. As shown in Figure 5.7, the drift force was measured for all regular wave tests in test series A, B and C. For periods greater than 6 seconds there is a good agreement between tests with a consistent drift force of approximately 25 Newtons. For wave periods less than 6 seconds, there is a dramatic increase to 120 Newtons at 3 seconds.

From Figure 5.8, it is obvious that the non-crossed mooring system results in the lowest mooring forces, with the crossed non-connected and crossed connected configurations being 17 and 28 percent larger respectively. When the wave periods exceed 8 seconds, the curves take on a linear form, increasing in magnitude as the period increases. Below 8 seconds, the values for the RAO become erratic and highly non-linear.

Chapter 6

Conclusions and Recommendations

6.1 Conclusions

The main objective of this study was to develop a model that was geometrically and dynamically similar to a typical floating dock and to use it to measure the dynamic motion response over a full range of wave periods (3 to 15 secs.) for both regular and irregular waves in beam seas. Experiments were conducted in a wave tank equipped with a pseudo random wave making facility. Extreme care was taken to ensure correct calibration and accurate measurements in all aspects of the experiment. Mass properties were established using appropriate materials, scales and tools, and then are reflected in the measured GM and natural period. Combinations of rubberbands in each mooring line were calibrated for correct stiffness. To obtain the response amplitude operator (RAO) from the ambient response data, spectral analysis techniques were used.

Based on the reported results and evaluations, important conclusions can be reached. Among these are the following:

- The results of the decay tests indicated the natural periods of motion were higher

than determined through calculations. It was suggested the error was due to the added mass factor which according to the test results should be in the range of 1.5 to 2.0.

- A comparison of the free-floating and moored-motion response parameters indicated the mooring system reduced the natural periods of motion leading to increased accelerations but reduced translation and rotation.

- The natural periods of motion in roll, heave and sway are such that they should not have detrimental effects on the dock response in the range of wave heights and periods tested.

- There is good agreement between regular and irregular data, except that data obtained from regular wave tests are more indicative of maximum values and data obtained from irregular wave tests are more indicative of significant values.

- The stiffness of the mooring system was calibrated through elastic bands which provide a linear system. The catenary chain system is elastic up to a specific transverse displacement when the inelastic system governs. The RAO's and mooring forces should be considered in light of this fact.

- For roll response, the magnitude of the RAO decreased exponentially as the period increased from 3 to 15 seconds. The general trend indicated roll motion decreased as the period increased. The non-crossed mooring configuration proved to be most effective in roll, with approximate 25% and 20% decreases in the RAO with respect to the crossed non-connected and crossed connected, respectively.

- For sway response, the magnitude of the RAO increased exponentially as periods increased from 3 to 15 seconds. The crossed non-connected mooring configuration proved to be most effective in sway, with a 20% decrease in the RAO with respect to the crossed connected and non-crossed systems.

- For heave response, the RAO remains relatively constant at 0.6 m/m regardless of wave height and mooring configuration. There appears to be no benefit in either of the mooring designs.

- The drift force remains constant at 25 N for periods greater than 6 seconds but increases dramatically to 120 N for a wave period of 3 seconds.

- For mooring forces, when the wave periods exceed 8 seconds, the curves take on a linear form, increasing in magnitude as the period increases. Below 8 seconds, the values for the RAO become erratic and highly non-linear.

- The non-crossed mooring system results in the lowest mooring forces, with the crossed non-connected and crossed connected configurations being 17 and 28 percent larger respectively.

6.2 Recommendations

From the experience gained in this study, the following recommendations are made:

- The non-crossed mooring configuration should be employed where the situation permits. This will serve to decrease the roll motion and mooring forces.

- Further studies into mooring configurations would be warranted to investigate

other possible mooring arrangements. One such example would be the use of a clump weight mid-way along the mooring line to prevent entanglement with boats berthed at the structure. Other variables to be considered are stiffness and pretension.

- The low frequency or second-order wave drift force should be investigated further to examine its effect on mooring system performance.

- Studies into the design and testing of dock connections should be considered.

- Methods of dampening the wave energy to reduce dock motions should be investigated.

References

1. Adee, B.T. and Martin, W. (1974). "Theoretical Analysis of Floating Breakwater Performance," *Floating Breakwater Conf. Papers*, Univ. of Rhode Island, pp. 21-39.

2. Alexandrov, M. (1971). "On the Dynamics of Cables with Application to Marine Use," *Marine Technology*, January, pp. 84-92.

3. Anderson, A.R. (Jan. 1973). "A 65,000 Ton Prestressed Concrete Floating Facility for Offshore Storage of LPG," *Marine Technology*, Vol. 15, No. 1, SNAME, New York.

4. Anspach, G. et al. (May 1980). "Floating Terminal for Storage and Sendout of LNG," *Proc. ASCE*, Ports '80, Spec. Conf., Norfolk, Va.

5. Bhattacharyya R. (1978). "Dynamics of Marine Vehicles" A Wiley-Interscience Publishing, N.Y., Toronto.

6. Bomze, H. (May 1974). "Analytical Determination of Ship Motions and Mooring Forces," *Proc. OTC*, Paper No. 2072, Houston, Tex.

7. Bomze, H. (1980). "Math Model for Harbor Waves/Ship Motions/Moorings," *Proc. ASCE*, Ports '80, Spec. Conf., Norfolk, Va.

8. Cammaert, A.B., Curran, P., and Murphy, D. (1992). "Investigation into alternate Design and Use of New Materials in the Construction of Fishing Harbours for the Gulf Region - Phase II". *OERC Report* No. TR-FIS-92001.

9. Casarella, M.J. (1970). "A Survey of Investigations on the Configuration and Motion of Cable Systems under Hydrodynamic Loading," *Marine Technology Soc. J.*, 4 (4), 27-43.

10. Chakrabarti, S.K. (May 1980): "Steady and Oscillating Drift Forces on Floating Objects," *Proc. ASCE*, Vol. 106, WW-2.

11. Chakrabarti, S.K. (May 1982). "Experiments on Wave Drift Force on a Moored Floating Vessel," *Proc. OTC*, Paper No. 4436, Houston, Tex.

12. Choo, Y. and Casarella, M.J. (1973). "A Survey of Analytical Methods for Dynamic Simulation of Cable-Body Systems," Report 73-1, Dept. of Civil and Mechanical Engineering, Institute of Ocean Science and Engineering, The Catholic University of America, Washington, D.C. 20017.

13. Cummins, W.E. (1962). "The Impulse-Response Function and Ship Motions," David Taylor Model Basin Report No. 1661, Washington, D.C.

14. Dillon, D.B. (Feb. 1973). "An Inventory of Current Mathematical Models of Scientific Data-Gathering Moors," HCI TR4450 0001, Hydro-Space-Challenger, Inc., Rockville, Maryland 20850.

15. Faltinsen, O.M. and Michelsen, F.C. (1974). "Motions of Large Structures in Waves at Zero Froude Number," *Proc. Int. Symp.* on the Dynamics of Marine Vehicles and Structures in Waves, University College, London.

16. Garrison, C.J. (1974). "Dynamic Response of Floating Bodies," *Offshore Technol. Conf.*, Paper No. OTC2067.

17. Gaythwaite, J.W. (1990) "*Design of Marine Facilities*". Van Norstrond Reinhold Publishing Company, New York.

18. Ijima, T. (1972). "Motion of a Rectangular Body by Waves in Finite Water Depth," *Proc. Japan Soc. Civil Eng.*, pp. 33 (in Japanese).

19. Ikegami, K. and Matsuura, M. (1983). "Study on Motions of Floating Bodies under Composite External Loads," *Mitsubishi Technical Bulletin*, No. 158.

20. Ito, Y. and Chiba, S. (1972). "An Approximate Theory of Floating Breakwaters," *Rept. Port and Harbor Res. Inst.*, Vol. 11, No. 2, June pp. 137-166, (in Japanese).

21. Jahren, C.T. and Davis, D.A. (May 1986). "Construction Approaches to the Navy's Floating Pier Concept," *Proc. ASCE*, Ports '86, Spec. Conf., Oakland, Calif.

22. John, F. (1950). "On the Motion of Floating Bodies," II *Commun. Pure Appl. Math.* 3, (1-4), 45.

23. Kaplan, P. and Putz, R.R. (1962). "The Motions of a Moored Construction-Type Barge in Irregular Waves and Their Influence on Construction Operation," N By-32206, Marine Advisors, Inc. La Jolla.

24. Kilner, F.A. (1960). "Model Tests on the Motion of Moored Ships Placed on Long Waves," *Proc. 7th Conf. on Coastal Engineering*, The Hague, Vol. 2 pp. 723-745.

25. Kim, C.H. (1968). "The Influence of Water Depth on the Heaving and Pitching Motions of a Ship Moving in Longitudinal Regular Head Waves," Schiffstechnik, Vol. 15, No. 79, pp. 127-132.

26. Kim, C.H., Henry, C.J. and Chou, F., (1971). "Hydrodynamic Characteristics of Priamatic Barges," *Offshore Technology Conference Preprints*, Paper No. 1417.

27. Kulsvehagen, T. and Sandvik, A. (1988). "Dynamic Motions and Mooring Line Dynamics of Floating Production System," *Proc. of the 7th International Conference on Offshore Mechanics and Arctic Engineering*, Houston, Tex.

28. Langley, R.S. and McWilliam, S. (1992). "A Statistical Analysis of First and Second Order Vessel Motions Induced by Waves and Wind Gusts," *Applied Ocean Research*, 0141-1187.

29. Lean, G.H. (1971). "Subharmonic Motions of Moored Ships Subjected to Wave Action," *Transactions of the Royal Institution of Naval Architects*, Vol. 113, pp.

387-399.

30. Leendertse, J.J. (1963). "Analysis of the Response of Moored Surface and Subsurface Vessels to Ocean Waves," Rand Corporation Memorandum RM-3368 PR.

31. Loken, A.E. and Olsen, O.A. (May 1979). "The Influence of Slowly Varying Wave Forces on Mooring Systems," *Proc. OTC*, Paper No. 3626, Houston, Tex.

32. Maeda, H. and Morooka, C.K. (1986). "Motions of Floating Type Offshore Structures In Directional Waves," *Proc. of the 5th International Offshore Mechanics and Arctic Engineering Symposium*, Tokyo, Japan.

33. Migliore, H.J. and Zwibel, H.S. (1976). "Rigorous Treatment of Cable Systems Which Change Length With Time," *Technical Memorandum* TM-44-76-8.

34. Morey, B.J., Cammaert, A.B. and Rong, Y. (1993). "Investigation Into Alternate Designs and Use of New Materials in the Construction of Fishing Harbours for the Gulf Region" Memorial University of NFLD, OERC, *Report* No. TR-FIS-93001A.

35. Muga, B.J. (1967). "Experimental and Theoretical Study of Motion of a Barge as Moored in Ocean Waves," University of Illinois, Hydraulic Engineering Series No. 13.

36. Natvig, B.J. (1976). "Motion Response of Floating Structures to Regular Waves," Aker Engineering A/S, Tjurholmen, Oslo, Norway and Pell Frischman Offshore, Oslo, Norway.

37. Newman, J.N. (1970). "Applications of Slender Body Theory in Ship Hydrodynamics," *Annual Review of Fluid Mechanics*, Vol. 2.

38. Nogata *et al.* (1993). "Motions of FLoating Bodies in Waves, Moored by Elastic Lines in a Sea with a Breakwater," *Proc. 3th Int. Offshore and Polar Eng. Conf.*, Singapore.

39. Ogilvie, T.F. (1964). "Recent Progress Toward the Understanding and Prediction of Ship Morions," *5th Symposium on Naval Hydrodynamics*, Bergen.

40. Seidl, L.H. (1973). "Prediction of Motions of Ships Moored in Irregular Seas," *Proc. N.A.T.O.* Advanced Study Institute on Analytical Treatment of Problems in the Berthing and Mooring of Ships, Wallingford, pp. 221-229.

41. Sugin, L. (1983). "Conventional vs. Offshore Loading and Unloading," *Indonesian Coal/Lignite Dev. and U.S. Tech. Symp.*, Jakarta, Indonesia.

42. Takeshi Kinoshita (1990). "Numerical and Physical Simulation of Slow Drift Motion of a Moored Floating Structure in Waves," *4th Int. Symp. on Integrity of Offshore Structures*, Glasgow, Scotland.

43. Tsinker, G.P. (1986). *Floating Ports: Design and Construction Practices.* Gulf Publishing, Houston, Tex.

44. van Oorshot, J.H. (1975). "Subharmonic Components in Hawser and Fender Forces," *Proc.* 15th Coastal Engineering Conf., *ASCE*, New York.

45. van Oortmerssen, G. (1976). "The Motions of a Moored Ship in Waves," *Ph.D. thesis* Univ. of Tech. of Delft, NSME No. 510, Delft, The Netherlands.

46. van Oortmerssen, G. et al. (Mar. 1986). "Computer Simulation of Moored Ship Behaviour," *Proc. ASCE*, JWPCOE Div., Vol. 112, No. 2.

47. Vugts, J.H. (1968). "Cylinder Motions in Beam Waves," *Netherlands Ship Research Centre TNO*, Delft, Report No. 115s.

48. Wehausen, J.V. (1971). "The Motion of Floating Bodies," *Annual Review of Fluid Mechanics*, Vol. 3.

49. Wilson, J.F. and Awadalla, N.G. (1971). "Subharmonic Response in the Non-Linear Oscillations of Moored Ships," *Offshore Technology Conference*, Houston, paper OTC 1420, Vol. II pp. 65-80.

50. Wilson, J.K. and Awadalla, N.G. (1973). "Computer Simulation of Non-Linear Motion of Moored Ships," *Proc. N.A.T.O.* Advanced Study Institute on Analytical Treatment of Problems in the Berthing and Mooring of Ships, Wallingford, pp. 277-298.

51. Wilson, B.W. (1959). "The Energy Problem of Ships Exposed to Waves," The Princeton University Conference.

52. Wilson, B.W. (1973). "Progress in the Study of Ships Moored in Waves," *Proc. N.A.T.O.* Advanced Study Institute on Analytical Treatment of Problems in the Berthing and Mooring of Ships, Wallingford, pp. 143-213.

53. Yamamoto, T. (1978). "Response of Moored Objects to Waves. Part II: Random Wave Tests and Periodic Wave Tests on Elastically Moored Floating Breakwaters in a Large Wave Tank," *Tech. Report for NSF*, Cullen College of Engineering, University of Houston.

54. Yamashita, S. (1981). "Motions of a Box-Shaped Floating Structure in Regular Waves," *IHI Engineering Review*, Vol. 14, No. 2, pp. 21-30.

55. Yang, I-Min. (1972). "Motions of Moored Ships in Six Degrees of Freedom," *9th Symposium on Naval Hydrodynamics*, Paris.

APPENDIX A

Catenary Mooring Calculations

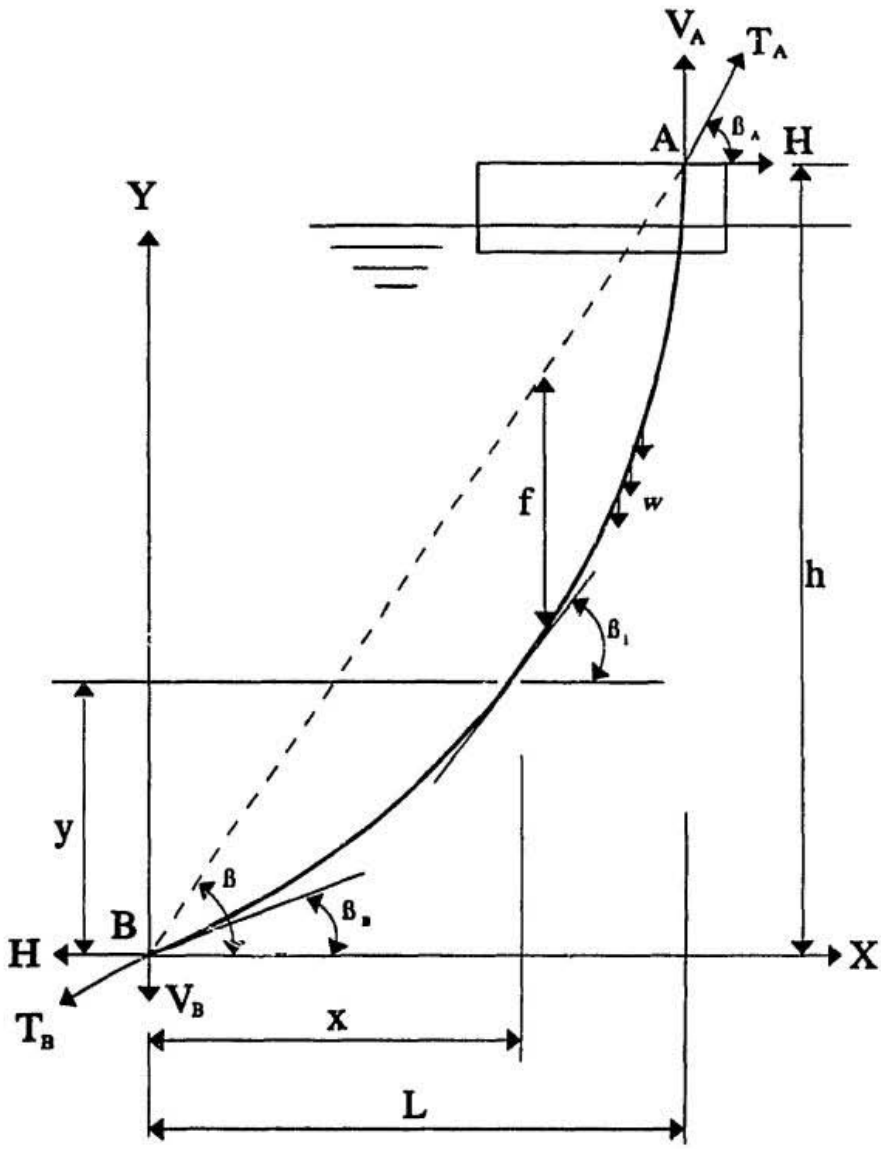

Figure A.1 Mooring Line Diagram

L	h	H (0 deg)	beta	Va	beta B	Vb	Ta
m	m	N	deg	N	deg	N	N
0.000	0.500	0.000	90.0	---	0.0	0.00	0.000
0.200	0.500	0.060	78.7	0.298	0.0	0.00	0.303
0.400	0.500	0.238	68.2	0.595	0.0	0.00	0.641
0.600	0.500	0.536	59.0	0.893	0.0	0.00	1.041
0.800	0.500	0.952	51.3	1.190	-0.0	-0.00	1.524
1.000	0.500	1.488	45.0	1.488	0.0	0.00	2.104
1.200	0.500	2.142	39.8	1.785	0.0	0.00	2.789
1.400	0.500	2.916	35.5	2.083	0.0	-0.00	3.583
1.600	0.500	3.808	32.0	2.380	-0.0	-0.00	4.491
1.800	0.500	4.820	29.1	2.678	0.0	0.00	5.514
2.000	0.500	5.951	26.6	2.975	0.0	0.00	6.653
2.200	0.500	7.200	24.4	3.273	0.0	0.00	7.909
2.350	0.500	8.216	23.1	3.496	0.0	0.00	8.929
2.360	0.500	8.286	23.0	3.511	0.0	0.00	8.999
2.370	0.500	8.356	22.9	3.526	-0.0	-0.00	9.070
2.380	0.500	8.427	22.8	3.541	-0.0	-0.00	9.140
2.390	0.500	8.498	22.7	3.556	-0.0	-0.00	9.212
2.400	0.500	8.569	22.6	3.570	0.0	0.00	9.283
2.410	0.500	8.641	22.5	3.585	0.0	0.00	9.355
2.420	0.500	8.712	22.5	3.600	0.0	0.00	9.427
2.430	0.500	8.785	22.4	3.615	-0.0	-0.00	9.499
2.440	0.500	8.857	22.3	3.630	0.0	0.00	9.572
2.450	0.500	8.930	22.2	3.645	0.0	0.00	9.645
2.460	0.500	9.003	22.1	3.660	0.0	0.00	9.718
2.470	0.500	9.076	22.0	3.675	0.0	0.00	9.792
2.480	0.500	9.150	22.0	3.689	0.0	0.00	9.866
2.490	0.500	9.224	21.9	3.704	0.0	0.00	9.940
2.500	0.500	9.298	21.8	3.719	0.0	0.00	10.014

Displacement m	Horizontal Forces C1 Seaward N	C2 Leeward N	2 * (C1−C2) Global N
−0.500	5.95	13.39	−14.88
−0.300	7.20	11.66	−8.93
−0.150	8.22	10.45	−4.46
−0.140	8.29	10.37	−4.17
−0.130	8.36	10.29	−3.87
−0.120	8.43	10.21	−3.57
−0.110	8.50	10.13	−3.27
−0.100	8.57	10.06	−2.98
−0.090	8.64	9.98	−2.68
−0.080	8.71	9.90	−2.38
−0.070	8.78	9.83	−2.08
−0.060	8.86	9.75	−1.79
−0.050	8.93	9.67	−1.49
−0.040	9.00	9.60	−1.19
−0.030	9.08	9.52	−0.89
−0.020	9.15	9.45	−0.60
−0.010	9.22	9.37	−0.30
0.000	9.30	9.30	0.00
0.010	9.37	9.22	0.30
0.020	9.45	9.15	0.60
0.030	9.52	9.08	0.89
0.040	9.60	9.00	1.19
0.050	9.67	8.93	1.49
0.060	9.75	8.86	1.79
0.070	9.83	8.78	2.08
0.080	9.90	8.71	2.38
0.090	9.98	8.64	2.68
0.100	10.06	8.57	2.98
0.110	10.13	8.50	3.27
0.120	10.21	8.43	3.57
0.130	10.29	8.36	3.87
0.140	10.37	8.29	4.17
0.150	10.45	8.22	4.46
0.300	11.66	7.20	8.93
0.500	13.39	5.95	14.88
Stiffness	7.44	−7.44	29.75
Tension	9.30	9.30	0.00

Displacement m	Vertical Forces		
	C1 Seaward N	C2 Leeward N	2 * (C1−C2) Global N
−0.500	2.98	4.46	−2.98
−0.300	3.27	4.17	−1.79
−0.150	3.50	3.94	−0.89
−0.140	3.51	3.93	−0.83
−0.130	3.53	3.91	−0.77
−0.120	3.54	3.90	−0.71
−0.110	3.56	3.88	−0.65
−0.100	3.57	3.87	−0.60
−0.090	3.59	3.85	−0.54
−0.080	3.60	3.84	−0.48
−0.070	3.62	3.82	−0.42
−0.060	3.63	3.81	−0.36
−0.050	3.64	3.79	−0.30
−0.040	3.66	3.78	−0.24
−0.030	3.67	3.76	−0.18
−0.020	3.69	3.75	−0.12
−0.010	3.70	3.73	−0.06
−0.000	3.72	3.72	0.00
0.010	3.73	3.70	0.06
0.020	3.75	3.69	0.12
0.030	3.76	3.67	0.18
0.040	3.78	3.66	0.24
0.050	3.79	3.64	0.30
0.060	3.81	3.63	0.36
0.070	3.82	3.62	0.42
0.080	3.84	3.60	0.48
0.090	3.85	3.59	0.54
0.100	3.87	3.57	0.60
0.110	3.88	3.56	0.65
0.120	3.90	3.54	0.71
0.130	3.91	3.53	0.77
0.140	3.93	3.51	0.83
0.150	3.94	3.50	0.89
0.300	4.17	3.27	1.79
0.500	4.46	2.98	2.98
Stiffness	1.49	−1.49	5.95
Tension	3.72	3.72	0.00

Displacement m	Tension C1 Seaward N	Tension C2 Leeward N	Tension 2 * (C1−C2) Global N
−0.500	6.65	14.11	−14.92
−0.300	7.91	12.38	−8.95
−0.150	8.93	11.17	−4.48
−0.140	9.00	11.09	−4.18
−0.130	9.07	11.01	−3.88
−0.120	9.14	10.93	−3.58
−0.110	9.21	10.85	−3.28
−0.100	9.28	10.77	−2.98
−0.090	9.35	10.70	−2.69
−0.080	9.43	10.62	−2.39
−0.070	9.50	10.54	−2.09
−0.060	9.57	10.47	−1.79
−0.050	9.64	10.39	−1.49
−0.040	9.72	10.31	−1.19
−0.030	9.79	10.24	−0.90
−0.020	9.87	10.16	−0.60
−0.010	9.94	10.09	−0.30
−0.000	10.01	10.01	0.00
0.010	10.09	9.94	0.30
0.020	10.16	9.87	0.60
0.030	10.24	9.79	0.90
0.040	10.31	9.72	1.19
0.050	10.39	9.64	1.49
0.060	10.47	9.57	1.79
0.070	10.54	9.50	2.09
0.080	10.62	9.43	2.39
0.090	10.70	9.35	2.69
0.100	10.77	9.28	2.98
0.110	10.85	9.21	3.28
0.120	10.93	9.14	3.58
0.130	11.01	9.07	3.88
0.140	11.09	9.00	4.18
0.150	11.17	8.93	4.48
0.300	12.38	7.91	8.95
0.500	14.11	6.65	14.92
Stiffness	7.46	−7.46	29.84
Pretension	10.01	10.01	0.00

APPENDIX B

Structure Characteristics Calculations

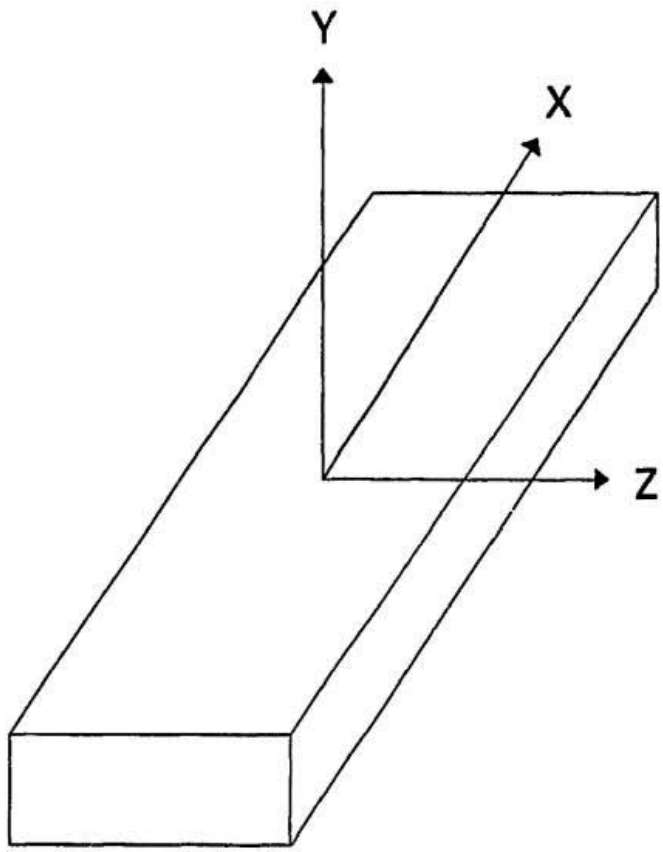

Figure B.1 Coordinate System

Calculation of Motion Response Characteristics – Prototype

Description	Xi (m)	Yi (m)	Zi (m)	Mass (kg)	Ixx (m)	Iyy (m)	Izz (m)
Skids	0.000	1.405	0.489	292.8	647.6	70.0	577.6
Skids	0.000	0.500	0.489	214.6	105.0	51.3	53.7
Level1 – Longitudinals	0.580	1.430	0.324	81.8	175.9	36.1	194.8
Level1 – Longitudinals	1.740	1.430	0.324	81.8	175.9	256.3	415.1
Level1 – Longitudinals	2.900	1.430	0.324	81.8	175.9	696.7	855.5
Level1 – Cross Ties	0.000	0.000	0.324	60.2	6.3	6.3	0.0
Level1 – Cross Ties	1.160	0.000	0.324	120.3	12.6	174.5	161.9
Level1 – Cross Ties	2.320	0.000	0.324	120.3	12.6	660.3	647.7
Level1 – Cross Ties	3.480	0.000	0.324	120.3	12.6	1469.8	1457.2
Slats	0.274	0.000	0.413	2.0	0.3	0.5	0.2
Slats	0.478	0.000	0.413	2.0	0.3	0.8	0.5
Slats	0.682	0.000	0.413	2.0	0.3	1.3	0.9
Slats	0.886	0.000	0.413	2.0	0.3	1.9	1.6
Slats	1.434	0.000	0.413	2.0	0.3	4.5	4.1
Slats	1.638	0.000	0.413	2.0	0.3	5.8	5.4
Slats	1.842	0.000	0.413	2.0	0.3	7.2	6.8
Slats	2.046	0.000	0.413	2.0	0.3	8.6	8.4
Slats	2.594	0.000	0.413	2.0	0.3	13.9	13.6
Slats	2.798	0.000	0.413	2.0	0.3	16.1	15.8
Slats	3.002	0.000	0.413	2.0	0.3	18.5	18.2
Slats	3.206	0.000	0.413	2.0	0.3	21.1	20.7
Billets	0.580	0.000	0.101	84.6	0.9	29.3	28.5
Billets	1.740	0.000	0.101	84.6	0.9	257.1	256.2
Billets	2.900	0.000	0.101	84.6	0.9	712.5	711.6
Level2 – longitudinals	0.000	1.430	0.108	421.1	865.9	4.9	861.1
Level2 – Cross Ties	0.000	0.000	0.108	68.8	0.8	0.8	0.0
Level2 – Cross Ties	1.160	0.000	0.108	137.7	1.6	186.8	185.2
Level2 – Cross Ties	2.320	0.000	0.108	137.7	1.6	742.5	740.9
Level2 – Cross Ties	3.480	0.000	0.108	137.7	1.6	1668.7	1667.1
Level2 – Cross Ties	4.040	0.000	0.108	137.7	1.6	2248.4	2246.8
Level3 – Longitudinals	0.580	1.430	−0.109	81.8	168.3	26.5	194.8
Level3 – longitudinals	1.740	1.430	−0.109	81.8	168.3	248.7	415.1
Level3 – longitudinals	2.900	1.430	−0.109	81.8	168.3	689.1	855.5
Level3 – longitudinals	3.709	1.430	−0.109	25.5	52.5	351.2	403.1
Level3 – Cross Ties	0.000	0.000	−0.109	60.2	0.7	0.7	0.0
Level3 – Cross Ties	1.160	0.000	−0.109	120.3	1.4	163.3	161.9
Level3 – Cross Ties	2.320	0.000	−0.109	120.3	1.4	649.1	647.7
Level3 – Cross Ties	3.480	0.000	−0.109	120.3	1.4	1458.7	1457.2
Level3 – Cross Ties	4.014	0.000	−0.109	251.0	3.0	4046.7	4043.7
Level4 – longitudinals	0.000	1.380	−0.274	421.1	832.9	31.6	801.3
Level4 – Longitudinals	1.390	0.367	−0.274	103.5	21.7	207.8	214.0
Level4 – Longitudinals	2.550	0.456	−0.274	60.2	17.0	395.9	403.8
Level4 – Cross Ties	3.781	0.880	−0.274	76.8	65.3	1103.8	1157.5
Level4 – Cross Ties	3.749	0.000	−0.274	41.6	3.1	587.8	584.7
Decking	0.000	0.000	−0.362	682.2	89.4	89.4	0.0
Chocks	1.740	1.430	−0.411	4.0	8.8	12.7	20.1
Chocks	2.900	1.430	−0.411	4.0	8.8	34.1	41.5
Chocks	0.000	1.430	−0.411	13.0	28.8	2.2	28.6
Railing	0.000	1.430	−0.487	119.8	273.3	28.4	245.0
Siding	0.000	1.507	−0.058	92.8	210.9	0.3	210.6
Bolts	-----	-----	-----	133.6	-----	-----	-----

Data Summary – Prototype		
Radius of Gyration	Kxx =	0.91 m
	Kyy =	1.94 m
Moment of Inertia	Ixx =	4329 kg m^2
	Iyy =	19503 kg m^2
Natural Periods	Txx =	1.07 secs
	Tyy =	2.27 secs

Data Summary – Model		
	Kxx =	0.101 m
	Kyy =	0.215 m
	Ixx =	0.073 kg m^2
	Iyy =	0.330 kg m^2
	Txx =	0.356 secs
	Tyy =	0.756 secs

CALCULATION OF THE CENTER OF GRAVITY – PROTOTYPE

	# MEM	Length (mm)	Height (mm)	Width (mm)	Volume (m^3)	Density (kg/m^3)	Mass (kg)	Z–BAR (m)	Moment (kg m)
Skids – Wide	2	7300	140	191	0.390	750	293	0.070	20
Skids – Narrow	2	7300	140	140	0.286	750	215	0.070	15
Level1 – longitudinals	12	1020	191	140	0.327	750	245	0.236	58
Level1 – Cross Ties	7	140	191	3000	0.562	750	421	0.236	99
Slats	24	38	13	2720	0.032	750	24	0.147	4
Billets	6	1020	610	2720	10.154	25	254	0.458	116
Level2 – Longitudinals	2	8320	241	140	0.561	750	421	0.452	190
Level2 – Cross Ties	9	140	241	2720	0.826	750	619	0.452	280
Level3 – Longitudinals	12	1020	191	140	0.327	750	245	0.668	164
Level3 – Longitudinals	4	318	191	140	0.034	750	26	0.668	17
Level3 – Cross Ties	7	140	191	3000	0.562	750	421	0.668	281
Level3 – Cross Ties	2	292	191	3000	0.335	750	251	0.668	168
Level4 – Longitudinals	2	8320	140	241	0.561	750	421	0.833	351
Level4 – Longitudinals	2	5540	140	89	0.138	750	104	0.833	86
Level4 – Longitudinals	2	3220	140	89	0.080	750	60	0.833	50
Level4 – Cross Ties	4	241	140	759	0.102	750	77	0.833	64
Level4 – Cross Ties	2	241	140	822	0.055	750	42	0.833	35
Decking	57	140	38	3000	0.910	750	682	0.922	629
Chocks – Short	8	305	62	140	0.0[illegible]	750	16	0.972	15
Chocks – Long	2	1000	62	140	0.017	750	13	0.972	13
Railing	2	6410	89	140	0.160	750	120	1.048	125
Siding	2	8320	572	13	0.121	750	91	0.617	56
Lifting – Hooks	4	----	----	----	0.004	6300	24	0.537	13
Skid Bolts	14	----	331	----	0.001	6300	9	0.166	2
Stringer Bolts	20	----	331	----	0.002	6300	13	0.738	10
Through Blots	8	----	572	----	0.001	6300	9	0.617	6
Through Bolts	30	----	903	----	0.009	6300	54	0.452	24
				SUMS	16.58		5169		2890
						KG =	0.559		

CALCULATION FOR THE CENTER OF BUOYANCY – PROTOTYPE

Submerged Volume =	5.169 m^3
Draft =	0.358 m
Freeboard =	0.583 m

	# MEM	Length (m)	Height (m)	Width (m)	Volume (m^3)	Density (kg/m^3)	Mass (kg)	Z–BAR (m)	Moment (kg m)
Skids – Wide	2	7.300	0.140	0.191	0.390	750	293	0.070	20.5
Skids – Narrow	2	7.300	0.140	0.140	0.286	750	215	0.070	15.0
Level1 – Longitudinals	12	1.020	0.191	0.140	0.327	750	245	0.236	57.8
Level1 – Cross Ties	7	0.140	0.191	3.000	0.562	750	421	0.236	99.2
Slats	24	0.038	0.013	2.720	0.032	750	24	0.147	3.5
Billets	6	1.020	0.205	2.720	3.416	25	65	0.256	21.8
Level2 – Longitudinals	2	8.320	0.027	0.140	0.063	750	48	0.345	16.4
Level2 – Cross Ties	9	0.140	0.027	2.720	0.093	750	70	0.345	24.1
				SUMS	5.170		1401		258.4
						KB =	0.184		

CALCULATION FOR THE METACENTRIC RADIUS – PROTOTYPE

Submerged Volume =	5.170 m^3

	# MEM	Along X (m)	Along Z (m)	X–bar (m)	Z–bar (m)	AREA (m^2)	box (m^4)	Izz (m^4)
Billets	2	1.020	2.720	0.580	0.000	5.5	3.42	2.35
Billets	2	1.020	2.720	1.740	0.000	5.5	3.42	17.28
Billets	2	1.020	2.720	2.900	0.000	5.5	3.42	47.15
Level2 – Longitudinals	2	8.320	0.140	0.000	1.430	2.3	4.77	13.44
Level2 – Cross Ties	1	0.140	2.720	0.000	0.000	0.4	0.23	0.00
Level2 – Cross Ties	2	0.140	2.720	1.160	0.000	0.8	0.47	1.03
Level2 – Cross Ties	2	0.140	2.720	2.320	0.000	0.8	0.47	4.10
Level2 – Cross Ties	2	0.140	2.720	3.480	0.000	0.8	0.47	9.22
Level2 – Cross Ties	2	0.140	2.720	4.090	0.000	0.8	0.47	12.74
					SUMS	22.4	17.14	107.31
					BMbox =	3.3		
					BMzz =	20.8		

METACENTRIC HEIGTHS – PROTOTYPE

GMbox = 2.94 m

GMzz = 20.38 m

CALCULATION OF THE CENTER OF GRAVITY – MODEL

	# MEM	Length (mm)	Height (mm)	Width (mm)	Volume (m^3)	Density (kg/m^3)	Mass (kg)	Z–BAR (m)	Moment (kg m)
Skids – Wide	2	811	16	21	0.00054	750	0.409	0.008	0.00318
Skids – Narrow	2	811	16	16	0.00042	750	0.311	0.008	0.00242
Ends–A	2	16	27	302	0.00026	750	0.196	0 050	0.00982
Ends–B	2	32	21	302	0.00041	750	0.304	0.074	0.02258
Dividers	7	16	68	302	0.00230	750	1.725	0.040	0.08529
Sides–A	2	811	21	16	0 0054	750	0.409	0.026	0.01070
Sides–B	2	924	48	16	0 00142	750	1.064	0.061	0.06469
Billets	6	113	68	302	0.01392	25	0.348	0.049	0.01721
Level4 – Longitudinal A	2	924	16	27	0.00080	750	0.599	0.093	0.05542
Level4 – Longitudinal B	2	924	16	10	0.00030	750	0.222	0.093	0.02053
Level4 – Cross ties A	4	27	16	84	0.00015	750	0.109	0.093	0.01008
Level4 – Cross Ties B	2	27	16	91	0.00008	750	0.059	0.093	0.00546
Decking	1	924	5	333	0.00154	750	1.154	0.102	0.11821
Chocks – Short	8	34	7	16	0.00003	750	0.023	.108	0.00247
Chock – Long	2	111	7	16	0.00002	750	0.019	0.108	0.00201
Railing	2	712	10	16	0.00023	750	0.171	0.116	0 01989
				SUMS	0.02295		7.121		0.450
						KG =	0.063		

CALCULATION FOR THE CENTER OF BUOYANCY – MODEL

Submerged Volume =	0.0071 m^3
Draft =	0.0388 m
Freeboard =	0.0657 m

	# MEM	Length (m)	Height (m)	Width (m)	Volume (m^3)	Density (kg/m^3)	Mass (kg)	Z–BAR (m)	Moment (kg m)
Skids – Wide	2	811	16	21	0.0005	750	0.409	0.0080	0.0033
Skids – Narrow	2	811	16	16	0.0004	750	0.311	0.0080	0.0025
Ends–A	2	16	2	302	0.0000	750	0.015	0.0378	0.0006
Dividers	7	16	23	302	0.0008	750	0.590	0.0276	0.0163
Sides–A	2	811	21	16	0.0005	750	0.409	0.0265	0.0108
Sides–B	2	924	2	16	0.0001	750	0.045	0.0380	0.0017
Billets	6	113	23	302	0.0048	25	0.119	0.0276	0.0033
				SUMS	0.0071		1.897		0.0384
						KB =	0.020		

CALCULATION FOR THE METACENTRIC RADIUS – MODEL

Submerged Volume =	0.007 m^3

	# MEM	Along X (m)	Along Z (m)	X–bar (m)	Z–bar (m)	AREA (m^2)	Ixx (m^4)	Izz (m^4)
Ends–A	2	0.016	0.302	0.454	0.000	0.00966	0.00007	0.00199
Dividers	1	0.016	0.302	0.000	0.000	0.00483	0.00004	0.00000
Dividers	2	0.016	0.302	0.129	0.000	0.00966	0.00007	0.00016
Dividers	2	0.016	0.302	0.258	0.000	0.00966	0.00007	0.00064
Dividers	2	0.016	0.302	0.387	0.000	0.00960	0.00007	0.00145
Side–B	2	0.924	0.016	0.000	0.166	0.02957	0.00082	0.00210
Billet	2	0.113	0.302	0.064	0.000	0.06825	0.00052	0.00035
Billet	2	0.113	0.302	0.193	0.000	0.06825	0.00052	0.00261
Billet	2	0.113	0.302	0.322	0.000	0.06825	0.00052	0.00715
					SUMS	0.27781	0.00270	0.01646
					BMxx =	0.379		
					BMzz =	2.309		

METACENTRIC HEIGHTS – MODEL

GMxx = 0.336 m

GMzz = 2.266 m

APPENDIX C

Time History Plots

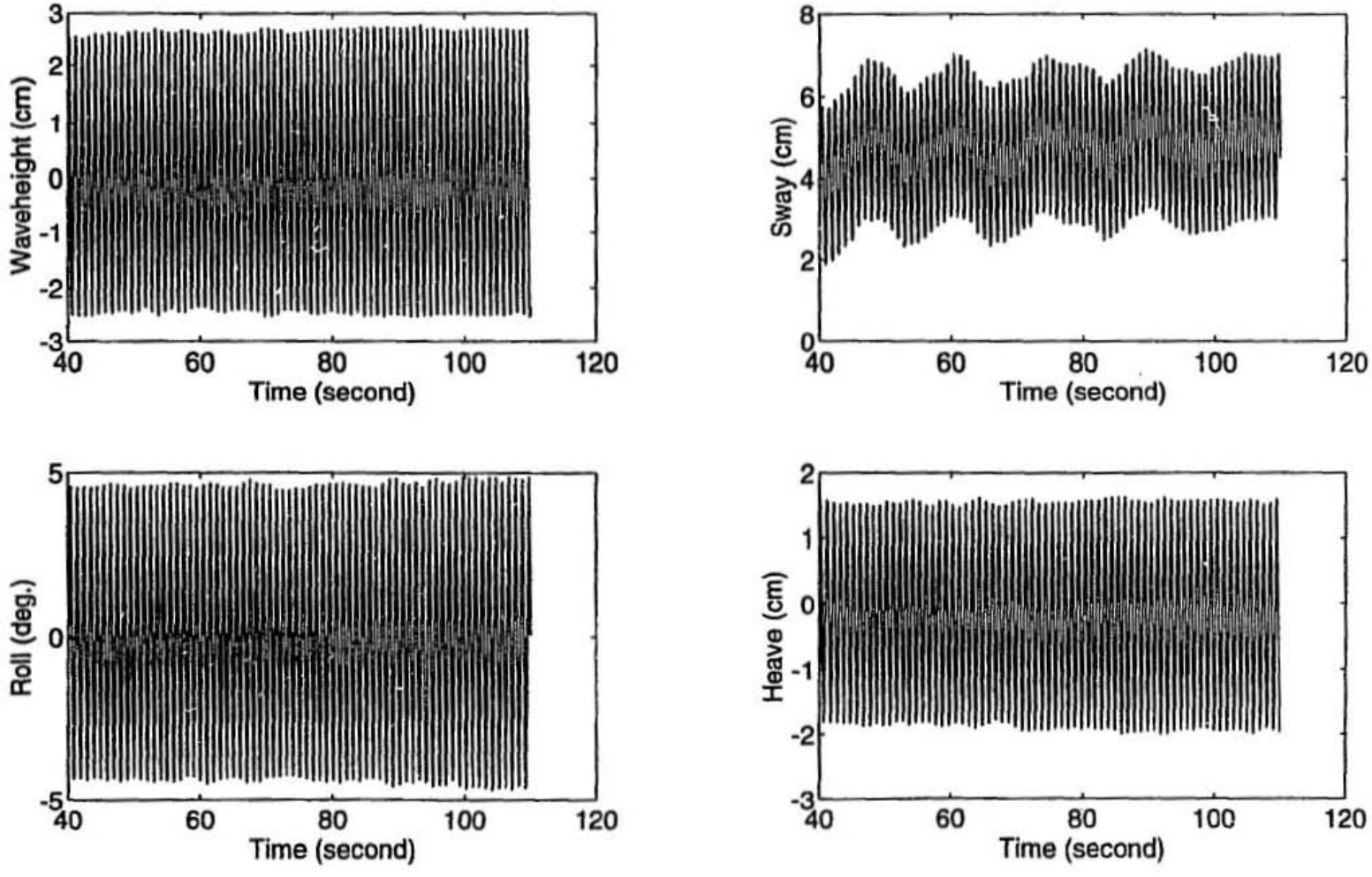

C2

Figure C.1 Test Series A1M1

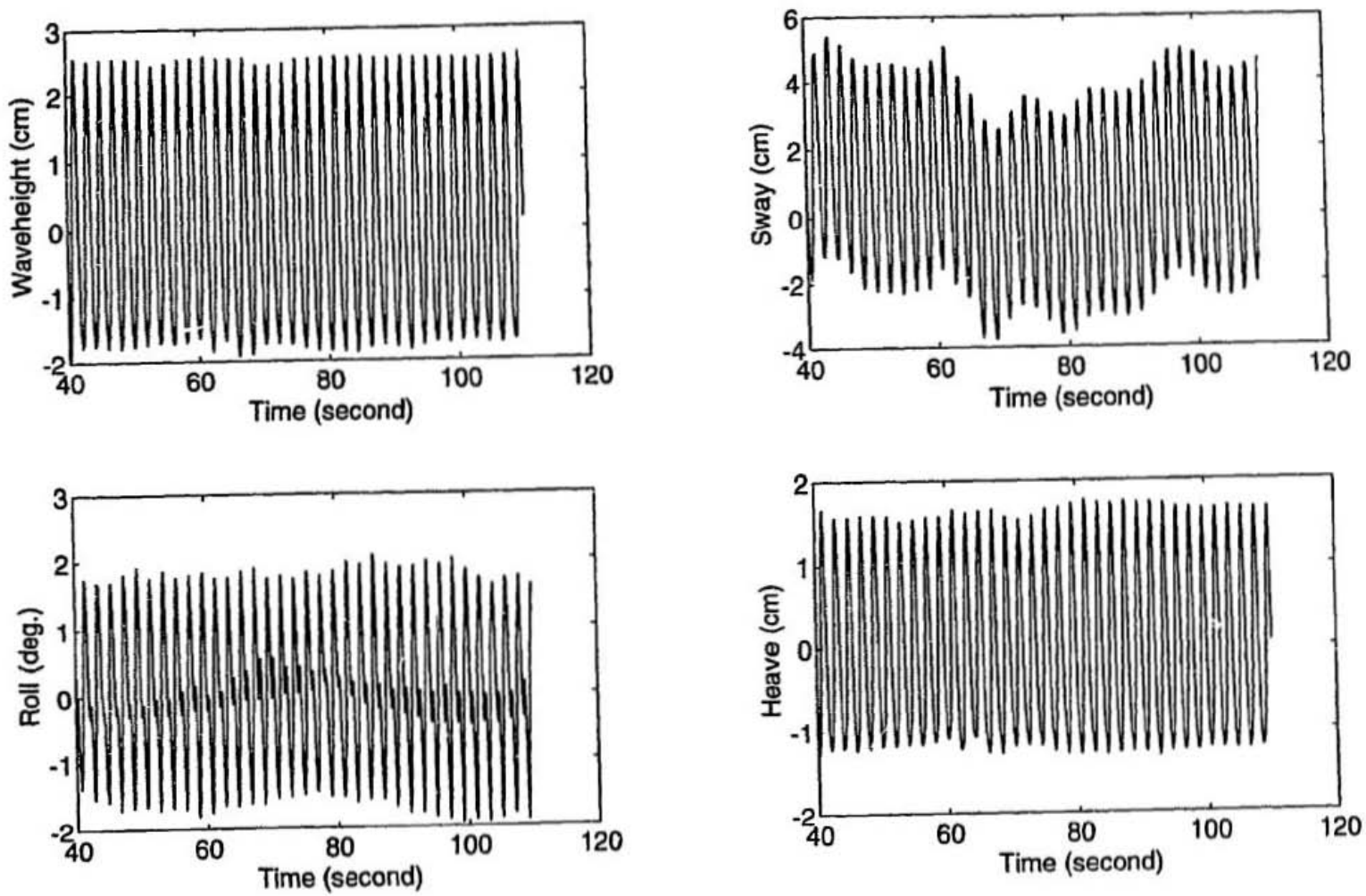

C3

Figure C.2 Test Series A2M1

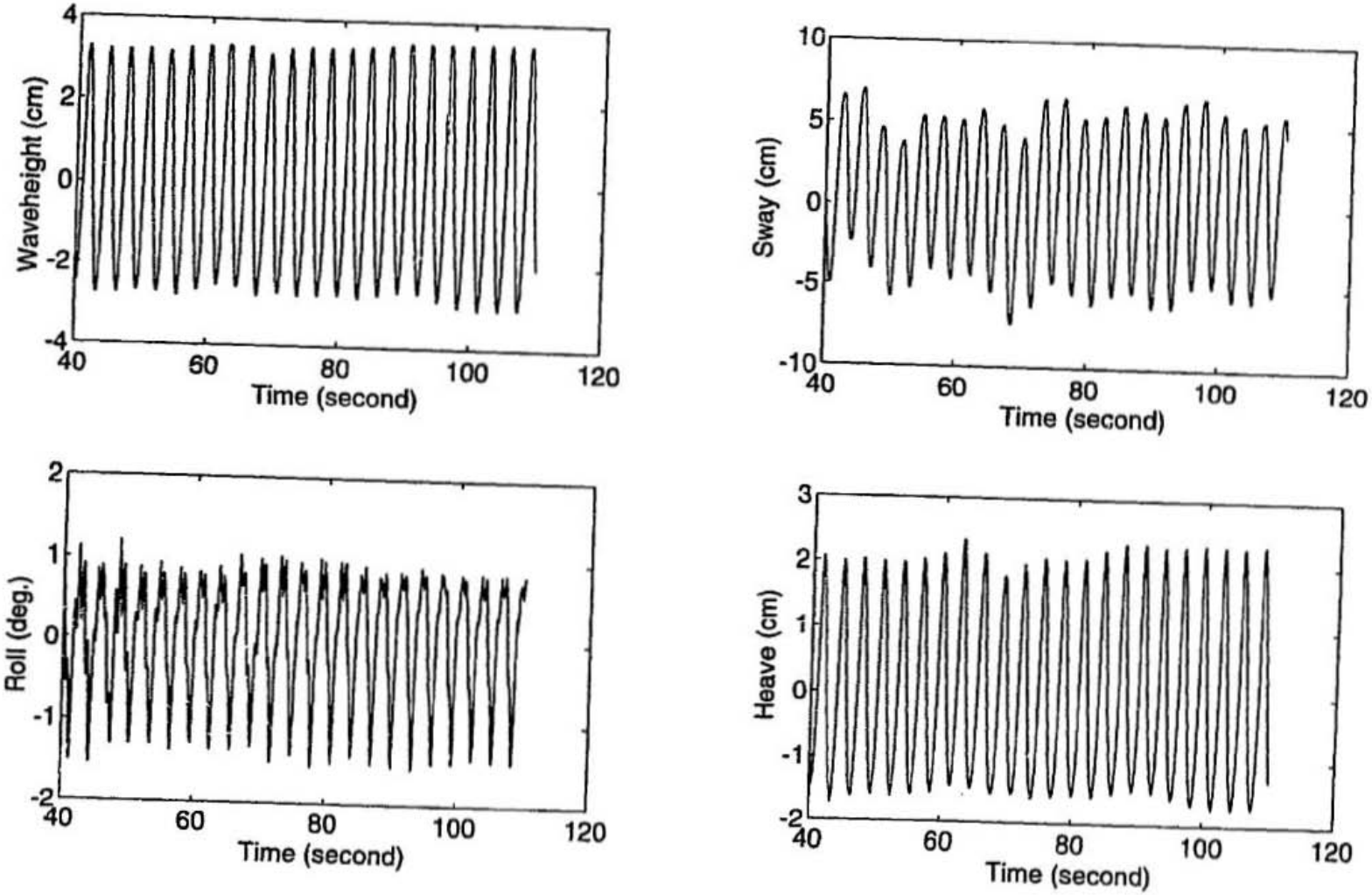

Figure C.3 Test Series A3M1

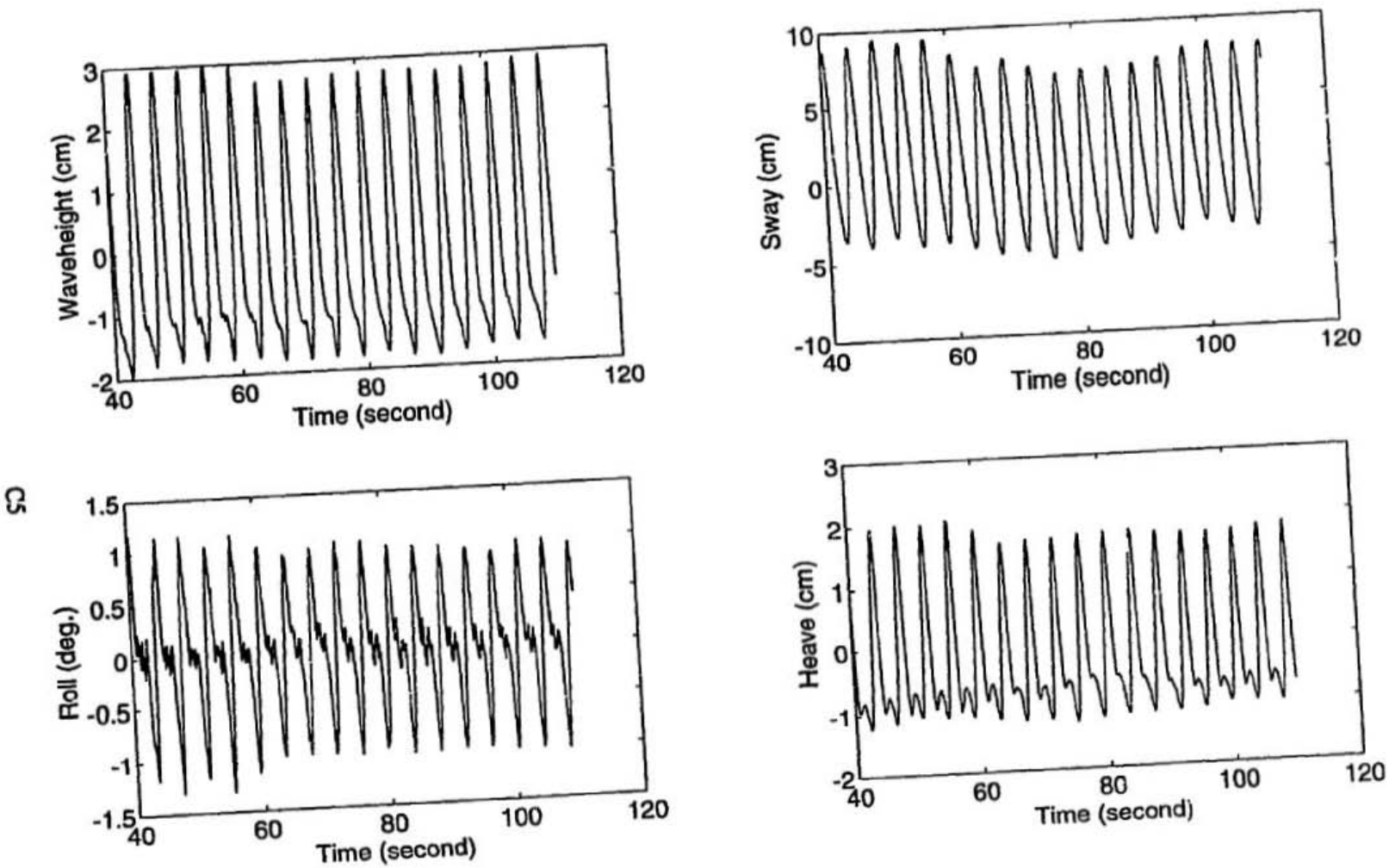

Figure C.4 Test Series A4M1

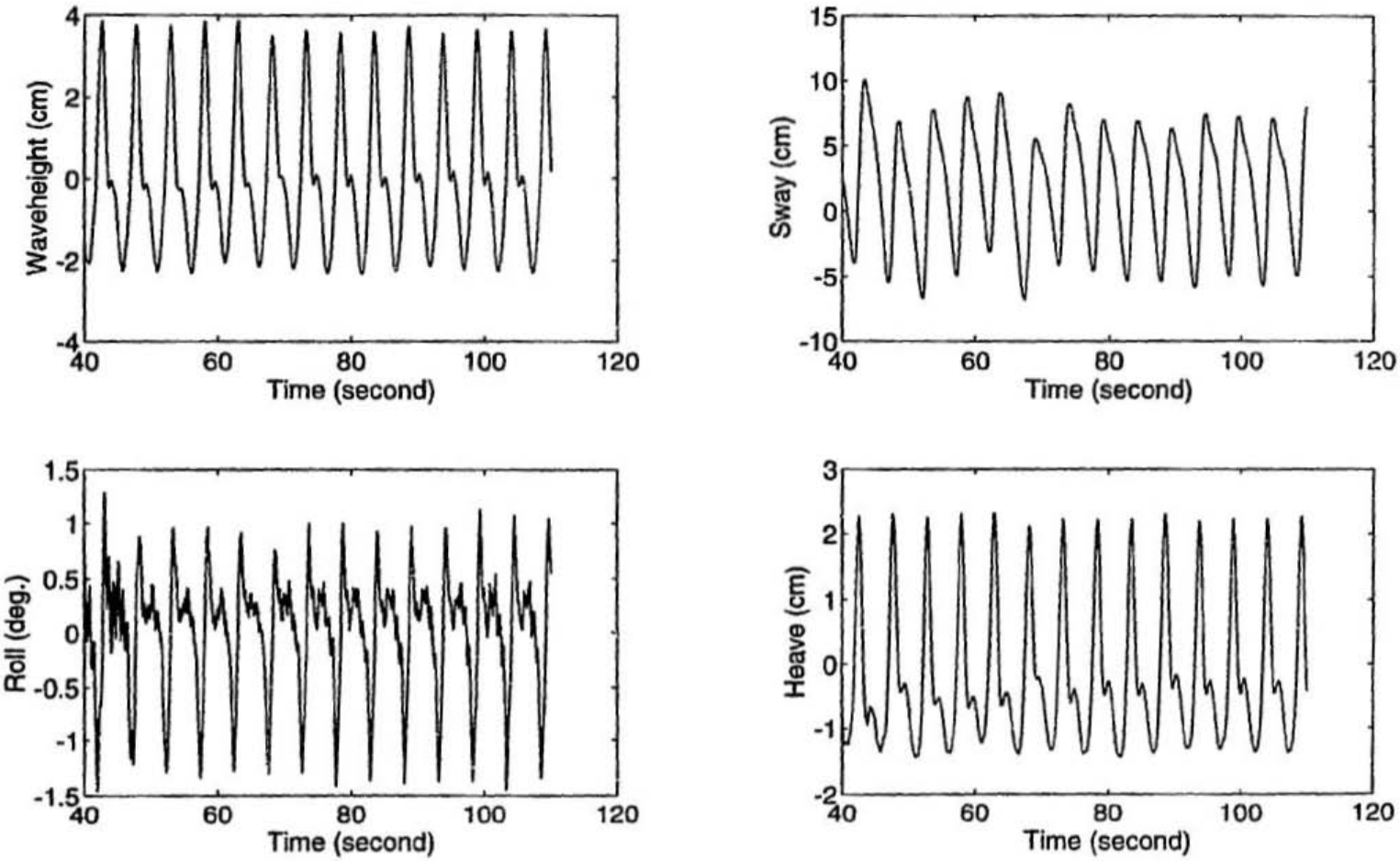

Figure C.5 Test Series A5M1

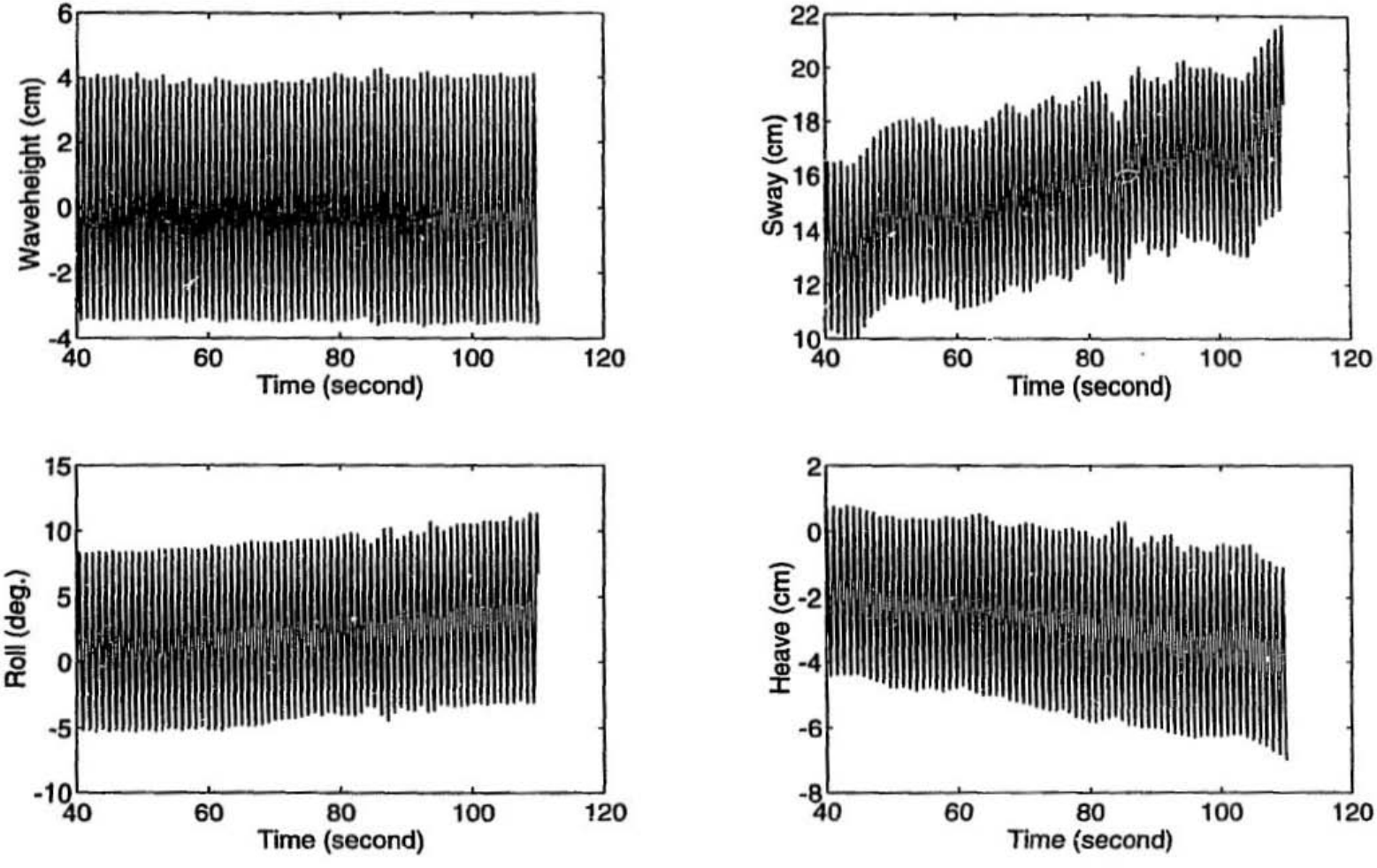

Figure C.6 Test Series B1M1

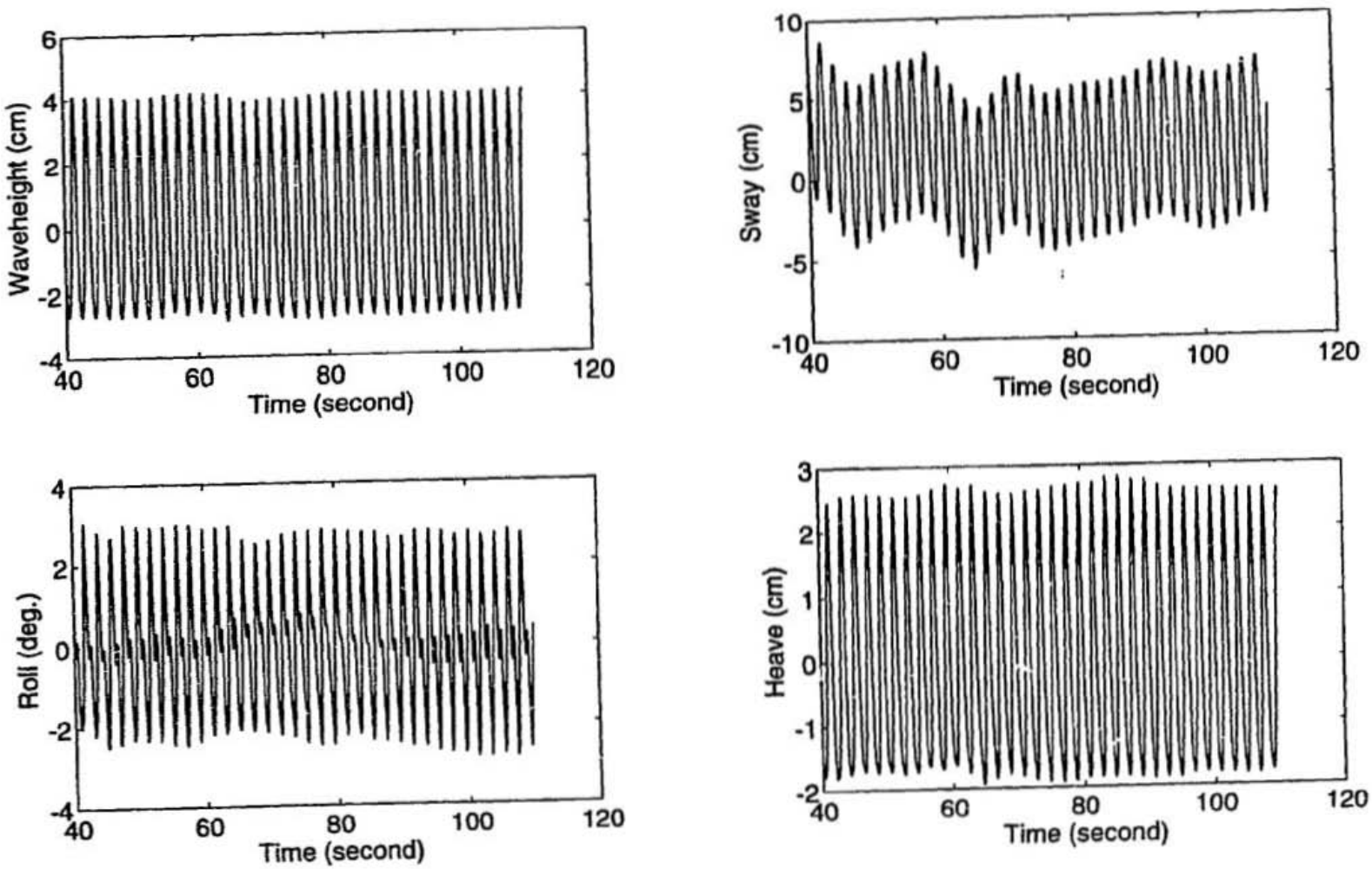

Figure C.7 Test Series B2M1

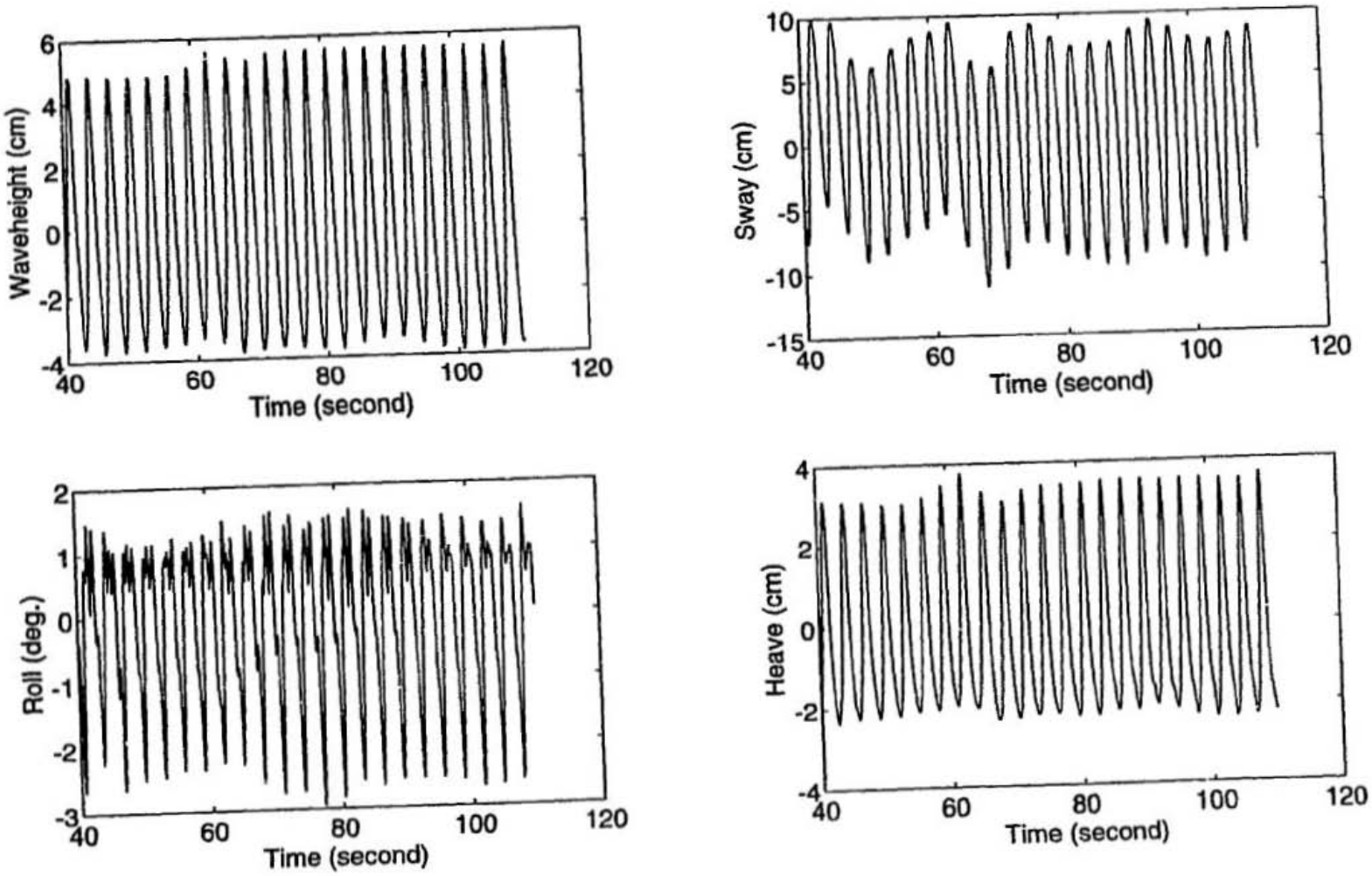

Figure C.8 Test Series B3M1

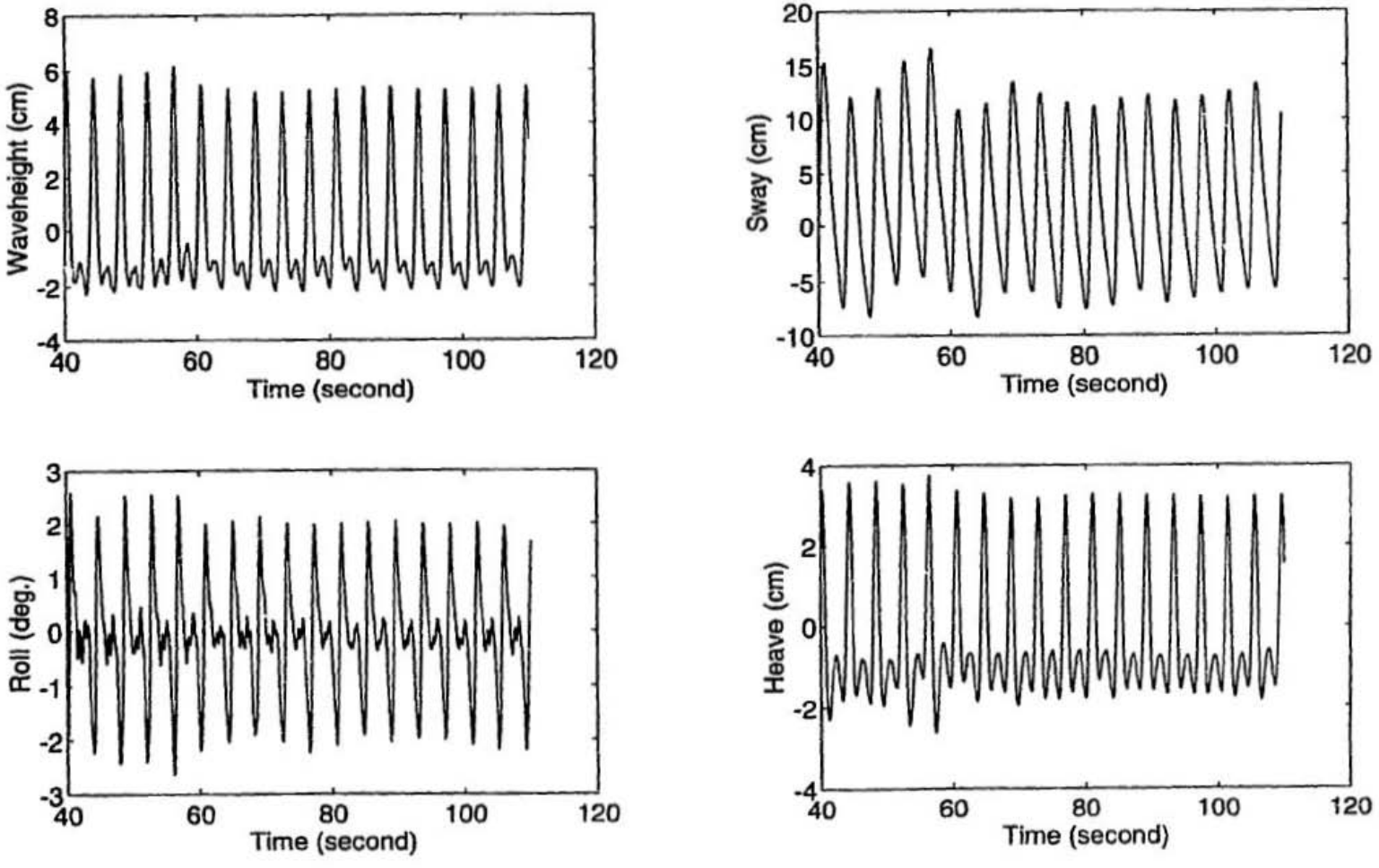

Figure C.9 Test Series B4M1

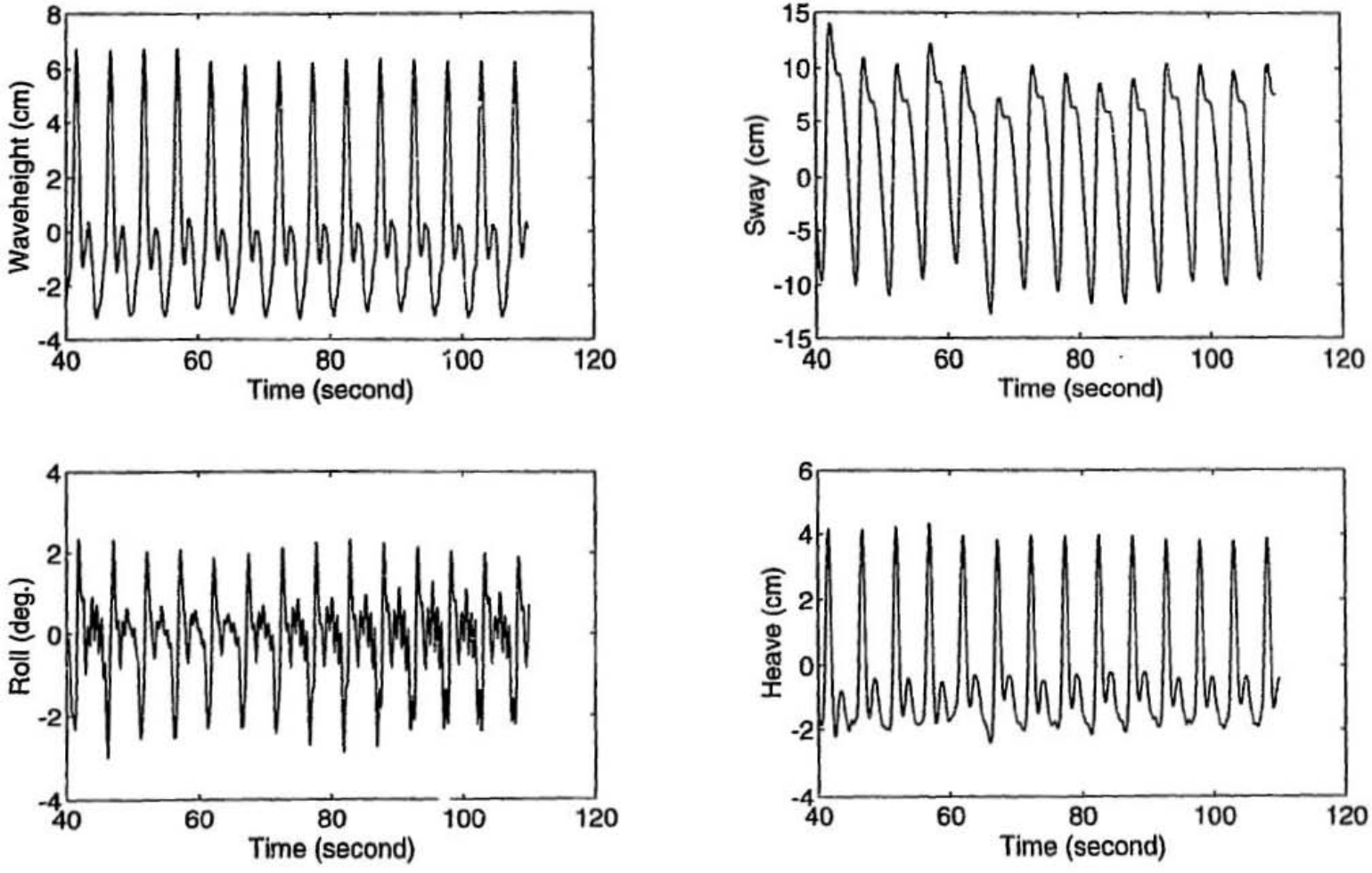

Figure C.10 Test Series B5M1

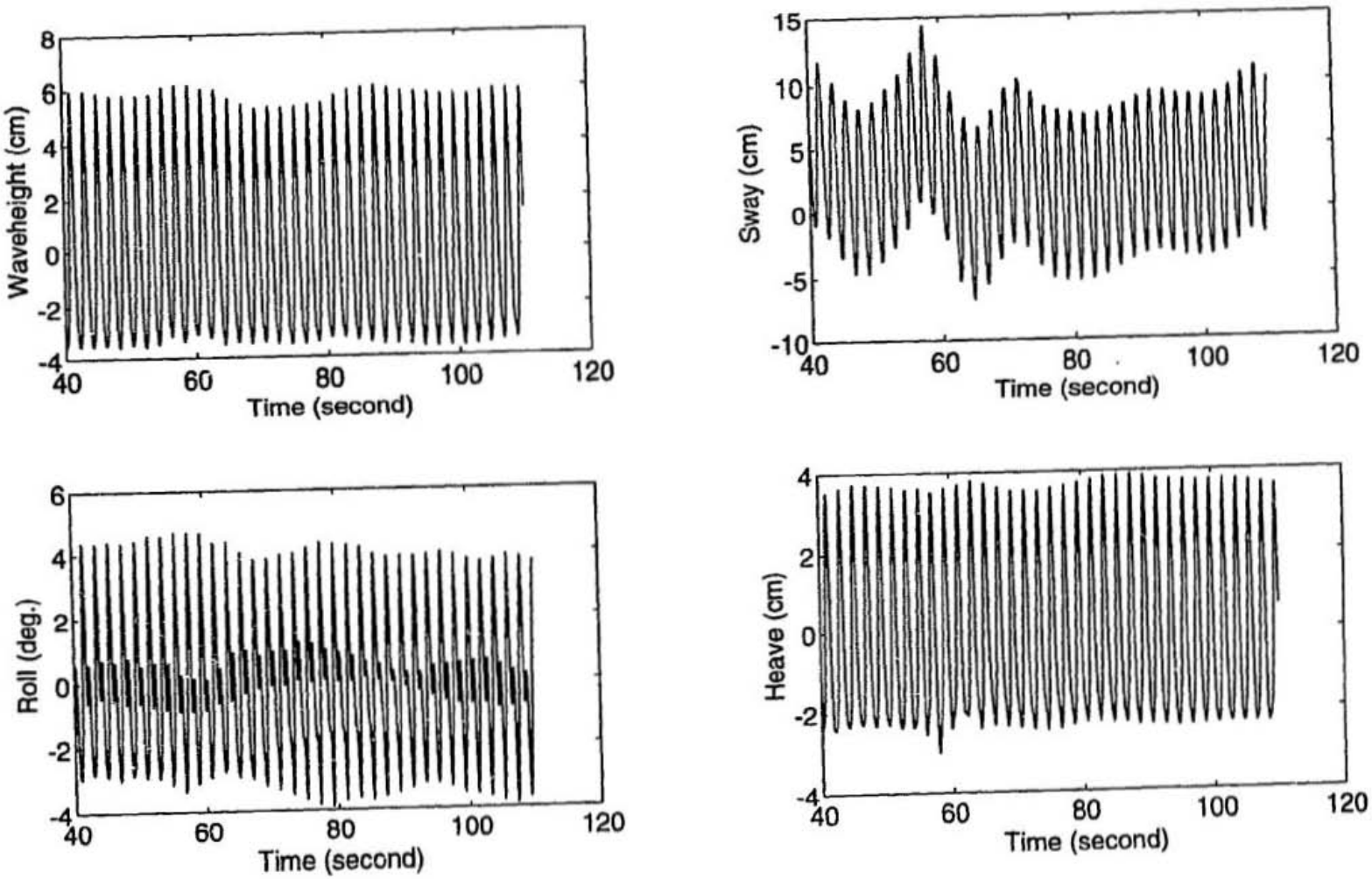

Figure C.11 Test Series C2M1

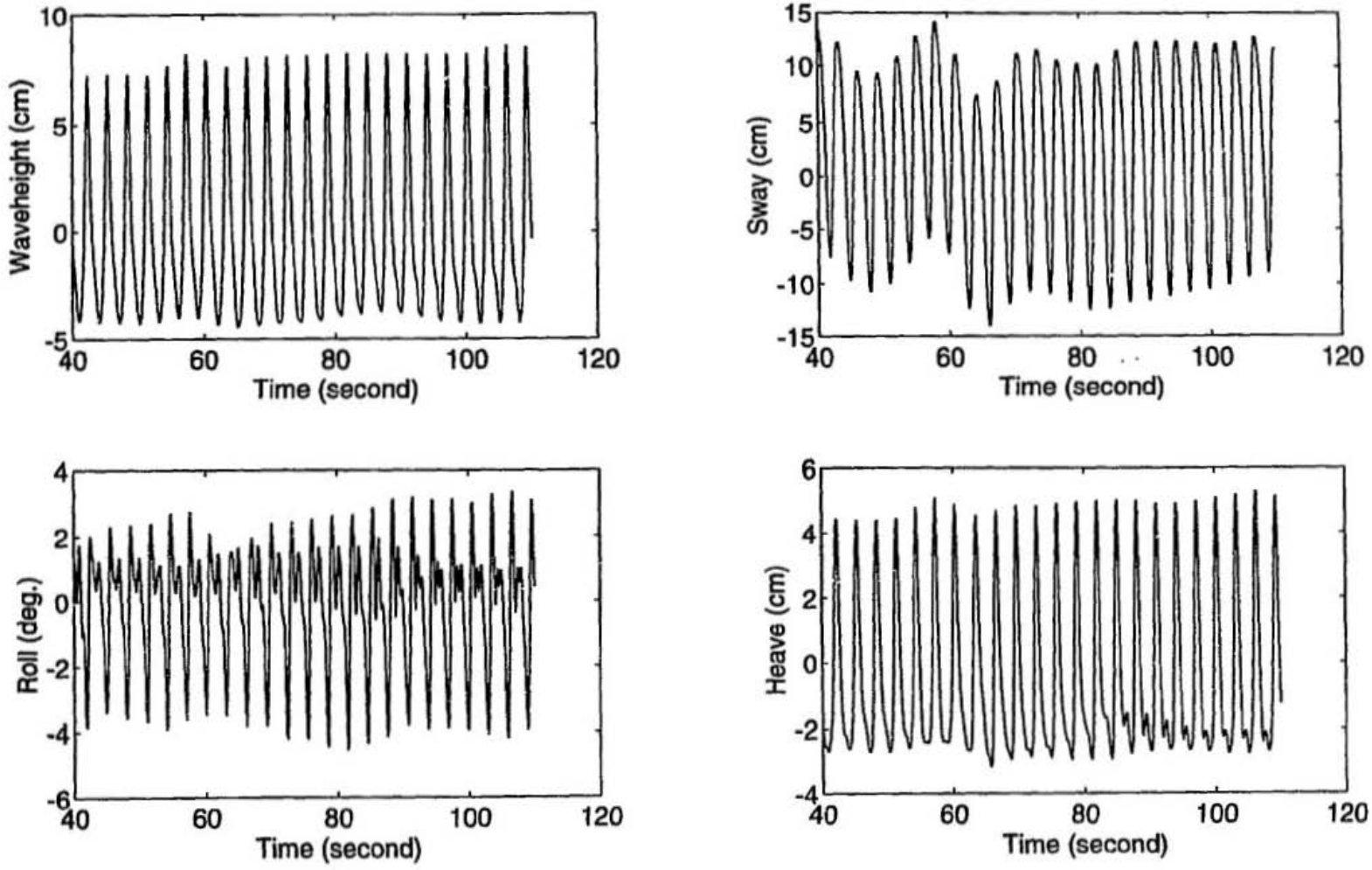

Figure C.12 Test Series C3M1

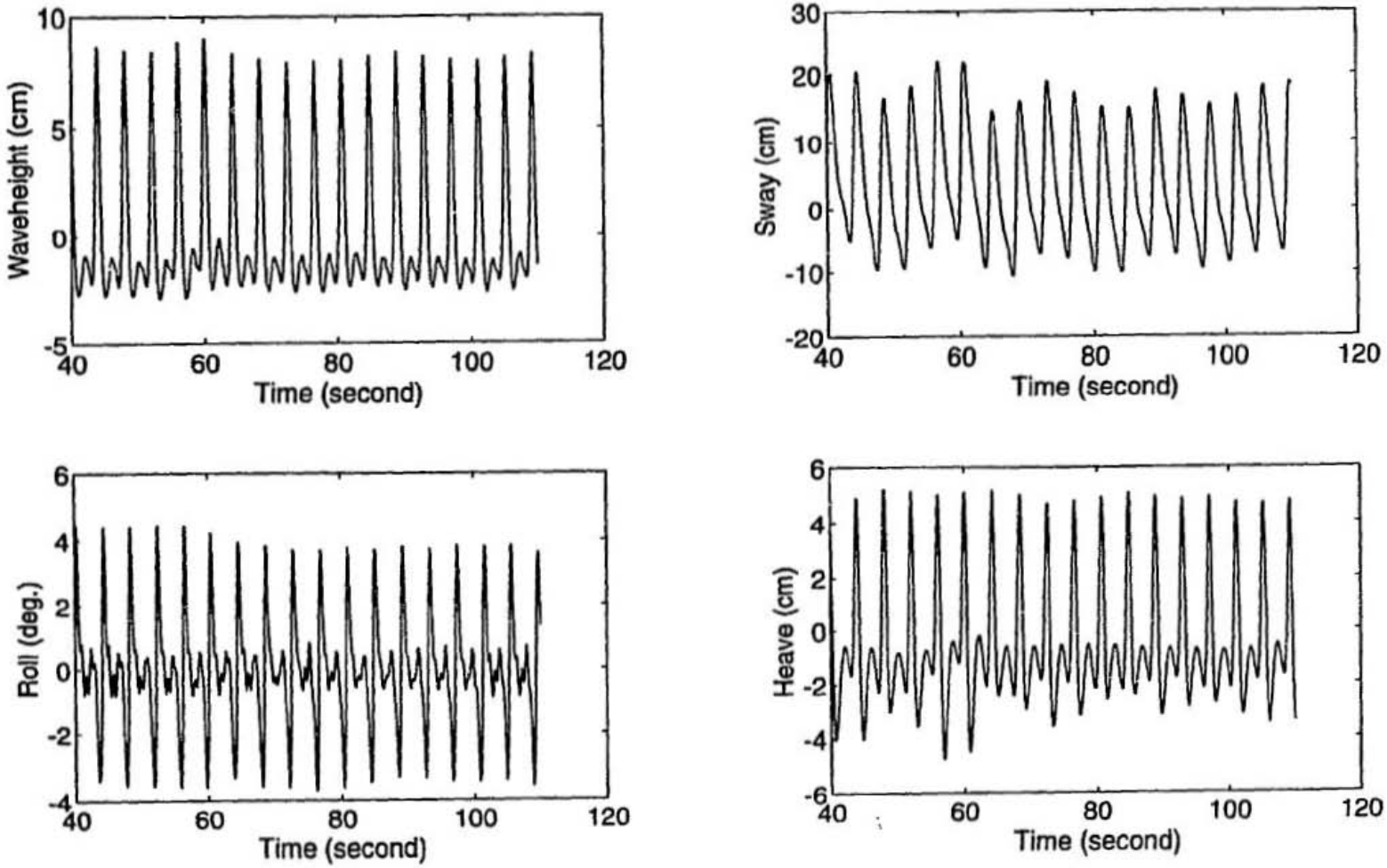

Figure C.13 Test Series C4M1

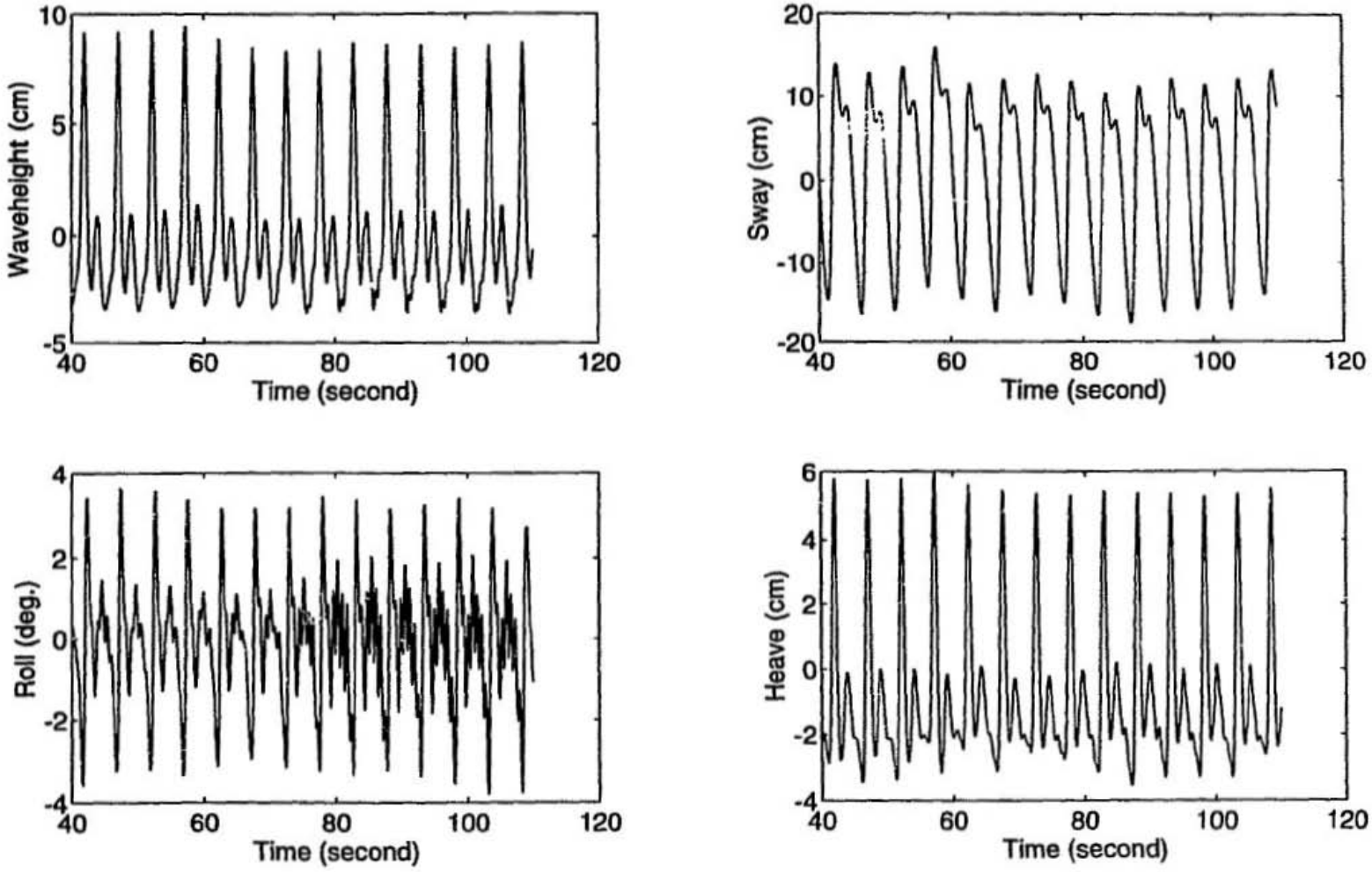

Figure C.14 Test Series C5M1

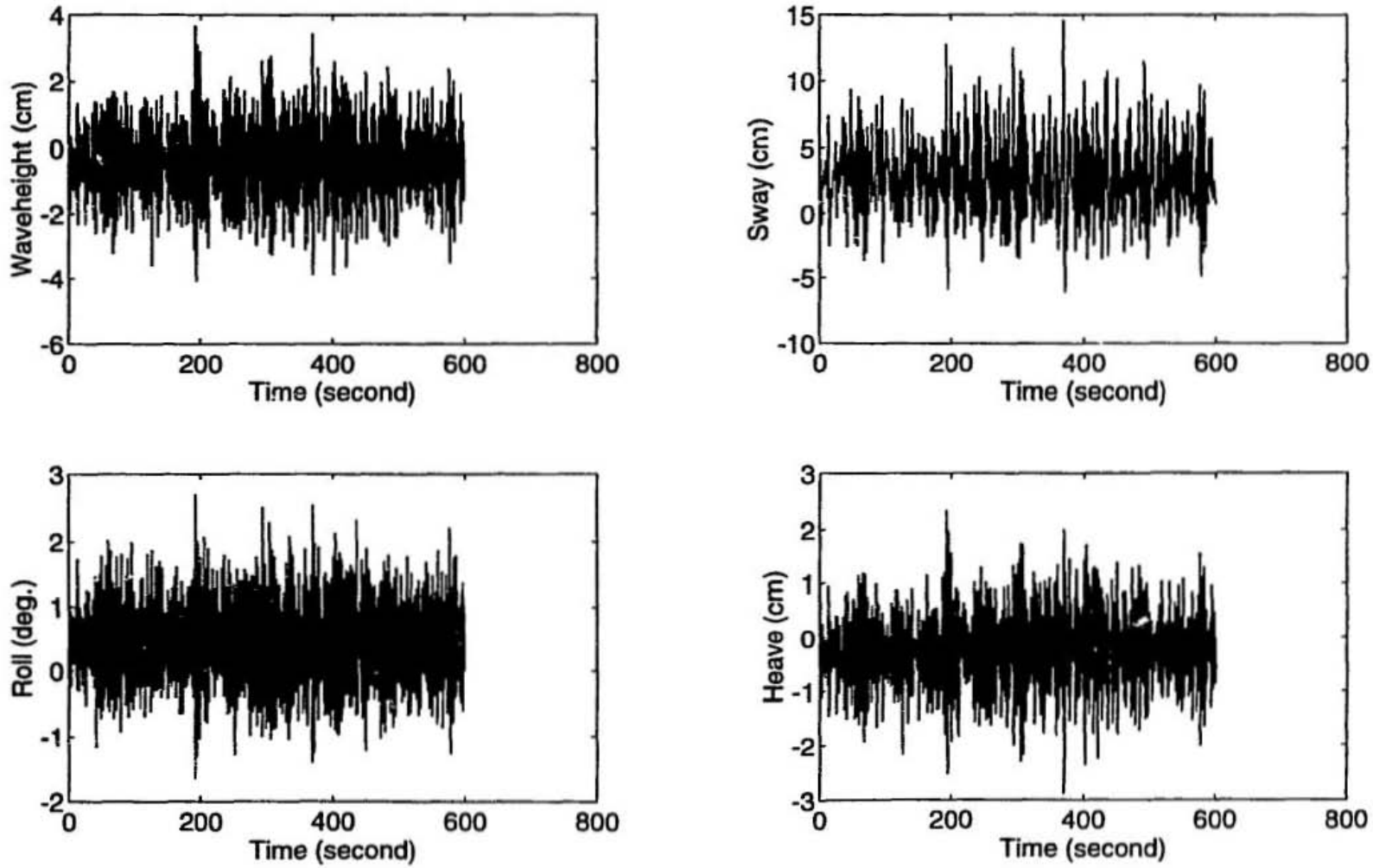

Figure C.15 Test Series D1M1

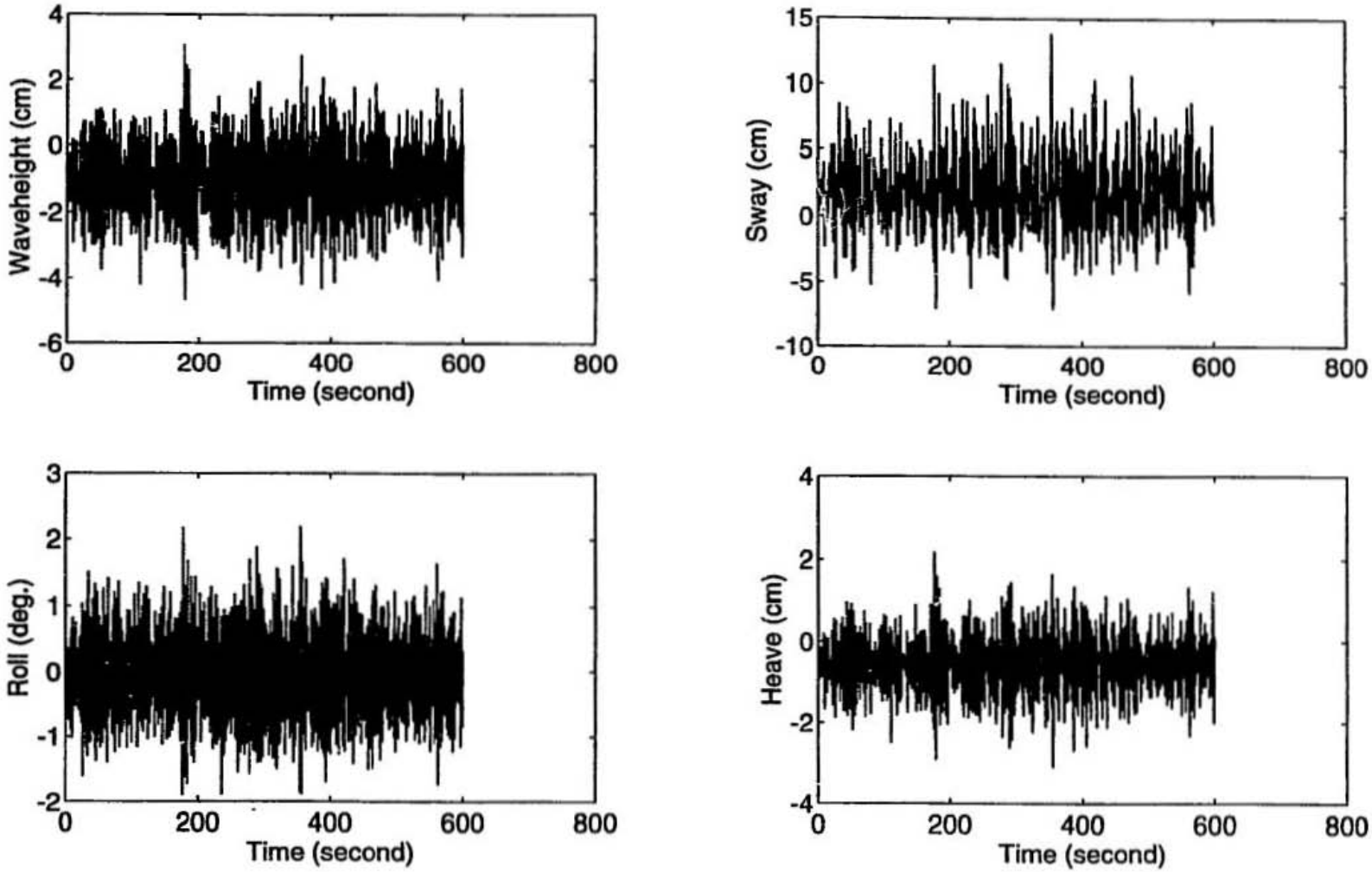

Figure C.16 Test Series D2M1

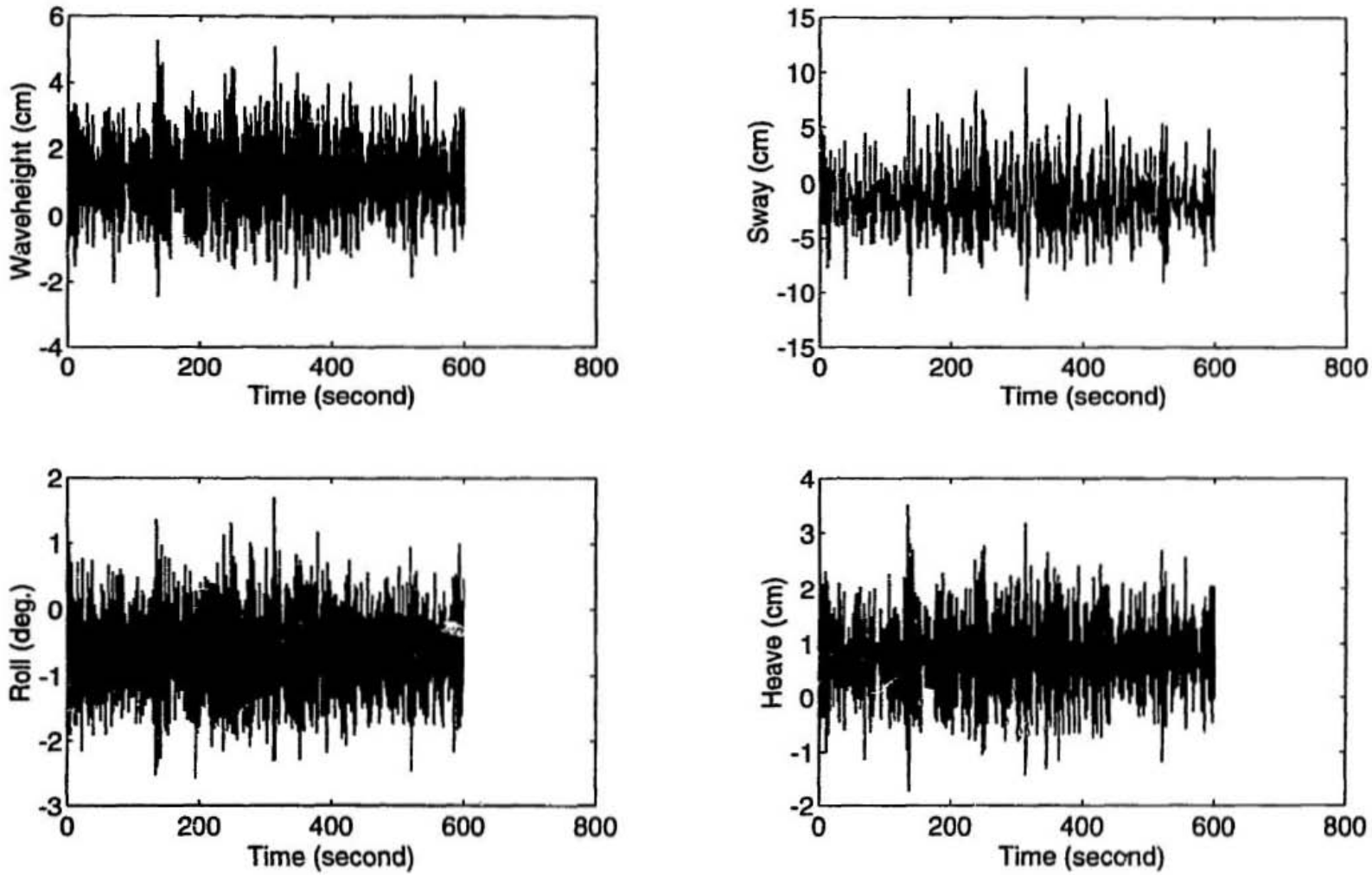

Figure C.17 Test Series D3M1

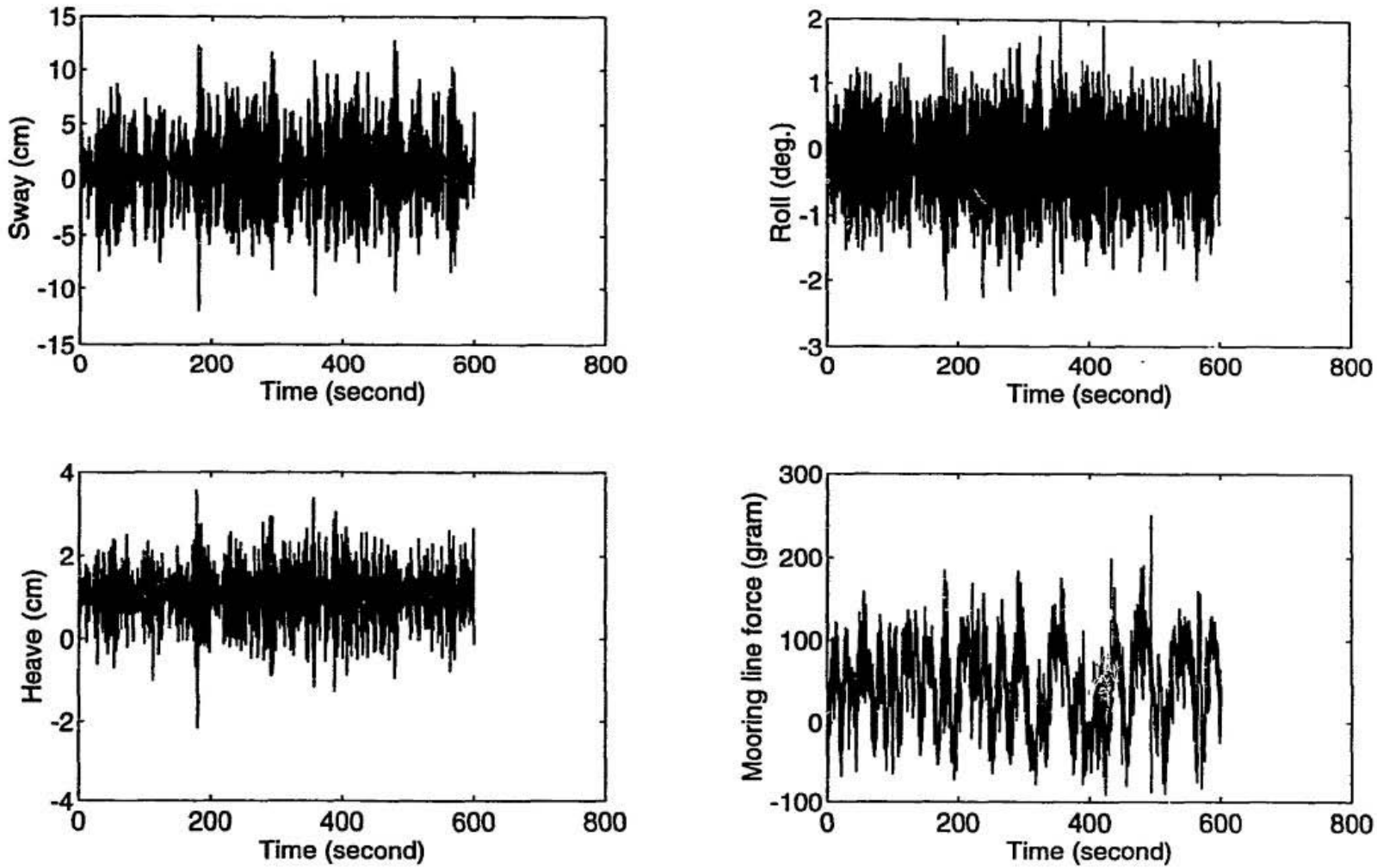

Figure C.18 Test Series D1M2

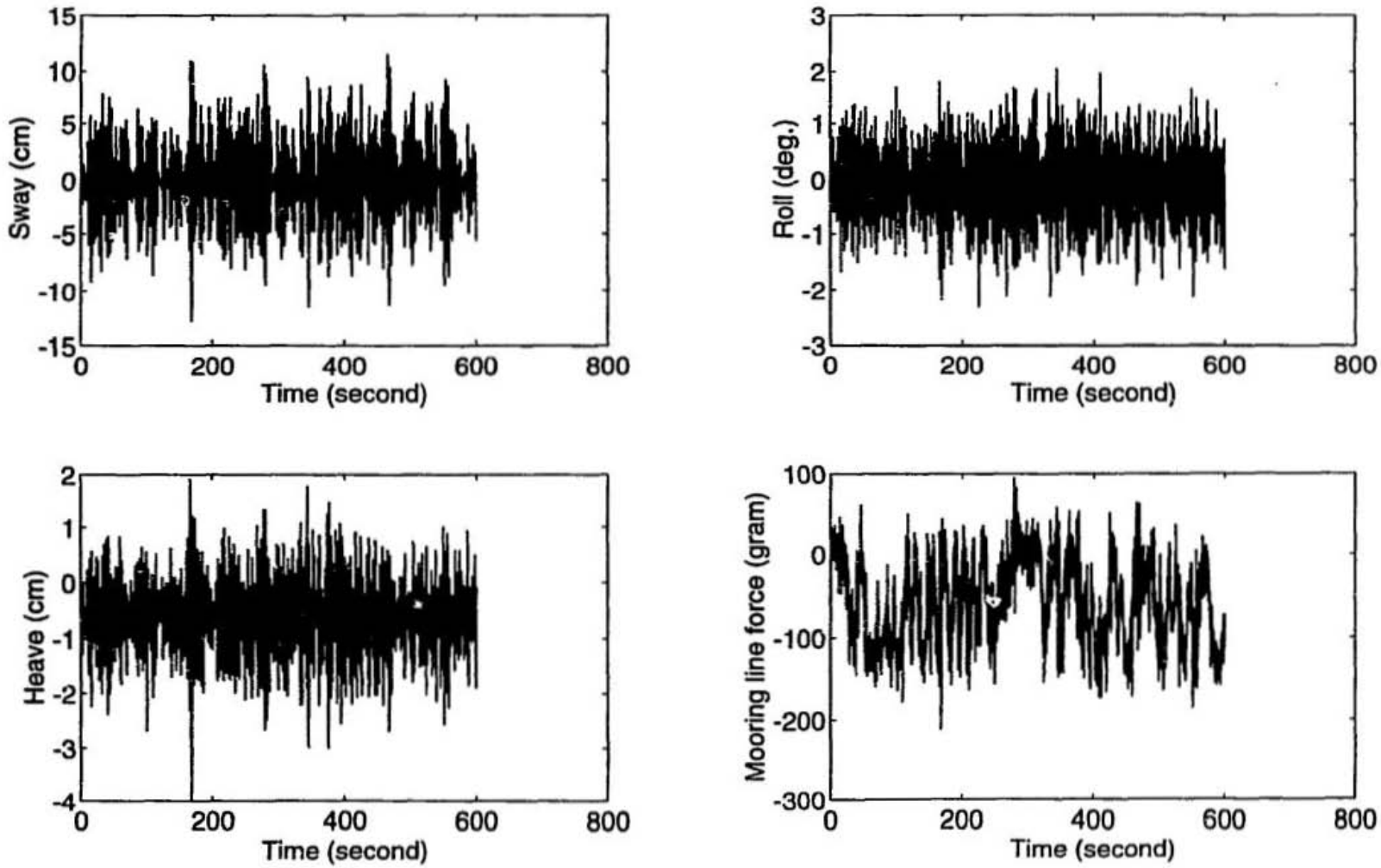

Figure C.19 Test Series D2M2

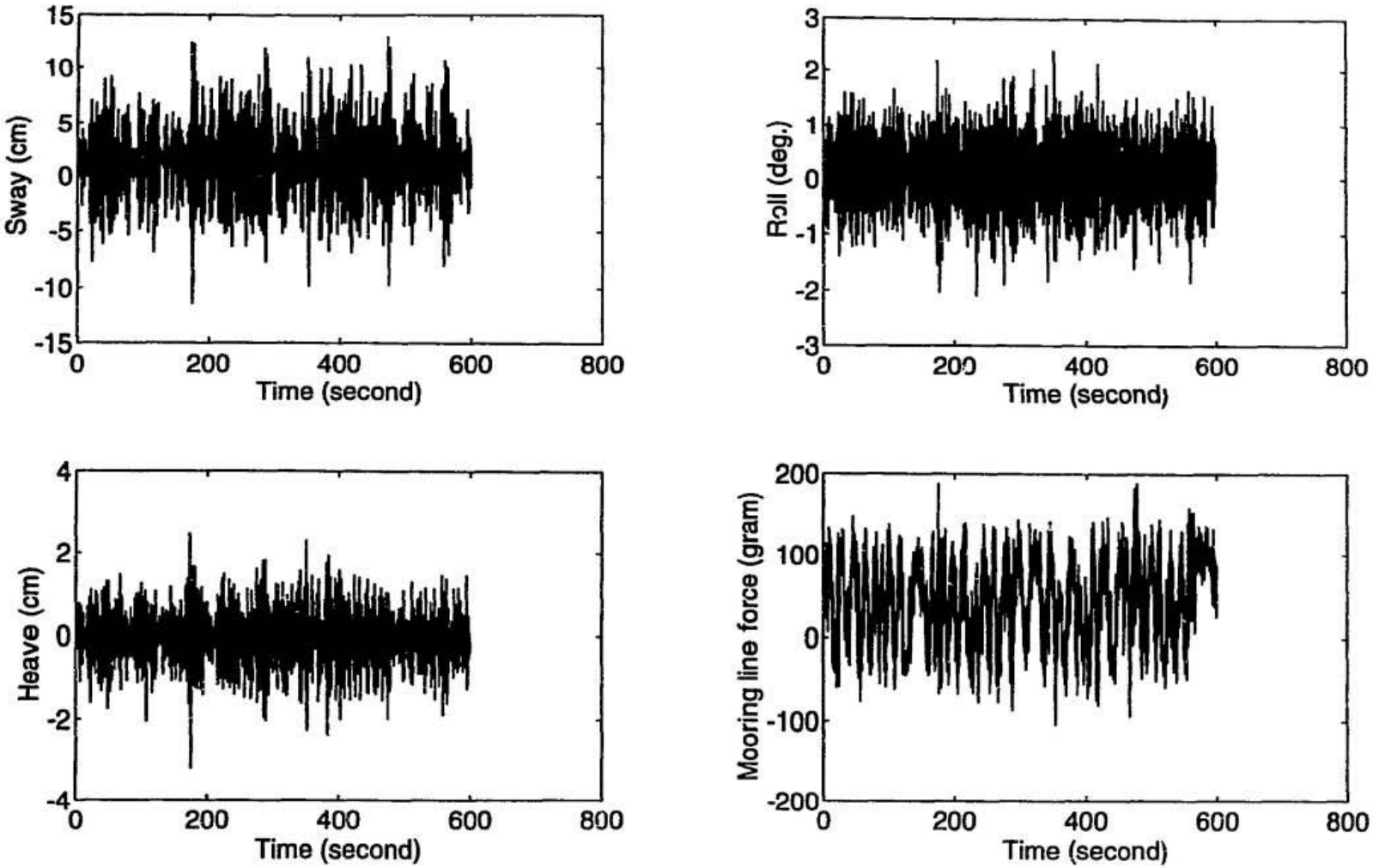

Figure C.20 Test Series D3M2

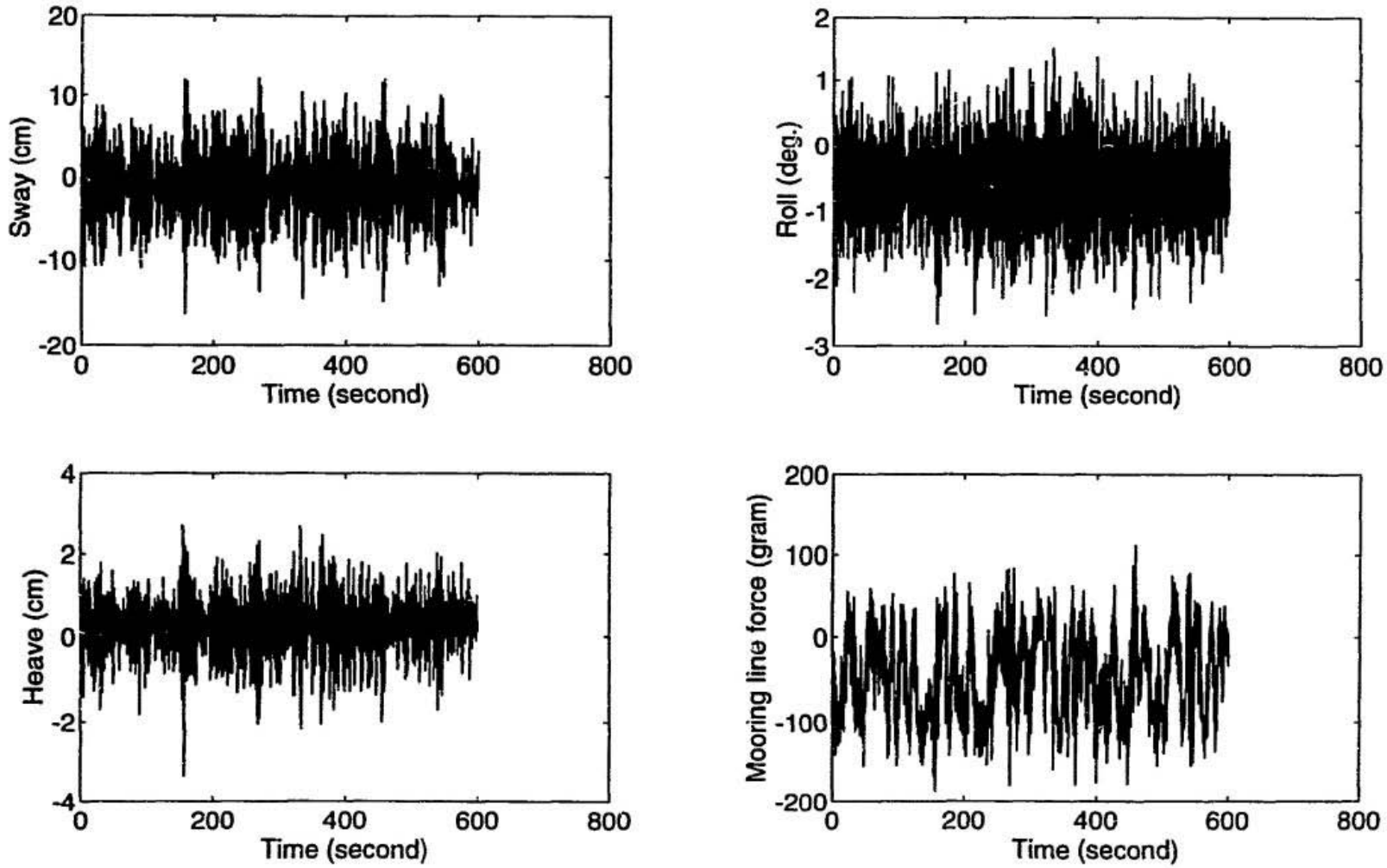

Figure C.21 Test Series D1M3

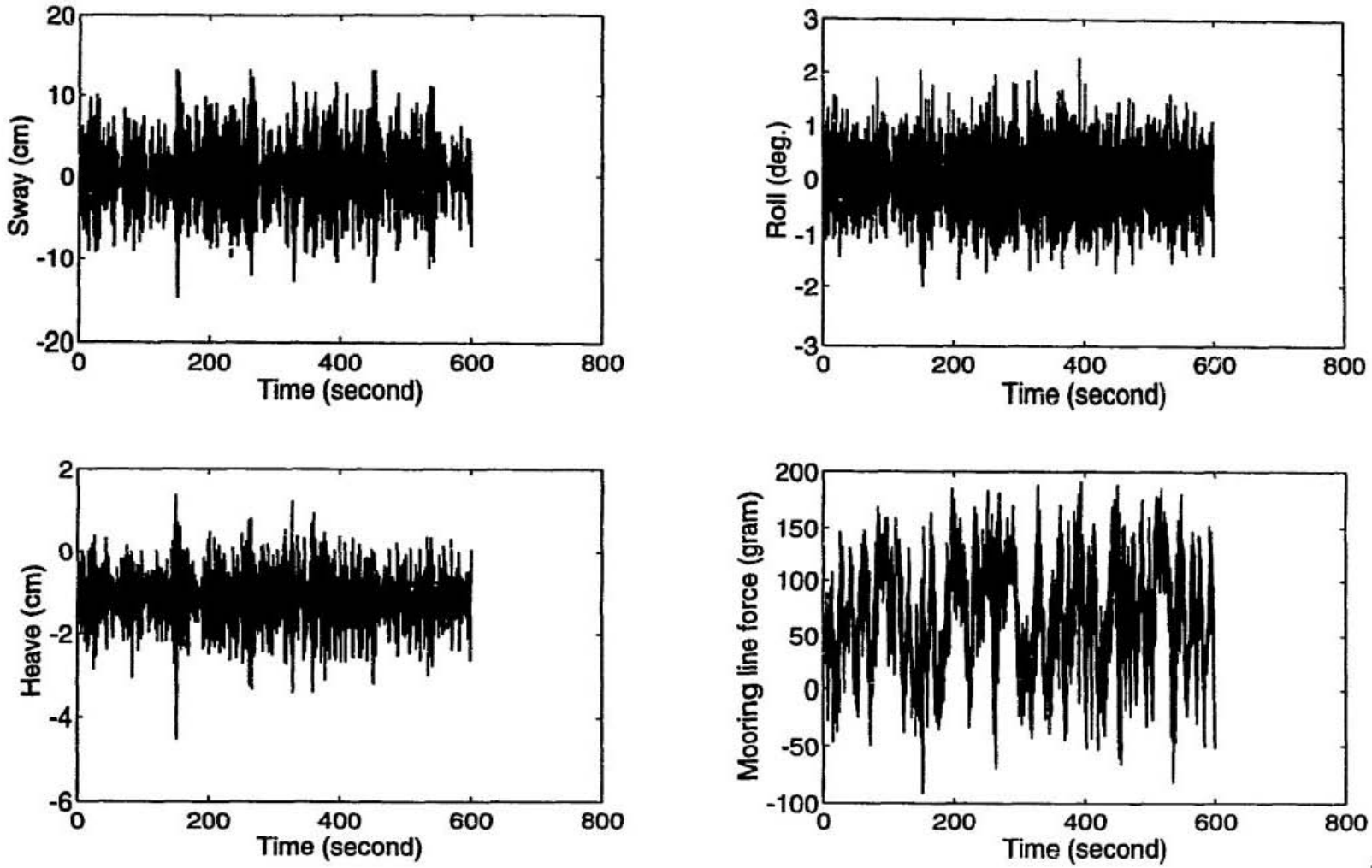

Figure C.22 Test Series D2M3

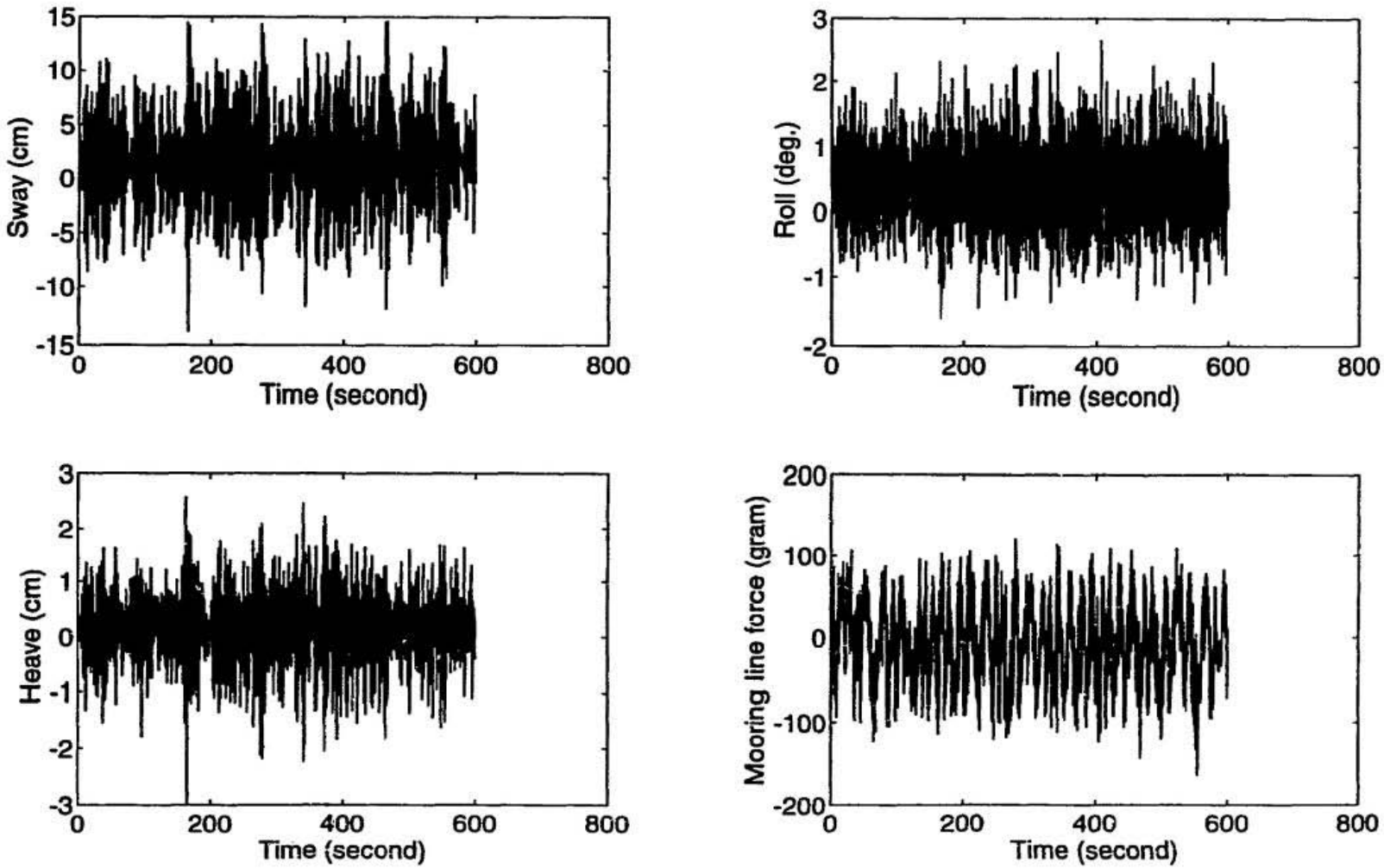

Figure C.23 Test Series D3M3

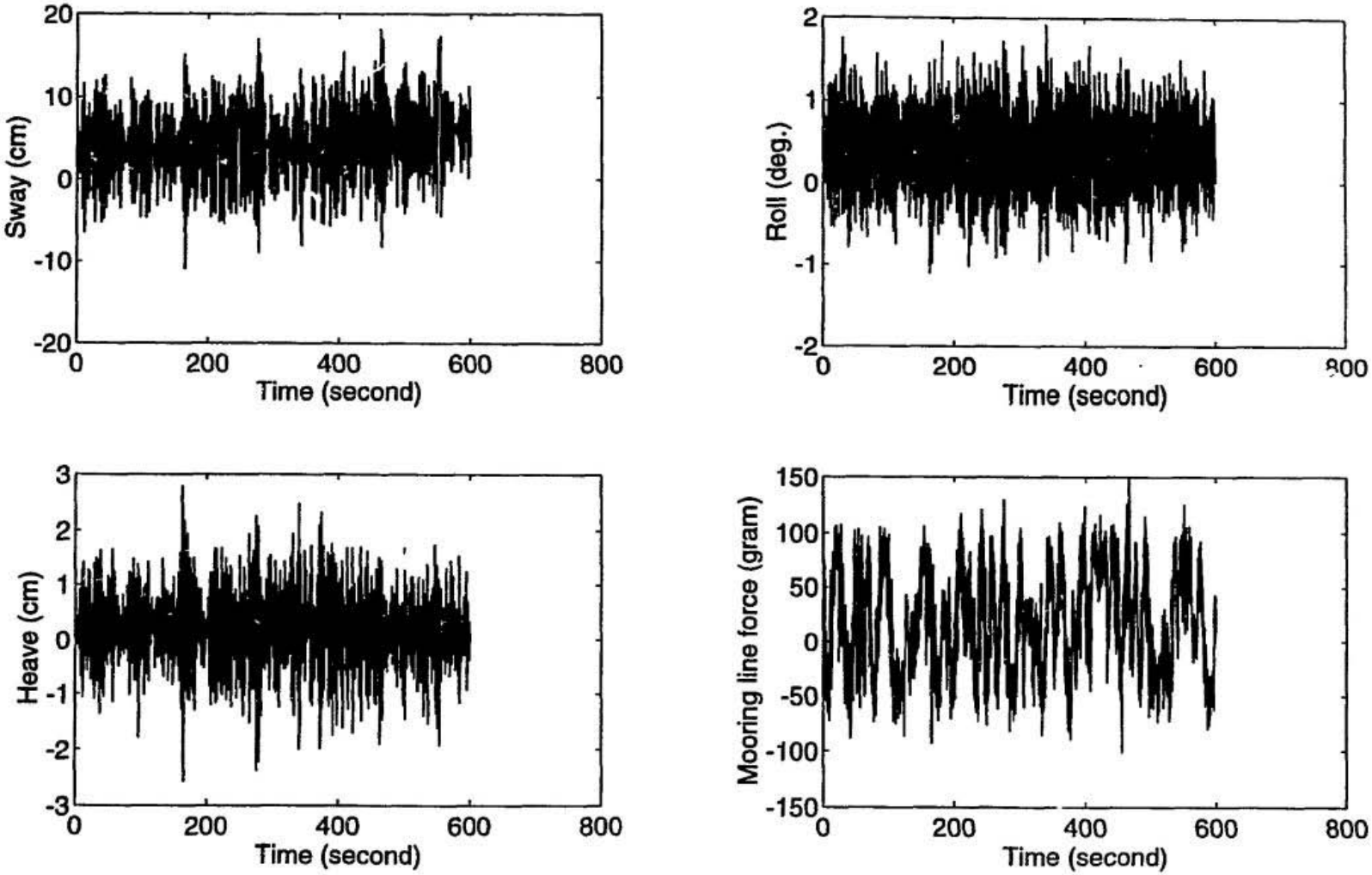

Figure C.24 Test Series D1M4

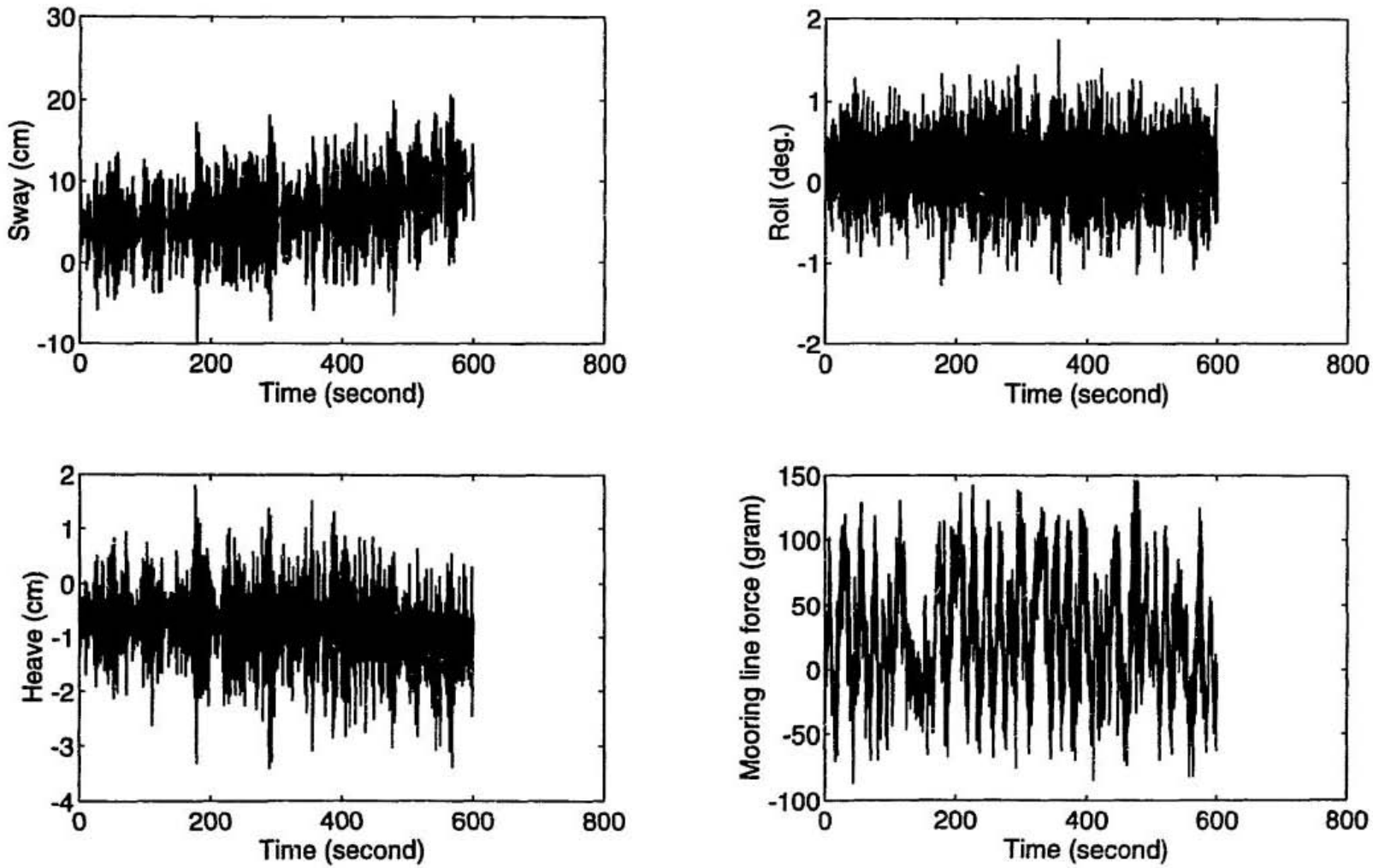

Figure C.25 Test Series D2M4

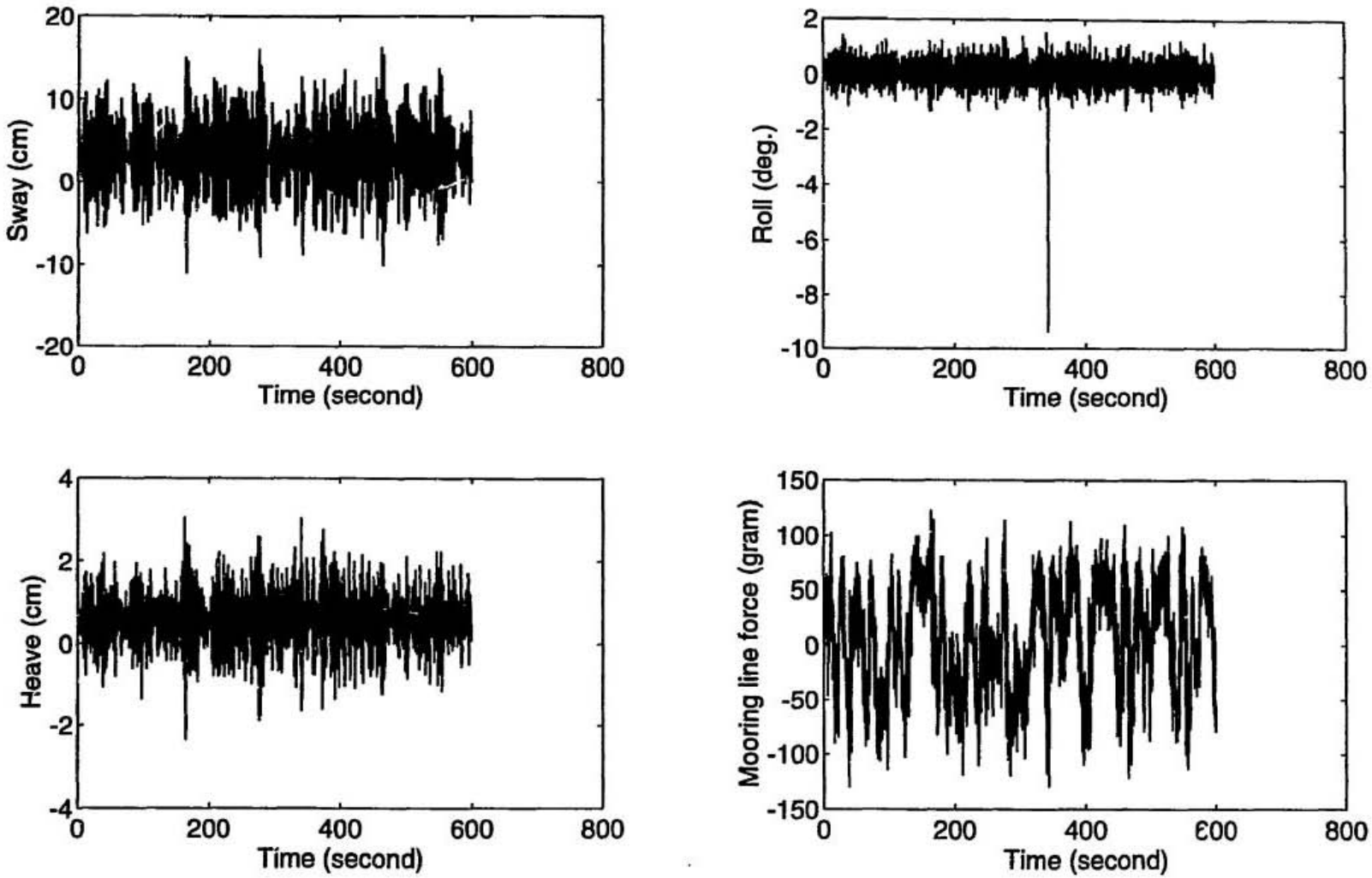

Figure C.26 Test Series D3M4